TARGETING THE PI3K/AKT/MTOR PATHWAY IN TRAUMATIC BRAIN INJURY AND DEVELOPMENTAL DISEASE

By

INA NIKOLAEVA

A dissertation submitted to the

Graduate School – New Brunswick

And

The Graduate School of Biomedical Sciences

Rutgers, The State University of New Jersey

In partial fulfillment of the requirements

For the degree of

Doctor of Philosophy

Graduate Program in Microbiology/Molecular Genetics

Written under the direction of

Gabriella D'Arcangelo, Ph.D.

And approved by

_____

_____

_____

_____

New Brunswick, New Jersey

May, 2016

ABSTRACT OF THE DISSERTATION

Targeting the PI3K/Akt/mTOR pathway in traumatic brain injury and developmental disease

By INA NIKOLAEVA

Dissertation Director:

Gabriella D'Arcangelo, Ph.D.

The PI3K/Akt/mTOR signaling pathway mediates many aspects of cell growth and regeneration. Dysregulation of the pathway during development or following injury can lead to severe symptoms, including behavioral disorders, intellectual disability and seizures. We investigated the effects of excess PI3K/Akt/mTOR signaling in the mouse brain during embryonic development and following traumatic brain injury; we then tested out known inhibitors of the pathway for their potential to prevent or reverse the resulting damage. Here, we described the time course and cell specificity of mTORC1 signal activation in the mouse hippocampus after moderate controlled cortical impact (CCI), and identified an early neuronal peak of activity that occurs within few hours after injury. We suppressed this peak activity by a single injection of the mTORC1 inhibitor rapamycin one hour after CCI, and showed that this acute treatment significantly diminishes the extent of neuronal death and astrogliosis within 24 hours after injury. We investigated two other suppressor compounds of the pathway, mTORC1 inhibitor RAD001 and Akt inhibitor MK-2206, in an *in vitro* mouse model of excess developmental PI3K/Akt/mTOR activity; increased signaling in this pathway is associated with multiple

brain overgrowth disorders in humans. We used excitatory neuron-specific gene deletion of the PI3K antagonist Pten as a method for disinhibiting the pathway. We established Pten-mutant forebrain neuronal cultures as an *in vitro* model of brain overgrowth that may facilitate the identification of pharmacological treatments. We found that Pten-mutant neurons exhibit dramatic cellular hypertrophy, including increased soma size and dendrite complexity, which can be reversed partially with mTORC1 inhibitor RAD001 and fully with Akt inhibitor MK-2206. Our findings suggest that acute Akt and mTORC1 inhibition may offer viable therapeutic approaches for preventing or reversing pathologies caused by excess PI3K/Akt/mTOR signaling, both in the developing and healing brain.

Acknowledgements

First and foremost, I would like to thank my dissertation advisor, Dr. Gabriella D'Arcangelo, for her incredible mentorship and support during this journey. Dr. D'Arcangelo has been a force of calm and clarity throughout all the projects we pursued in the last five years. Her willingness to listen, discuss scientific ideas and create research plans together have taught me to appreciate the art of scientific inquiry. She has created a strong, hardworking laboratory of close-knit colleagues who take interest in each other's work and support each other scientifically and personally. I have thoroughly enjoyed working in a laboratory where new technologies and fields of exploration are always welcome, while sticking to the core foundation of concepts that Dr. D'Arcangelo's research is based on.

I also want to express my gratitude to the following faculty members for agreeing to join my committee and providing invaluable feedback on my progress in graduate school: Dr. Janet Alder, Dr. Bonnie Firestein, Dr. Smita Varia, and Dr. Ping Xie. My committee members have helped me develop both scientifically and professionally outside of the lab, and I am very thankful for all of those experiences.

These acknowledgements would not be complete without my mentioning the first two scientists who gave me a chance at scientific research: my undergraduate mentor Dr. Danton O'Day and (then-PhD candidate) Dr. Robert Huber at the University of Toronto-Mississauga. They showed me how working with an organism as small as the slime mold *D. discoideum* can lead to complex scientific inquiries with vast implications to larger organisms.

My colleagues at Nelson labs, including current and former D'Arcangelo lab members, Alina Afinogenova, Carolina Cocito, Beth Crowell, Valentina Dal Pozzo, Dr. Tatiana Kazdoba-Leach, Dr. Gum Hwa Lee, Giulia Maestri, and Avery Zucco, have been an extraordinary team to work with! Their hard work and scientific curiosity inspires me

every day. Discussing procedures and sharing knowledge is a huge part of our approach and everyone is committed to their projects and to the overall progress of the lab. Together, we have explored new fields, from traumatic brain injury to tuberous sclerosis complex and induced pluripotent stem cells. We have faced many scientific challenges, changing hypotheses and unexpected data, and celebrated every paper, grant or new PCR machine! A special thanks to Beth Crowell for all of the laughter, phone conversations and texts, joint trips to the animal facility and the gym, and the overwhelming amount of skill, organization and resilience she brings to the lab.

There is one more colleague at Nelson Labs that has made a huge difference in my life. Przemyslaw Swiatkowski was first a stranger, then friend, and now my fiancé. He has been an amazing force of scientific curiosity and has helped motivate me in times of failing experiments over and over again. He also performed all electrophysiology mentioned in this dissertation. His talent and drive as a scientist continue to inspire me every day.

Finally, I want to acknowledge our funding sources for the work discussed here: the New Jersey Commission on Brain Injury Research, the Department of Defense, the Department of Cell Biology and Neuroscience, the Department of Microbiology and Molecular Genetics, and the National Institutes of Health.

TABLE OF CONTENTS

LIST OF TABLES

LIST OF FIGURES

CHAPTER 1: INTRODUCTION

1. PI3K/Akt/mTOR Pathway

The phosphoinositide 3-kinase (PI3K)/Akt/Mammalian target of rapamycin (mTOR) pathway integrates signals from growth factors, insulin, and cell energy status in order to control protein synthesis, metabolism and cytoskeletal dynamics. The order of the signaling cascade was elucidated in the late 1990s and early 2000s, and all components have been implicated in a variety of cancers, neurodegenerative diseases, autism, diabetes and epilepsy (Prestwich, 2004; Sarbassov et al, 2004; Ma et al, 2005; Sarbassov et al, 2005; Karisson et al, 2015). The pathway functions via a series of activating and inactivating phosphorylation events, and diseases arise from mutations that cause increased signaling activity of the kinases PI3K, Akt and mTOR, or inactivation of the two key negative effectors, phosphatase and tensin homolog on chromosome ten (Pten) and tuberous sclerosis complex 1 and 2 (Tsc1 and Tsc2) (Garami et al, 2003; Tee et al, 2003; Sarbassov et al, 2005; Jansen et al, 2015). Research has therefore focused on identifying effective, nontoxic inhibitors of PI3K, Akt and mTOR as potential treatment options for patients suffering from diseases secondary to dysregulation of this signaling cascade. Rapamycin is the defining small molecule inhibitor of downstream effects of PI3K/Akt/mTOR, although new compounds such as Akt antagonist MK-2206 and safer, more soluble analog of rapamycin (rapalog) RAD001, are swiftly making their way through clinical trials (Oki et al, 2015; Rugo et al, 2016).

1.1 PI3K

PI3K is a major effector of insulin-like growth factors (IGFs) and other growth factors, which activate receptor tyrosine kinases (RTKs) in order to stimulate protein synthesis in growing and dividing cells (Karisson et al, 2015). PI3K is recruited to the cytoplasmic leaflet of the cellular membrane via Src-homology 2 (SH2) domains by

phosphatidylinositol-4,5-bisphosphate (PIP_2) molecules. PI3K phosphorylates the 3-hydroxyl group of PIP_2, converting it into phosphatidylinositol-3,4,5-trisphosphate (PIP_3) (Deane and Fruman, 2004; Prestwich, 2004; Briaud et al, 2005). While PIP_2 and PIP_3 form only a small component of the plasma membrane, they undergo transient increases as second messengers involved in PI3K/Akt/mTOR pathway signal transduction. Resting cell levels of PIP_3 are especially low, and accumulation of PIP_3 due to loss of Pten severely disrupts glucose homeostasis in the cell (Prestwich, 2004).

There are three classes of PI3Ks, called I, II and III, but only Class I targets PIP_2. Class I PI3K usually consists of one of three 110kDa catalytic subunits (p110) and one of five possible regulatory subunits, ranging from 50 to 85kDa (p85), which dictate localization and activity. All five regulatory subunits have the SH2 domains necessary for recruitment to the cell membrane by PIP_2 (Deane and Fruman, 2004; Briaud et al, 2005). p85 has an N-terminal and C-terminal SH2 domain, with an inter-SH2 domain in the center, which interacts with the N-terminal adaptor domain of p110. p85 can downregulate PI3K activity by sequestering into the nucleus or binding Pten to prevent its degradation (LoPiccolo et al, 2015). Hyperactivation of PI3K generally results in increased cell size and division, mainly through the Akt/mTORC1 signaling pathway.

1.2 Pten

Pten is the main upstream inhibitor of the entire PI3K/Akt/mTOR pathway by reversing PI3K's addition of a phosphate on the 3-hydroxyl group of PIP_2 through its lipid phosphatase activity on PIP_3 (Prestwich, 2004; Laplante and Sabatini, 2009). Therefore, Pten-inactivating mutations can give rise to a similar host of phenotypes as PI3K- and Akt-activating mutations. Pten was initially identified through the study of glioblastomas and mutations associated with tumors in a variety of tissues including breast, prostate and melanocyte (Backman et al, 2001). Since then, dysregulation of Pten has been implicated in a variety of neurologic diseases in addition to cancer, including Autism

Spectrum Disorder (ASD), Lhermitte-Duclos, brain overgrowth disorders, and Pten hamartoma tumor syndromes (PHTS) such as Cowden syndrome and Bannayan-Riley-Ruvalcaba syndrome (Backman et al, 2001; Spinelli et al, 2014; Jansen et al, 2015; Nakanishi et al, 2016).

The *PTEN/MMAC1* gene is located in the 10q23 region of the chromosome, within a section that commonly undergoes somatic mutations during tumorigenesis (Sansal and Sellers, 2004). Pten is a 403 amino acid, 55kDa protein with two defined domains, a catalytic dual-specificity phosphatase domain, and a C2 Calcium-independent domain (Lee et al, 1999; Hopkins et al, 2013; Spinelli et al, 2014; Naguib et al, 2015). The C2 domain contains a CBR3 loop specific for binding Phosphatidylinositol-3-phosphate (PI[3]P), and allows Pten to localize to a variety of membranes, including the endoplasmic reticulum, and mitochondrial membranes. Furthermore, Pten can localize to the microtubule network, thus allowing for a variety of surfaces and subcellular locations where it can modulate local Akt/mTOR activity and protein synthesis (Kreis et al, 2014; Spinelli et al, 2014; Naguib et al, 2015). Pten also localizes to the cellular membrane by interacting with PIP_2 via an N-terminal PIP_2 binding motif (PBM), where it can gain access to PIP_3. The C-terminus of Pten contains a flexible tail with regulatory functions and a PDZ binding motif thought to help Pten localize to dendritic spines (Lee et al, 1999; Kreis et al, 2014). The phosphatase domain of Pten contains a HCXXGXXR phosphatase motif, at residues 123-130, with Cysteine-124 as the catalytic amino acid (Lee et al, 1999). Pten can dephosphorylate lipids and has predicted protein phosphatase activity on Serine, Threonine and Tyrosine residues of peptides based on *in vitro* experiments (Lee et al, 1999; Naguib et al, 2015). Finally, the 49 residues of the C-terminal tail appear to form a flexible structure, which, upon phosphorylation, fold into a closed conformation to disrupt Pten's interaction with PIP_2 and its localization to the cellular membrane (Lee et al, 1999; Kreis et al, 2014).

It is important to note that a second form of Pten, the 75kDa Pten-Long, is translated *in vivo* and contains 173 extra amino acids at its N-terminus. Pten-Long is equally capable of dephosphorylating PIP_3 and inhibiting the PI3K/Akt/mTOR signaling cascade. Finally, Pten-Long has a signal sequence for extracellular secretion, and has been shown to undergo both secretion and cell entry (Hopkins et al, 2013). Regular Pten can also make it into the extracellular space in exosomes (Kreis et al, 2014). Pten can be sequestered into the nucleus, potentially as a way to disinhibit PI3K signaling at the cellular membrane. Nuclear localization of Pten occurs during cell cycling, and stressful events such as excitotoxicity and traumatic brain injury (Kreis et al, 2014). It is clear that Pten has a number of functions that can be disrupted by mutations and lead to tumorigenesis, such as overactive PI3K/Akt/mTOR activity and disinhibition of apoptotic signalsThe symptoms of a patient with a Pten-related disorder vary depending on the severity of the mutation. The presence of phosphatase-inactive Pten appears to be more detrimental than unstable and active or completely absent Pten. Therefore, mutations in the catalytic domain of Pten correlate with the most severe syndromes. Missense mutations that destabilize, but do not inactivate, Pten are associated with ASD, while truncation mutations result in tumors and PHTS (Kreis et al, 2014; Spinelli et al, 2014). Another very curious Pten mutation found in tumors involves a change of function, namely from a 3-phosphatase to a 5-phosphatase (Costa et al, 2015). Since absence of Pten is less detrimental than inactive Pten, change of function mutations are just as destructive and tumorigenic as loss of function mutations that do not affect Pten synthesis. Pten-mediated disease in humans can come from a variety of genetic conditions, such as germline mutations and somatic mutations leading to type 1 or 2 mosaicism (heterozygous and homozygous condition, respectively). Germline nonsense and missense mutations in *PTEN* are more commonly associated with Cowden and Lhermitte-Duclos disease, while sporadic loss of function mutations in the brain lead to

brain overgrowth disorders such as hemimegalencephaly and focal cortical dysplasia. Patients tend to be heterozygous for mutations, although rare cases of homozygosity do exist (Liaw et al, 1997; Nelen et al, 1997; Jansen et al, 2015).

. Homozygous deletion of *Pten* in mice is embryonic lethal, whereas heterozygous mice are prone to tumors (Kwon et al, 2006). In neurons, Pten is expressed ubiquitously in the soma, but can also localize specifically to dendritic spines or the dendritic shaft. Pten modulates neurite outgrowth in differentiating and immature neurons, and controls synaptic plasticity in mature neurons (Kreis et al, 2014). Since Pten downregulates Akt signaling, and thus leads to increased Glycogen Synthase Kinase 3 (GSK3) activity, Pten also indirectly regulates a major pathway for establishing neuronal polarity (Jiang et al, 2005). Furthermore, there is evidence that Pten interferes with axonal regeneration after injury and axonal branching during development, but little else is known about Pten's direct effects on axonal growth (Park et al, 2008; Drinjakovic et al, 2010; Ohtake et al, 2014; Ohtake et al, 2015).

1.3 Akt

Akt, also known as Protein Kinase B (PKB), is a ubiquitously expressed 57-60kDa Serine/Threonine protein kinase activated by the PIP_3 signal downstream of PI3K (Auguin et al, 2004; Muddassar et al, 2008). There are three isoforms of the Akt enzyme, Akt1, Akt2 and Akt3, whose expression levels vary between tissues and organs, and have 70-80% amino acid sequence homology to each other (Auguin et al, 2004; Muddassar et al, 2008). The structure of Akt includes a C-terminal hydrophobic domain with regulatory function, a catalytic kinase domain, and an N-terminal pleckstrin homology (PH) domain (Auguin et al, 2004). The PH domain is a sequence of about 100 amino acids specifically used to interact with phosphoinositides such as PIP_3, which uses the PH domain to recruit Akt to the cellular membrane (Auguin et al, 2004; Prestwich, 2004). At the cellular membrane, Akt gets phosphorylated by

phosphoinositide-dependent kinase 1 (PDK1), also recruited by PIP_3 via a PH domain, at Threonine residue 308 (Thr308), within the activation loop of Akt's catalytic domain. A further activating phosphorylation, at the Serine 473 (Ser473) residue in the hydrophobic loop of the C-terminal regulatory domain, can be performed by several kinases, including mTORC2 and protein kinase C (PKC), allowing activation of Akt to be moderated by different signaling cascades (Das et al, 2016). Studies choose to focus on either or both of these phosphorylation sites as indicators of Akt activity, but researchers agree that pAkt(Thr308) is mainly a readout of PI3K activity, while pAkt(Ser473) is mainly indicative of of mTORC2 activity (Auguin et al, 2004; Sarbassov et al, 2005; Sarbassov et al, 2006; Karisson et al, 2015; Shimobayashi and Hall, 2016). Two other phosphorylation sites have been identified on Akt, at residues Threonine 450 and Serine 124. The former negatively regulates Thr308 phosphorylation, while the latter appears to be insensitive to cell stimulation and does not influence Akt activity (Auguin et al, 2004; Hiraoka et al, 2011).

The Thr308 and Ser473 phosphorylation events have a complex functional effect on Akt activity. There is evidence that Thr308 is sufficient for Akt kinase activity, but the Ser473 site is necessary for "full activation" (Hietakangas and Cohen, 2006). For example, regulation of FoxO1,3 and 4 by Akt requires the presence of phosphate groups on both Ser473 and Thr308. Studies in *Drosophila* mutants with impaired mTORC2 function show lowered levels Akt signaling and present with a minor growth defect of approximately 10% reduction in mass (Hietakangas and Cohen, 2006). Interestingly, the same homozygous mutation in mice, deletion of *Rictor*, an essential component of mTORC2, leads to embryonic lethality, suggesting either a greater requirement for maximal Akt signaling or other roles of the Ser473 phosphate group in mammalian development (Hietakangas and Cohen, 2006). Finally, recent studies demonstrate that the presence of a phosphate group on Ser473 may promote the Thr308 phosphorylation

event, adding another layer of complexity to the regulation of Akt activity (Das et al, 2016).

Once Akt is activated at the cell membrane, it targets and phosphorylates many substrates involved in the control of cell growth. One major target of Akt is TSC2, which is phosphorylated at the surface of the lysosome, releasing the TSC1/2 complex from the lysosomal membrane and disinhibiting Ras homology enriched in brain (Rheb) GTPase (Buel and Blenis, 2016; Shimobayashi and Hall, 2016). Free Rheb is responsible for activating the mTOR kinase by interacting with its catalytic domain and leading to the formation of mTOR complex 1 (mTORC1), which stimulates protein synthesis, cell growth and cell survival (Garami et al, 2003; Shimobayashi and Hall, 2016). PI3K and Akt are two of five downstream effectors of IGF-like receptors, the others being Ras, Raf, and Src. However, PI3K/Akt is the only signaling cascade that is sufficient to block apoptosis. Akt phosphorylates and inhibits pro-apoptotic transcription factors FoxO1, FoxO3, and FoxO4, indirectly inhibiting other pro-apoptotic transcription factors including BAD and p53 (Downward, 2004; Kennedy et al, 1997). Finally, Akt modulates glycogen metabolism in the cells by inhibiting GSK3 and promoting glycogen synthesis (Downward, 2004; Cortes-Vieyra et al, 2015).

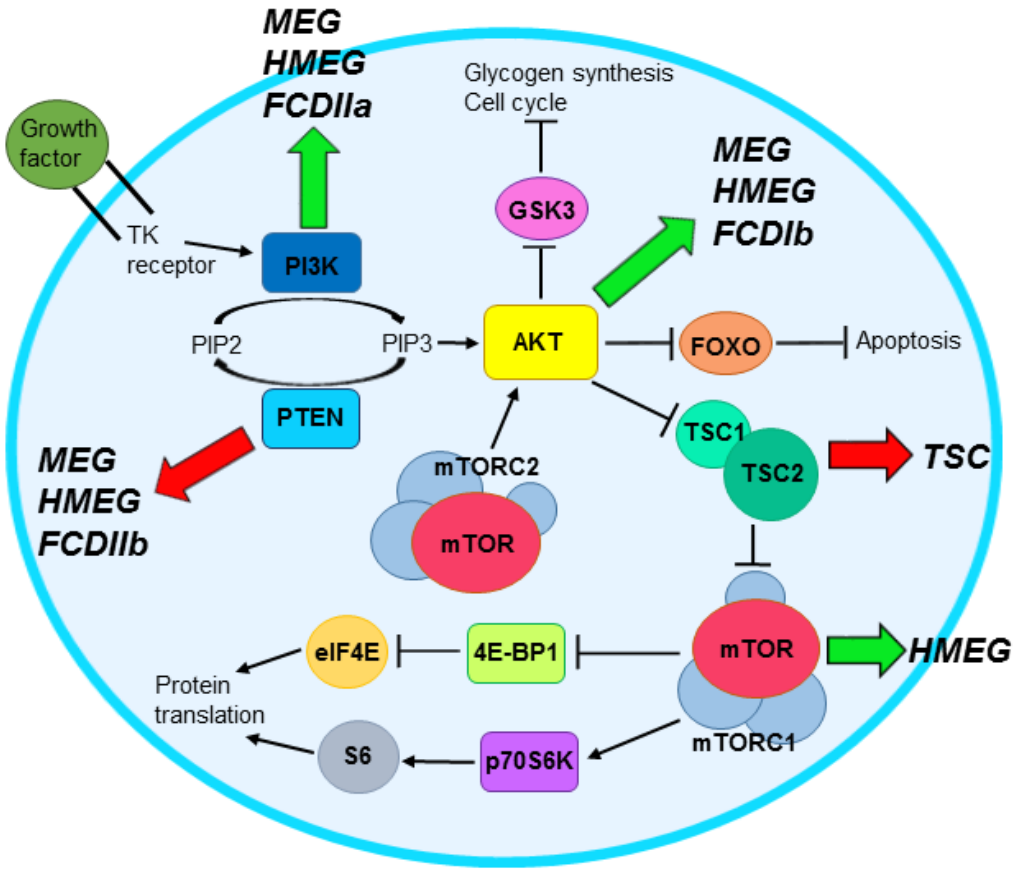

Figure 1. Simple schematic of the PI3K/Akt/mTOR pathway. Thin black arrows (→) signify activation, while thin black lines (--|) signify inhibition. Large red arrows indicate that inactivating mutations of the protein lead to the diseases listed, while large green arrows indicate activating mutations lead to diseases.

1.4 Tsc1/2

TSC1 and *TSC2* were first identified as genes mutated in patients with tuberous sclerosis complex, a disorder discussed in detail in section 4 of the Introduction. *TSC1* encodes a 130kDa protein called hamartin (Inoki et al, 2002). Although structural analysis reveals no putative catalytic domains in hamartin, the amino acid sequence does suggest a transmembrane domain (Tee et al, 2003). Since mutations in the *TSC1*

gene yield the same disease phenotypes as *TSC2* and homozygous deletion of either gene leads to embryonic lethality in mice and rats, it was suggested early on that the two proteins work in a complex. *TSC2* encodes the 200kDa tuberin, which has a C-terminal GTPase activating protein (GAP) domain and GAP activity, promoting GTP hydrolysis (Tee et al, 2003; Ma et al, 2005). Studies have now confirmed that hamartin and tuberin indeed function as a complex, with tuberin as the catalytic subunit and hamartin in a regulatory role, to promote GTP hydrolysis to GDP on Rheb, thereby inhibiting its ability to activate mTOR. This inhibition occurs at the lysosomal membrane (Garami et al, 2003; Inoki et al, 2003; Shimobayashi and Hall, 2016). When Akt phosphorylates Tsc2, Tsc1 and 2 dissociate, releasing Rheb. Akt-mediated phosphorylation on Tsc2 also downregulates its GAP activity and primes it for ubiquitination (Inoki et al, 2002). Other than Pten, Tsc1/2 is the major negative effector of the mTOR pathway. Loss of Tsc1/2 function leads to hyperactivity of mTORC1 effector S6 kinase (S6K), while overexpression suppresses it (Tee et al, 2003). Therefore, Tsc1/2 works to counteract insulin and growth factor-mediated PI3K/Akt signaling and downregulates protein synthesis and cell growth.

Other pathways beside PI3K/Akt can modulate Tsc1/2 function. Tsc1/2 activity is stimulated by high AMP:ATP ratio, i.e. low available cell energy, and integrates signals from several major cellular pathways. Both Tsc1 and Tsc2 are targeted with activating phosphorylation by GSK3 and 5'-activated protein kinase (AMPK) during high AMP:ATP conditions to conserve cell energy spent on mTORC1-mediated protein synthesis. A proposed mechanism by Inoki et al, 2006, is that the AMPK-mediated phosphorylation primes Tsc2 for the GSK3-mediated addition of a phosphate group for maximum Tsc2 GAP domain activity and thereby optimal mTORC1 inhibition (Ma et al, 2005; Inoki et al, 2006; Shimobayashi and Hall, 2016). Finally, cross-talk with the Ras- extracellular signal-regulated kinases (Erk) cascade allows Tsc1/2 to incorporate signals from

transcription regulation into protein synthesis activity. Erk itself negatively regulates Tsc2 by phosphorylation, causing it to dissociate from Tsc1 and the lysosomal membrane (Ma et al, 2005).

1.5 mTOR

mTOR is a major regulator of protein synthesis, and therefore of cellular growth, repair and survival. In neurons, mTOR mediates both global and local protein translation, modulating overall cell growth as well as synapse dynamics such as plasticity (Kwon et al, 2006). The evolutionarily conserved Serine/Threonine kinase was first identified in a rapamycin-insensitive yeast strain as the specific target of the drug (Kafferkey et al, 1993; Edinger et al, 2003; Coffey et al, 2016). mTOR is a 289kDa PI3K-related protein kinase (PIKK) with two lobes, one on the N- and one on the C-terminus, connected by an ATP-binding domain (Yang et al, 2013). The N-terminal lobe contains the FK506 binding protein 12 (FKPB12)-rapamycin binding domain (FRB), where the mTORC1 inhibitory complex of FKBP12 and rapamycin interact to disrupt kinase activity (Sarbassov et al, 2006; Yang et al, 2013).

The mTOR kinase can form one of two complexes, mTOR complex 1 or 2 (mTORC1 and mTORC2). mTORC1 forms downstream of Rheb activation and is nucleated by two mTOR molecules held together by the protein regulatory-associated protein of mTOR (Raptor). Raptor is proposed to both stabilize the mTOR dimer and regulate substrate access to the catalytic domain deep within the mTORC1 structure (Edinger et al, 2003; Buel and Blenis, 2016). Another important subunit of mTORC1 is FKBP12, which is responsible for mTORC1's rapamycin sensitivity. Rapamycin complexes with FKBP12 and binds free mTOR and the FRB. While this event does not prevent the interaction between mTOR and Raptor, the presence of rapamycin weakens it to the point of almost completely inhibiting all mTORC1 activity (Sarbassov et al, 2006). mTORC1 signals downstream of Akt, Erk and Wnt pathways by inducing protein

synthesis through two different phosphorylation events: the activation of S6K and inhibition of eukaryotic initiation factor 4E (eIF4E)-binding protein (4EBP). S6K activates ribosomal protein S6, allowing for ribosomal assembly and protein translation. After mTORC1-mediated phosphorylation, 4EBP releases eIF4E, allowing it to complex with eIF4F and initiate protein translation (Bhattacharya et al, 2015; Coffey et al, 2016, Wang et al, 2016). Levels of phosphorylation of S6K, ribosomal protein S6 and 4EBP are all used as reliable readouts of mTORC1 activity across a variety of tissues and organisms (Bhattacharya et al, 2015). It is important to note that only S6K and S6 activation are fully rapamycin-sensitive, while the phosphorylation of 4EBP is only partially responsive to rapamycin treatment (Edinger et al, 2003). S6K further mediates a negative feedback loop by phosphorylating mTOR at Serine 2448, inhibiting its kinase activity (Coffey et al, 2016). Finally, mTORC1 negatively regulates lysosome-mediated protein and organelle degradation, called autophagy, by inhibitory phosphorylation of autophagy-related protein 13 (Atg13) and Unc51-like autophagy-activating kinase (Ulk) 1 and 2 and preventing formation of the phagosome (McMahon et al, 2012; Coffey et al, 2016). Depending on the cell type, prolonged suppression of mTORC1 can lead to either induction, suppression or no effect on Akt signaling activity (Sarbassov et al, 2006; Karisson et al, 2015). Since many neurodegenerative diseases, including Alzheimer's disease (AD), ASD, Fragile X syndrome (FXS) and epilepsy, can be traced back to improper protein translation and/or degradation, the mTORC1 signaling cascade is a central focus of study for researchers of those diseases (Bhattacharya et al, 2015).

While mTORC1's effects on cell growth, metabolism and glucose homeostasis have been studied extensively, mTORC2's roles in the cell have remained more elusive. mTORC2 is the Raptor-independent, rapamycin-insensitive complex, held together by the rapamycin-insensitive companion of mTOR (Rictor) and is heavily involved in cell survival through Akt and cytoskeletal dynamics through Protein Kinase C 1 (Sarbassov

et al, 2004; Karisson et al, 2015). Structurally, Rictor appears to play a similar role in mTORC2 as Raptor in mTORC1 (Buel and Blenis, 2016). mTORC2 activity correlates with insulin signaling, and is responsible for phosphorylating Serine 473 of Akt's hydrophobic motif and Threonine 450 of Akt's turn motif (Sarbassov et al, 2006; Shin et al, 2011).

1.6 Available inhibitors

Due to the PI3K/Akt/mTOR pathway's heavy involvement in tumorigenesis and progression, finding clinically safe inhibitors for various proteins in this signaling cascade has been at the forefront of cancer research for decades. The standard drug of choice for any PI3K/Akt/mTOR related disorder, rapamycin (also called sirolimus), was initially studied heavily because of its ability to extend the lifespan of yeast, *C. elegans, D. melanogaster* and even mice and rats (Baar et al, 2015; Coffey et al, 2016). Once rapamycin's method of action through specific, reversible suppression of mTORC1 was elucidated, the drug underwent FDA approval and became widely used as an immunosuppressant in transplant patients in order to prevent organ rejection (Kahan, 1992; Edinger et al, 2003; Sarbassov et al, 2006; Zeng et al, 2009; Cardamone et al, 2014). Rapamycin has varying effects on mTORC2 signaling, which are predominantly cell type- and time-dependent. For example, brief and acute treatments with rapamycin almost always have no effects on mTORC2 and Akt activity. However, prolonged treatments in some cells can cause either a hyperactivation of Akt via mTORC2-dependent Ser473 phosphorylation, a dampening of the Akt and mTORC2 signal, or no effect at all. It is generally thought that when rapamycin does perturb mTORC2 activity, it accomplishes it by binding so much free mTOR that it sequesters it away from the mTORC2 complex (Sarbassov et al, 2006; Wang et al, 2016).

Unfortunately, rapamycin has led to multiple negative effects in human patients including rare but acute pulmonary disease (Jimenez et al, 2006; Das et al, 2007),

disturbance of glucose homeostasis and increased risk for diabetes (Johnston et al, 2008; Shum et al, 2016), and strong immunosuppression. Research has therefore shifted into trying to identify three main categories of alternatives to rapamycin: analogous mTORC1-specific inhibitors (rapalogs); inhibitors that target global mTOR by competing with ATP for the active pocket; and finally, compounds that antagonize other components of the PI3K/Akt/mTOR pathway (Muddassar et al, 2008; Ewald et al, 2015; Coffey et al, 2016; Shum et al, 2016).

Two prominent drugs that have recently emerged as potentially clinically safe are Akt inhibitor MK-2206 and rapalog RAD001 (Everolimus). Both have undergone multiple Phase II clinical trials for various cancers and have proceeded into Phase III (Mego et al, 2015; Oki et al, 2015; Rugo et al, 2016). Furthermore, both are highly soluble and can be delivered orally, which have long been two drawbacks to rapamycin treatment schemes (Oki et al, 2015; Rugo et al, 2016). Akt inhibitors can target the ATP binding site of Akt, an adjacent allosteric pocket or both (Muddassar et al, 2008). MK-2206 is the first allosteric inhibitor to show both high efficacy in Akt activity suppression and satisfactory safety in preclinical development (Oki et al, 2015). In cell lines, MK-2206 prevented proliferation and Akt/mTORC1 signaling, and suppressed tumor growth *in vivo* (Oki et al, 2015). MK-2206 is tolerated by humans with minimal side effects at doses of up to 60mg administered every other day, but can be given at higher dosages if the frequency of administration is decreased (Hirai et al, 2010; Yap et al, 2011; Oki et al, 2015). RAD001 has similar effects on mTORC1 activity to rapamycin. It is currently being used to treat solid tumors and TSC in clinical studies, and is the only mTOR inhibitor currently performing well in trials (Lee et al, 2015; Rugo et al, 2016). Side effects of RAD001 are mostly limited to inflammation of oral mucous membranes. Importantly, patients carrying certain somatic mutations experience increased sensitivity to RAD001 with improved tumor remission outcomes, paving the way for RAD001-based

personalized medicine (Iyer et al, 2012; Rugo et al, 2016). Since 2015, RAD001 has officially been approved for use on late-stage HER2-negative breast cancer patients (Lee et al, 2015).

2. Traumatic Brain Injury

Traumatic brain injury (TBI) is a leading cause of death for US residents under the age of 45 and the main cause of disability in children and young adults (Don et al, 2012; Zhou et al, 2012). Furthermore, blast-induced brain injury incidence has increased in recent years due to military conflict and the escalated use of homemade explosive devices in terrorist attacks (Okie, 2005). Survivors of TBI can develop depression, cognitive disturbances, motor issues, epilepsy and memory disorders days or months after the trauma (Zhou et al, 2012; Guo et al, 2013; Park et al, 2013). There is even evidence that blast-induced TBI may contribute to the physiological mechanisms behind post-traumatic stress disorder (Elder et al, 2015). The initial mechanical trauma causes physical damage and cell death referred to as primary damage and it is not preventable. Secondary damage includes a complex cell- and molecule-mediated inflammatory response, edema, increased intracranial pressure, vasospasm and hemorrhages (Erlich et al, 2007; Woodcock and Morganti-Kossmann, 2013; Chen et al, 2014; Elder et al, 2015). Furthermore, an immediate release of glutamate and other excitatory amino acids into the surrounding tissues of the cortex and hippocampus leads to excitotoxic cell death (Rose et al, 2002). Necrotic and apoptotic cell degenerations peak at around 24 hours post-TBI, and can continue to progress for days or months following the injury (Erlich et al, 2007; Zhou et al, 2012). Finally, TBI increases the risk of and exacerbates the effects of dementias such as Alzheimer's (Webster et al, 2015). Repetitive TBI is outside the scope of this study, but it is important to note that even mild concussions have additive negative effects on the brain (Xu et al, 2015).

2.1 Models of TBI

Current models for studying the physiological and molecular consequences of TBI have focused on small rodents such as rats and mice, and larger mammals like swine (Browne et al, 2011; Panzer et al, 2012). Methods of administrating brain injury have evolved from a simple weight drop model to more sophisticated procedures, becoming more precise and programmable (Erdman et al, 2011). TBI in rodents can be closed-head injury (CHI), meant to mimic concussions and blast-induced injury, or open and administered directly to the cortical surface (Panzer et al, 2012; Zhu et al, 2014). Other methods for modeling injury use air waves from controlled explosions, which pair wave transmission through the tissue with rotational acceleration of the head (Don et al, 2012; Elder et al, 2015). Even mild, closed-head injury with minimal cell death results in glial and microglial activation and induction of the same pathways as more severe, open-head traumas (Zhu et al, 2014). The magnitude of injury is generally classified into “mild”, “moderate” and “severe” categories, although the parameters for each vary depending on the TBI model used (Don et al, 2012).

Currently, the two predominant methods for open-head injury are controlled cortical impact (CCI), administered by pneumatic cylinder through a craniotomy in the skull, and fluid percussion (FP), which uses fluid displacement under pressure onto the brain surface to mimic shockwave effects (Faden et al, 1989; Dixon et al, 2010; Erdman et al, 2011). Both methods require anesthesia and the drilling of a craniotomy to expose the cortical surface. This added treatment necessitates that researchers control for the effects of the sedative and the surgery, but at the same time allows for very tight control on pressure and severity of the impact and thus increases the reproducibility of experimental procedure (Thompson et al, 2005; Dixon et al, 2010; Erdman et al, 2011). Furthermore, TBI caused by either method in rats and mice results in physical,

behavioral and neurological symptoms that are similar to those observed in human patients, such as seizures, apnea and impaired motor function (Thompson et al, 2005; Erdman et al, 2011). Despite the fact that mechanical damage usually targets the cortex, it is the dentate gyrus of the hippocampus that is most vulnerable and sensitive to TBI. It experiences increased cell loss of immature neurons early on after the injury, despite not being directly subjected to the mechanical impact (Gao et al, 2008; Zhou et al, 2012).

Finally, TBI can be studied *in vitro* using cultured neurons on a flexible surface such as a membrane or specially designed plates, which can be subjected to a stretch of calculable force. This method generates forces of stretch and displacement upon the cultured neural network and can elicit some of the effects of TBI *in vitro*, including cell death and altered electrical excitability, and which vary in response to the severity of the stretch injury (Choi et al, 1987; Panzer et al, 2012; Zhou et al, 2012; Liu et al, 2013).

2.2 TBI sequelae and potential treatments

Studies into TBI, brain lesions and the effects of glutamate excitotoxicity have all shown that brain trauma leads to an early release of glutamate and aspartate into the tissue, leading to a sufficiently high and prolonged increase of excitatory amino acids in the cerebrospinal fluid to cause excitotoxicity (Choi et al, 1987; Faden et al, 1989; Rose et al, 2002). These findings indicate that neurons untouched by the mechanical force of the injury can undergo cell death as a result of these secondary effects. Furthermore, the brain tissue's attempt to repair itself stimulates synaptogenesis and loss of glutamate receptors at the synapse, leading to a remodeling of the neuronal network that may be responsible for symptoms such as posttraumatic epilepsy in survivors and animal models (Park et al, 2013; Andersen et al, 2014). Unfortunately, clinical trials have shown no improvement in recovery after TBI from administration glutamate receptor blockers in human patients (Don et al, 2012). This inefficacy may be due to a number of reasons, one of which is that the therapeutic window for preventing initiation of excitotoxicity may

be too short and too close to the injury time to be a viable drug target. Timing studies of cell loss and inflammation indicate that these processes peak at around 24 hours of initial brain injury, allowing for a more realistic therapeutic window of treatment (Zhou et al, 2012; Elder et al, 2015).

Other studies have focused on the inflammation aspect of TBI. This response is mediated by the JAK/STAT pathway, activated glia and microglia, invading neutrophils, and release of cytokines (Lloyd et al, 2008; Don et al, 2012; Chen et al, 2014; Calikoglu et al, 2015). The density of microglia and astrocytes is increased in the injured brain, and levels of GFAP and various cytokines are elevated in the serum and cerebrospinal fluid of both animal models and human patients. These include, but are not limited to, major cytokines such as the pro-inflammatory Tumor Necrosis Factor (TNF) and interleukin-1β (IL-1β) and anti-inflammatory interleukin-10 (IL-10) (Woodcock and Morganti-Kossmann, 2013). These molecules have different expression timelines, the earliest of which is approximately 3-4 hours post-TBI. Similar to activated astrocytes and microglia, most cytokines are elevated at around 24 hours post-TBI, and some can stay elevated for days or months (Erlich et al, 2007; Park et al, 2013; Elder et al, 2015). Researchers are seeking treatments that can reduce the number of activated glial cells in the brain and return cytokine levels in the CSF back to normal (Elder et al, 2015). Furthermore, the variety and scope of TBI is wide and complex, scientists are hoping to characterize a panel of molecules that can be probed for in serum or CSF that will help predict the types of damage in a patient's brain, and allow for a more personalized pharmacological treatment of the injury (Woodcock and Morganti-Kossmann, 2013). In animal models, experiments with traditional and non-traditional anti-inflammatory drugs that successfully reduce the number of activated glia and cytokine levels have also led to improvements in neuronal loss, cerebral edema, and cognitive and behavioral performance (Lloyd et al,

2008; Chen et al, 2014; Calikoglu et al, 2015). However, no drugs have yet shown beneficial effects in human patients.

In recent years, the involvement of another signaling pathway has come under scrutiny. Depending on the severity of the injury, induction of the PI3K/Akt/mTOR pathway has been reported as early as 15 minutes post-TBI in the surrounding tissue, and was shown to remain elevated for up to 24 hours after the injury (Chen et al, 2007). This induction appears to be confined to the injured (ipsilateral or lesion-side) hippocampus and cerebral cortex and is not observed in the intact (contralateral) hemisphere of the brain (Chen et al, 2007; Park et al, 2012). Phosphorylation of mTORC1 downstream target S6 was observed in the cerebral cortex, and the CA1, CA3 and dentate gyrus regions of the hippocampus at time points between 15 minutes at 24 hours, while mTORC2-dependent phosphorylation of Akt at Serine 473 was observed only at 4 hours post-TBI (Chen et al, 2007; Zhao et al, 2012). Phosphorylation of the Akt target GSK3beta reached significant levels at 24-72 hours post-TBI (Zhao et al, 2012). Induced levels of phospho-AktS and phospho-GSK3beta however did not appear nearly as robust as those of phospho-S6. These data suggest a preferential induction of mTORC1 signaling as a result of TBI, and a modest involvement of mTORC2. Studies manipulating the PI3K/Akt/mTOR pathway after TBI have yielded conflicting results, possibly due to differential treatment doses and timing. Dual inhibition of Akt and mTORC1, beginning immediately prior to CCI, led to improvements in learning and memory performance in the Morris Water Maze test, and reduced cell death, but had no effects on inflammation. However, Akt or mTORC1 inhibition individually was not reported to yield any beneficial effects (Park et al, 2012). A similar study using the closed-head injury (CHI) of TBI found that mTORC1 inhibition with rapamycin immediately prior to injury actually worsened Morris Water Maze performance in rodents (Zhu et al, 2014). These results are in stark contrast with previous findings that a single

injection of rapamycin 4 hours after CHI reduced cell loss and microglia-mediated inflammation, and improved neurologic scores (Erlich et al, 2007). Repeated treatments with inhibitors yielded even more conflicting results. Increased Akt signaling via a 14-day long post-TBI treatment with Simvastatin, led to improved Morris Water Maze (MWM) performance, suggesting that the pathway is beneficial for recovery (Wu et al, 2008; Rozas et al, 2014). However, a 4-week long treatment with rapamycin that inhibits mTORC1 signaling, beginning 1 hour post-CCI also appeared to be beneficial, causing a reduction of cell loss and posttraumatic epilepsy in mice (Guo et al, 2013). Taken together, these studies indicate that the timing of intervention, and the modulation of specific components of the PI3K/Akt/mTOR pathway may influence recovery from TBI. It is therefore important to conduct further studies aimed at identifying the simplest treatment that confers maximum benefits with the minimal amount of detrimental effects.

3. Somatic brain overgrowth disorders

Brain overgrowth disorders include a range of developmental cortical malformations such as focal cortical dysplasia (FCDIIa and IIb), hemimegalencephaly (HMEG) and megalencephaly (MEG), which often present with medically intractable pediatric epilepsy (Jansen et al, 2015; Roy et al, 2015). The seizures that accompany these disorders do not respond to available anticonvulsant drugs. If epilepsy cannot be managed, the only effective treatment is surgical resection of the seizure foci or full hemispherectomy (Ljungberg et al, 2006; D'Arcangelo, 2009; Hu et al, 2015; Jansen et al, 2015). FCD is determined to be the underlying cause of intractable epilepsy in more than 60% of surgical candidates under age 16 (Kloss et al, 2002). This disorder is characterized by a localized disruption of the cortex with enlarged and irregular cells that become or produce a nearby seizure focus. The focal malformation can sometimes be identified by magnetic resonance imaging (MRI) prior to surgery, and the FCD diagnosis is based on the neuropathological examination of the brain biopsy after surgery (Hu et

al, 2015). The seizure foci can occur on one or both hemispheres, or affect an entire hemisphere in the case of HMEG. Both FCD and HMEG can necessitate full hemispherectomy (Hu et al, 2015). Furthermore, 15-37% of FCD seizure foci are undetectable by MRI, and only 60-70% of patients receiving hemispherectomy or other epilepsy surgery end up seizure-free or achieve good seizure control (Kloss et al, 2002; Hu et al, 2015). Since surgery in children and infants as young as several months and has numerous negative side effects on neurological function, there is a critical need to develop less invasive and more effective treatments for epilepsy associated with cortical malformations.

Brain tissue removed during epilepsy surgery has long been used as research and diagnostic material (D'Arcangelo, 2009). Studies performed on brain biopsy tissue have yielded insights into the underlying mechanisms of intractable childhood epilepsy. Two main types of irregular cells are used to diagnose FCD in seizure foci: balloon cells and dysmorphic neurons. Balloon cells, also known as neuroglial cells, have enlarged, distinguishable cellular morphology and express markers for both neurons and astrocytes, suggesting a differentiation defect (Ljungberg et al, 2006; D'Arcangelo, 2009; Yasin et al, 2013). Their exact origin is not currently known, although they seem to be related to neuronal precursors. These cells show increased mTORC1 signaling and disrupted autophagy, including prominent lysosomes and accumulation of autophagy cargo proteins (Yasin et al, 2013; Liu et al, 2014). Absence or presence of balloon cells determines the type of FCD (IIa and IIb, respectively) (Kloss et al, 2002; Palmini et al, 2004; D'Arcangelo, 2009). Dysmorphic, or dysplastic, neurons have neuronal morphology but are hypertrophic and hyperexcitable (Ljungberg et al, 2006). Since the PI3K/Akt/mTOR pathway is a major inducer of cellular growth, its dysregulation has been heavily investigated as a potential underlying mechanism for the hypertrophy in cortical malformation patients. Studies identified increased levels of phospho-S6, a

major downstream effector of mTORC1, in irregular cells of seizure foci in humans (Ljungberg et al, 2006; Liu et al, 2014). Furthermore, genetic studies have identified a high incidence of mutations in Pten, PI3K, or Akt in HMEG, FCD and dysplastic megalencephaly (DMEG) patients that are predicted to increase signaling through the pathway (Poduri et al, 2012; Jansen et al, 2015). These results have led researchers to focus on the PI3K/Akt/mTOR signaling cascade as a potential drug target in brain overgrowth disorders.

3.1 Rodent models of brain overgrowth disorders

Currently, researchers use a variety of genetic, chemical and lesion tools to induce brain cortical malformations in rodent brains. The freeze lesion model, which yields results potentially relevant to TBI as well, generates tissue disruption and network changes in the neurons surrounding the lesion. While rodents do not present with spontaneous seizures, area around the injury displays epileptiform activity and increased excitability (Albertson et al, 2011). This model induces increased synaptogenesis, which is potentially driven by an astrocytic response to the lesion. Hyperexcitability is improved when treated with gabapentin, which counteracts synaptogenesis, but is unresponsive to other common anticonvulsants (Andersen et al, 2014).

Embryonic administration of BCNU to rats is a chemical tool, which uses induced cell death to mimic disruption and thinning of cell body layers in the brain (Inverardi et al, 2013). However, this model leads to decreased hippocampal volume and does not replicate the dysmorphic nature of cell bodies in cortical dysplasia. Postnatal deletion of autophagy regulator Atg7 in mice also leads to spontaneous seizures, suggesting that autophagy downstream of mTOR contributes to epileptogenesis (McMahon et al, 2012). This finding suggests that although balloon cells are electrically inert, their mTORC1-driven defects may contribute to epilepsy caused by cortical malformations (D'Arcangelo, 2009).

Cre Promoter	Group	Phenotype
NEX (neuronal basic helix-loop-helix protein) Expresses starting at E11.5 in forebrain excitatory neurons	Kazdoba et al, 2012	Megalencephaly Hypertrophic neurons Premature death (within days of birth)
GFAP (Neuronal-Specific) Expressed in a subset of neuronal cells starting at E13.5	Ljungberg et al, 2009	Macrocephaly Hypertrophic neurons Epileptiform activity Seizures
Nse (neuron-specific enolase) Expressed in mature forebrain neurons; starting at 2 weeks of age	Kwon et al, 2006	Macrocephaly Hypertrophic neurons Impaired social interactions
CaMKiiα (Calmodulin Kinase iiα) Expressed in forebrain excitatory neurons starting after 16 days of age	Sperow et al, 2012	No neuronal hypertrophy Deficits in learning, memory and synaptic plasticity Death starting at 8 weeks of age

Table 1. Examples of different severities of phenotypes stemming from *Pten* gene deletion at different time points of development and in different populations of neurons.

Genetic manipulation of the PI3K/Akt/mTOR pathway removes some of the confounding variables that can occur with chemical or lesion models. As Pten is the main upstream suppressor of the mTOR pathway, its inactivation or deletion reproduces the increased PI3K/Akt/mTOR signal in balloon cells and dysmorphic neurons. A panel

of Pten conditional knockout mice has been generated by several laboratories, revealing differences and similarities among various developmental gene deletion strategies. Complete deletion of Pten is embryonically lethal in mice and rats, rendering the production of conditional knockouts necessary, and also prompting the analysis of heterozygous or hypomorphic mutants (Backman et al, 2001; Kazdoba et al, 2012). Oligodendrocyte-specific, excitatory neuron-specific or neuronal subset-specific *Pten* knockouts all present with macrocephaly, seizures, ataxia, and premature death. Brains of these mice reveal hypertrophy of neuronal cell bodies, increased dendritic branching, spine density, and defective synapses (Backman et al, 2001; Fraser et al, 2008; Ljungberg et al, 2009; Kazdoba et al, 2012). Severity of symptoms increases with earlier onset of Pten deletion and higher percentages of the affected neuronal population. Consequently, a late-onset knockout driven by CaMKIIa-Cre starting at postnatal day 16 in excitatory neurons led to variablel effects on neuronal soma size, even though electrophysiological properties were disrupted (Sperow et al, 2012).

3.2 NEX-Pten mouse line

One of the most severe *Pten* mutant mouse models is the NEX-*Pten* line, created and characterized at the D'Arcangelo lab by Tatiana M. Kazdoba, PhD. The mutation is made using the Cre-loxP strategy whereby the *Pten* gene, flanked by loxP sites, is deleted by Cre recombinase expressed under the control of the NEX promoter. This promoter begins to be active around embryonic day 11.5 in virtually the entire population of cortical and hippocampal excitatory neurons, resulting in the ablation of *Pten* in all these neurons (Kazdoba et al, 2012). Wildtype and heterozygous pups show normal levels of PI3K/Akt/mTOR activity, as well as normal neuronal size and survival. Knockout pups rarely survive past postnatal day 0 or 1, are severely underweight, and have increased brain weights as compared to wildtype or heterozygous littermates (Kazdoba et al, 2012). The widespread *Pten* deletion in the forebrain allows us to generate fairly

homogeneous knockout neuronal cultures, which can be used to assess the effectiveness of drug treatments on soma size and electrical activity *in vitro*.

3.3 Evidence for drug alternatives to surgery

Several studies suggest that the hypertrophic neuronal phenotype and epilepsy of brain overgrowth disorders is reversible and treatable. *In vitro*, transfection of Pten-deficient neurons with the wildtype *Pten* gene leads to recovery of normal soma size and spine density (Spinelli et al, 2014). Furthermore, long term treatment with mTORC1 inhibitor Rapamycin or RNAi knockdown of mTOR or Akt lead to reduction in soma size and dendritic branching (Jaworski et al, 2005). Epileptic seizures in mice with activating mutations in PI3K can be suppressed within an hour of administering PI3K inhibitor BKM120 (Roy et al, 2015). Rapamycin treatment *in vivo* can counteract effects of deletion of Pten in mice, such as macrocephaly, epileptiform activity, reduced life span, and increased neuronal soma size (Ljungberg et al, 2009; Zhou et al, 2009; Sunnen et al, 2011; Kazdoba et al, 2012). Thus, further studies should lead to the identification of effective pharmacological treatments for brain overgrowth syndromes.

4. Tuberous Sclerosis Complex – a hereditary brain overgrowth disorder

Tuberous Sclerosis Complex (TSC) is a hereditary, autosomal dominant disease with high penetrance (Napolioni et al, 2009). TSC has many symptoms in common with somatic brain overgrowth disorders, including intellectual disability, ASD, and intractable epilepsy (Inoki et al, 2002; Tee et al, 2003; Tsai et al, 2012). Other common symptoms include benign tumors, called hamartomas, in many tissues such as the skin, kidneys, eyes and brain (Tavazoie et al, 2005; Kwon et al, 2006; Moavero et al, 2015). Approximately 1 in 6000 babies is born with TSC (Ma et al, 2005). The disorder is caused by Tsc1/2 hemizygosity due to inactivating mutations in *TSC1* or *TSC2*, both of which have gene-dosage effects in mice and humans (Garami et al 2003; Tavazoie et al, 2005). Loss of heterozygosity is believed to occur in some cells within hamartomas,

which in the brain are known as cortical tubers. This results in the production of a limited number of homozygous null cells, which may profoundly affect the surrounding heterozygous tissue. TSC presents with a wide range of symptoms and severity levels, depending on the type and location of the mutation. Generally, mutations that prevent the Tsc2 GAP domain activity or translation present with the most debilitating forms of TSC and earliest onset of symptoms (Garami et al, 2003; Tee et al, 2003; Napolioni et al, 2009). Overall, mutations in *TSC1* and *TSC2* have equal frequencies in inherited TSC, while mutations in *TSC2* appear to be responsible for over 80% of sporadic TSC cases (Napolioni et al, 2009). Furthermore, 20-30% of TSC patients have no detectable mutations in either gene (Inoki et al, 2002; Garami et al 2003; Moavero 2015). In this subset of patients, TSC is diagnosed solely based on symptoms, although several potential alternative mechanisms have been proposed, including Rheb mutations and excess Erk activation (Garami et al 2003; Ma et al 2005).

Tsc1 and *Tsc2* are homozygous lethal in mice, restricting studies to heterozygous animals and conditional knockouts. Currently, many such mouse models exist and are being studied. Research into conditional knockouts has yielded pieces of the TSC puzzle, such as that homozygous deletion of *Tsc1* or *Tsc2* in either neurons or in oligodendrocytes leads to myelination defects in the brain (Meikle et al, 2007; Carson et al, 2015). Excitatory neuron-specific and astroglial-specific Tsc2 knockout mice have increased astrogliosis (Napolioni et al, 2009; Crowell et al, 2015). Other commonly observed phenotypes in TSC model rodents include seizures, learning deficits, impaired social interaction and shortened life span (Ehninger et al, 2008; Tsai et al, 2012; Crowell et al, 2015).

While conditional knockout mice generally present with TSC-like phenotypes, there is a need to understand whether heterozygous neurons are defective. Within the brain, TSC can present with various lesions and tumors, such as nodules, cortical tubers

and subependymal giant cell astrocytomas (SEGAs). The presence of dysmorphic neurons, giant cells and tumors in the brains of patients was for a long time explained by a loss of heterozygosity (LOH) of *TSC1* or *TSC2* in specific cells in the brain (Tsai and Sahin, 2011; Wong and Crino, 2012). However, human patient studies indicate rates of LOH in these lesions to be as low as low as 4% (Tee et al, 2003; Ma et al 2005; Tavazoie et al 2005). Therefore, either the hemizygous condition is sufficient for tumorigenesis and disease, or there are other associated mechanisms that drive cell enlargement, epileptogenesis, and network rearrangement in the brain. Studies of heterozygotes have shown to date that it is sufficient to delete one copy of *Tsc1* in the Purkinje cells of the cerebellum to cause cellular hypertrophy and social interaction deficits in mice (Tsai et al, 2012). Furthermore, homozygous Floxed*Tsc1* hippocampal neurons transfected with Cre in culture have enlarged somas and dendritic spines, as well as a higher density of spines (Tavazoie et al, 2005). Interestingly, in the former study rapamycin was able to rescue all phenotypes, while in the second study some spine size defects were unaffected by rapamycin. These findings suggest that TSC neurological defects may occur only partially through excess mTORC1 signaling, but other important mechanisms of disease remain to be elucidated.

5. Significance

The PI3K/Akt/mTOR pathway is highly conserved and plays major roles in neuronal growth and survival. While baseline levels of activity of this cascade are essential to normal development and function, excess signaling leads to deleterious effects to neurons in the brain. Activating mutations cause a range of pathologies including drug-resistant epilepsy, benign tumors and intellectual disability. Similarly, excess signaling following brain injury is associated with post-traumatic epilepsy and motor and behavioral disorders. Currently, both brain overgrowth disorders and traumatic brain injury patients have few pharmacological treatment options to ameliorate such

symptoms. The PI3K/Akt/mTOR pathway offers a list of potential drug targets, but no safe, effective inhibitors are available, none is FDA-approved for the treatment of these patients. Thus, there is an urgent need to investigate the potential of promising inhibitors in preclinical studies using animal models of TBI and brain overgrowth disorders..

CHAPTER 2: BENEFICIAL EFFECTS OF EARLY MTORC1 INHIBITION AFTER TRAUMATIC BRAIN INJURY

1. Introduction

Focus on the study of mild to severe traumatic brain injury (TBI) has increased in recent years and brought researchers' and clinicians' attention to the lack of available treatments for patients suffering from such injury. Even mild, closed-head trauma to the brain can lead to temporary or permanent neurological symptoms, including epileptic seizures, behavioral changes, and impaired motor and cognitive function (Okie, 2005; Merrit and Arnett, 2014; Kostyun et al, 2015). Negative consequences of TBI can arise due to a combination of direct neuronal tissue damage, inflammatory response, and secondary excitotoxic damage (Faden et al, 1987; Rose et al, 2002). However, spontaneous healing occurs and, in most cases, leads to at least a partial recovery of brain function. To optimize recovery, it is therefore critical to understand which TBI-induced molecular events contribute to damage of the neuronal tissue and which promote healing. Understanding the nature of these mechanisms and their time course of induction will then allow us to develop potential therapeutic approaches to minimize damage and facilitate functional recovery of the injured brain.

Research has so far identified three main signaling pathways that are modulated by TBI *in vivo*: the JAK-STAT, PI3K/Akt/mTOR and the MAPK pathways (Don et al, 2012). The focus of the present study is on the PI3K/Akt/mTOR pathway, which other groups have shown to be strongly induced *in vivo* post-TBI (Chen et al, 2007; Park et al, 2012). The PI3K/Akt/mTOR signaling pathway is a major player in the control of cell size, dendrite and axon outgrowth during brain development and repair (Fingar et al, 2002; Gong et al, 2006). Growth factors and hormones typically stimulate this pathway through the activation of receptor tyrosine kinases, leading to the activation of the PI3K

and downstream Akt, which in turn regulates the activity of many signaling molecules, including mTOR. This kinase forms two complexes, mTORC1 and mTORC2. mTORC1 activation specifically induces protein translation through activation of ribosomal protein S6Ks and disinhibition of the transcription initiation factor eIF4E through phosphorylation of the inhibitor 4EBP1 (Laplante and Sabatini, 2009). However, the role of this signaling pathway in TBI is controversial. Indeed studies have shown that both induction of PI3K activity by suppression of upstream inhibitor Pten and suppression of mTORC1 by the mTORC1-specific inhibitor rapamycin after TBI *in vivo* can have beneficial effects on recovery as measured by extent of tissue damage, motor function, neurological score, and learning and memory tasks in rodent models (Erlich et al, 2007; Wu et al, 2013). These findings raise the question of whether PI3K/Akt/mTOR induction plays a dual role in the TBI sequela, by affecting different cell types at different time points after injury.

To address this issue we examined the time course of PI3K/Akt/mTOR induction in the hippocampus after TBI in the whole tissue and at a cellular level, and discovered an early peak of mTORC1 activation that is specific to neurons. Furthermore, we investigated the role of early mTORC1 activity using a single systemic injection of rapamycin in the immediate aftermath of the injury. We reasoned that an early acute, short-term suppression of mTORC1 post-CCI best models the treatment a TBI victim might receive in an attempt to limit the extent of brain damage and promote recovery. We found that this simple treatment positively affects brain repair and promotes functional recovery, laying the foundation for further translational studies in TBI.

2. Methods

Controlled Cortical Impact (CCI), Drug Treatments, Morris Water Maze

These 3 procedures were performed by our collaborator Dr. David F. Meaney and his laboratory at University of Pennsylvania, and are described in full in Nikolaeva et al, 2015. Briefly, adult C57BL6 mice were anesthetized with isoflurane and

a 4-mm diameter craniotomy was produced on the left parietotemporal region of the skull with a trephine. A moderate CCI was produced at a velocity of 2.4m/s with an impact depth of 1.15mm, centering the impact at approximately -2.5mm bregma. In a control group (sham) animals were subjected to craniotomy, placed in the stereotaxic holder, but no CCI was delivered. At different time points after injury (1, 2, 4, 8, 24 hours or 7 days), animals were euthanized and processed for either immunohistochemistry or Western blot analysis. Drug treatment with rapamycin or vehicle (5% PEG, 5% Tween-80 in saline) were done by intraperitoneal injection at a dose of 1mg/kg of body weight. We selected this dose based on past studies (Erlich et al, 2007) and our preliminary dose-response studies. For immunohistochemistry, mice were transcardially perfused with 30 mL of ice-cold phosphate-buffered saline (PBS) (pH 7.4) and then with 40 mL of ice-cold 4% paraformaldehyde. Brains were harvested, post-fixed overnight in 4% paraformaldehyde at 4°C, and then cryoprotected in 24% sucrose. For Western blotting, brains were dissected and the hippocampi separated into lesion-side (L-side, experimental injury sample) and contralateral-side (C-side, internal control sample). The tissue was flash frozen in liquid nitrogen within 3 minutes of extraction for Western blot analysis. Cryoprotected brains for immunohistochemistry and Western blot were either shipped overnight by UPS or driven for 3 hours by staff from University of Pennsylvania to Dr. D'Arcangelo's laboratory Rutgers University, where they were stored at -80^{0}C until use. All experiments and animal housing were in accordance with procedures approved by the Animal Care and Use Committees at both University of Pennsylvania and Rutgers University, according to the National and Institutional Guidelines for Animal Care established by the National Institute of Health.

Western Blot Analysis

Hippocampal tissue was freshly dissected from the L-side and the C-side of the brain after CCI or sham injury, and lysed in RIPA buffer (50 mM Tris pH 7.4, 1% NP40,

0.25% sodium deoxycholate, 150 mM NaCl, 1nM EDTA supplemented with protease and phosphatase inhibitors). The tissue was homogenized and spun at 4^0C, at 3000 rcf for 5-7minutes to remove debris, and protein concentration was measured by a standard Bradford assay. Laemmli sample buffer was added to the lysates, and the samples were boiled for 3 minutes. Proteins (20 μg per sample) were separated by SDS-PAGE using 8.0% or 10.0% gels and transferred onto 0.2 μm nitrocellulose membrane at 4 ^{0}C in 20% methanol Tris-Glycine buffer for 2.5 hours at a constant 0.5 Amp. Membranes were blocked in 3% milk in TBS-T for 1 hour, and incubated in primary antibodies overnight at 4 ^{0}C. Membranes were then incubated for 1 hour in secondary HRP-conjugated antibodies, and subjected to ECL-Plus Western Blotting Detection System (Pierce/Thermo Fisher, Rockland, IL). Primary antibodies against phospho-ribosomal protein S6(Ser235/236) (pS6), phospho-Akt(Thr308) (pAktT), total Akt, and S6 were purchased from Cell Signaling, and anti-actin antibody was purchased from Millipore. All phosphorylated protein levels were normalized to the total amount of each protein. Quantification was performed using the band analysis function of Alpha Imager software (Protein Simple). For each condition, samples were analyzed from $n>3$ mice, average phosphorylated/total density values were calculated for each protein, and C-side values were set at 1. Statistical significance was calculated comparing L-side to C-side values using ANOVA and post-hoc Dunnett's test. A *p*-value of 0.05 or less was considered significant.

Immunofluorescence

Brains were frozen in a 30% sucrose/Cryo-OCT compound solution (30: 70 mixture; Fisher) and serially sectioned at 30-50 μm on a cryostat. Coronal slices were mounted directly on slides. Slides were thawed at room temperature, permeabilized in 0.1% Triton-X, and blocked in 5% normal goat serum (NGS). Slides were incubated with

primary antibody in 5% NGS in 0.1% Triton-X overnight at 4 ^{0}C. Slides were then washed in PBS, probed with fluorophore-conjugated secondary antibodies for 1 hour at room temperature, and mounted in Vectashield Mounting Medium with DAPI (Vector Laboratories). The following antibodies were used: fluorophore-conjugated AlexaFluor 488-anti-pS6 (Ser235/236) (1:250, Cell Signaling Technology), anti-GFAP (1:250, Cell Signaling Technology or 1:500, Dako), anti-NeuN (1:100, Millipore), and anti-Iba1 (1:250, Wako). Multiple sections from 3-4 mice per treatment were examined at each time point. Representative images were acquired using a Yokogawa CSU-10 spinning disk confocal head attached to an inverted fluorescence microscope (Olympus IX50), or an epifluorescence microscope (Olympus BX3-CBH). Positive cell counts were performed manually and in blind. Statistical significance in positive cell number was determined by the Student's *t*-test when only 2 datasets were compared, or by ANOVA and Dunnett's post-hoc analysis for more than 2 datasets. $p < 0.05$ was considered significant.

Fluoro-Jade B Staining

Slides were washed in PBS to remove OCT, then washed in TBS and dried. Dried tissue was serially washed in 1%NaOH and 80% Alcohol, 70% Alcohol, DI, 0.06% KMnO4, and DI. Slides were incubated in Fluoro Jade-B (FJB) staining solution (4%FJB, Millipore, in Acetic Acid) for 20 min. Slides were then washed in distilled water, dried, washed in Xylene and mounted in DPX (VWR). Representative images were acquired using a Yokogawa CSU-10 spinning disk confocal head attached to an inverted fluorescence microscope (Olympus IX50). Because FJB staining did not allow us to distinguish and count individual positive cells, an analysis of the fluorescence intensity was performed using ImageJ. Fluorescence analysis for hippocampal areas, such as dentate gyrus (DG) and CA3, was performed by measuring the Integrated Density of the cell body layer after subtracting the background (Area x Mean Gray Value of adjacent

background). Intensity values were normalized to the selected areas to obtain corrected total fluorescence values. Comparison between these values obtained from vehicle- versus rapamycin-treated brains was performed using the Student's *t*-test. $p < 0.05$ was considered significant.

Antibody	*Vendor*	*Catalogue#*	*Host*	*Dilution*	*Application*
pAkt(Thr308)	Cell Signaling	2965	Rb	1:1000	WB
pAkt(Ser473)	Cell Signaling	9271	Rb	1:1000	WB
Total Akt	Cell Signaling	4691	Rb	1:2000	WB
pmTOR(Ser2448)	Cell Signaling	2971	Rb	1:1000	WB
Total mTOR	Cell Signaling	2983	Rb	1:1000	WB
pS6K (Thr389)	Cell Signaling	9208	Rb	1:1000	WB
Total S6K	Cell Signaling	9202	Rb	1:1000	WB
pS6 (Ser235/236)	Cell Signaling	4858	Rb	1:1000	WB
Total S6	Cell Signaling	2317	M	1:1000	WB
488-pS6 (Ser235/236)	Cell Signaling	4803	Rb	1:1000	IF
MAP2	Covance	SMI-52R	M	1:250	IF
NeuN	Millipore	MAB377	M	1:100	IF
GFAP	Cell Signaling	3670	M	1:250	IF
Iba1	WAKO	019-19741	Rb	1:250	IF
GFAP	DAKO	Z 0334	Rb	1:250	IF

Table 2. Primary antibodies used in this study. WB= Western blot, IF=Immunofluorescence. Host: Rb=Rabbit, M=Mouse.

3. Results

Time course of CCI-induced PI3K/Akt/mTOR activity in the lesioned hippocampus

Adult C57Bl6 mice were subjected to moderate CCI or sham injury in Dr. Meaney's lab at U Penn and allowed to recover for 1, 2, 4, 8, 24 hours or 7 days before brain dissection. Frozen tissue was shipped to our lab at Rutgers for protein extraction and analysis. CCI caused extensive tissue damage to the cerebral cortex on lesion (L)-side of the brain, but the hippocampus was relatively spared (Fig. 2E). Therefore, the effect of the CCI injury on the PI3K/Akt/mTOR pathway was analyzed only in this tissue. No damage of the cerebral cortex or hippocampus in the contralateral (C)-side of the brain was observed (Fig. 2E). To minimize variability inherent the use of multiple mice and multiple blots, we measured signaling activity comparing L-side values to C-side values (set at 1) by Western blotting. Phospho-specific antibodies against pAktT (Thr308, a readout of PI3K activity), and pS6 (Ser235/236, a readout of mTORC1 activity) were used to probe the activity of the signaling pathway. Levels of phosphorylated proteins were normalized to total levels of proteins in $n>4$ mice per time point. Levels of pAktT were found to be significantly higher in the L-side than in the C-side of the hippocampus only at 2 hours post-CCI, and returned to normal by 8 hours (Fig. 2B,C). We also analyzed levels of pAkt(Ser473), a site targeted by mTORC2 and not strictly dependent on PI3K activity, but found no significant induction at any time point (Fig 2D). Levels of pS6, on the other hand, were significantly higher in the L-side over a broad time period (2-8 hours) post-CCI, and returned to lower levels at later time points (Fig. 2B,C). Levels of CCI-induced pS6 peaked by 3-4 fold between 2 and 4 hours in the L-side hippocampus. No induction of PI3K/Akt/mTOR pathway was observed in the hippocampus in response to sham craniotomy at any time point analyzed (Fig. 2B and data not shown). Craniotomy alone did cause activation of the PI3K/Akt/mTOR pathway in the L-side cerebral cortex, even though there was no evidence of tissue

damage resulting from craniotomy during perfusion, sectioning or immunostaining (Fig. 2A). Given the sham effect, and the extensive damage to this region resulting from CCI, the cerebral cortex was not analyzed further. Immunofluorescence experiments using a fluorophore-conjugated anti-pS6 antibody confirmed extensive phosphorylation of this mTORC1 target in the cell body layers of areas CA1, CA3 and DG in the L-side hippocampus 4 hours after CCI (Fig. 2F). The organization of these cellular layers appeared somewhat disrupted by the injury, however individual pS6-positive cells were readily observed. The pS6 signal was completely absent from similar regions of the C-side hippocampus, in which the cell body layers appeared intact (Fig. 2F). Together, these studies demonstrate a modest activation of PI3K/Akt, and a robust, but transient activation of mTORC1 in the injured hippocampus within few hours after CCI.

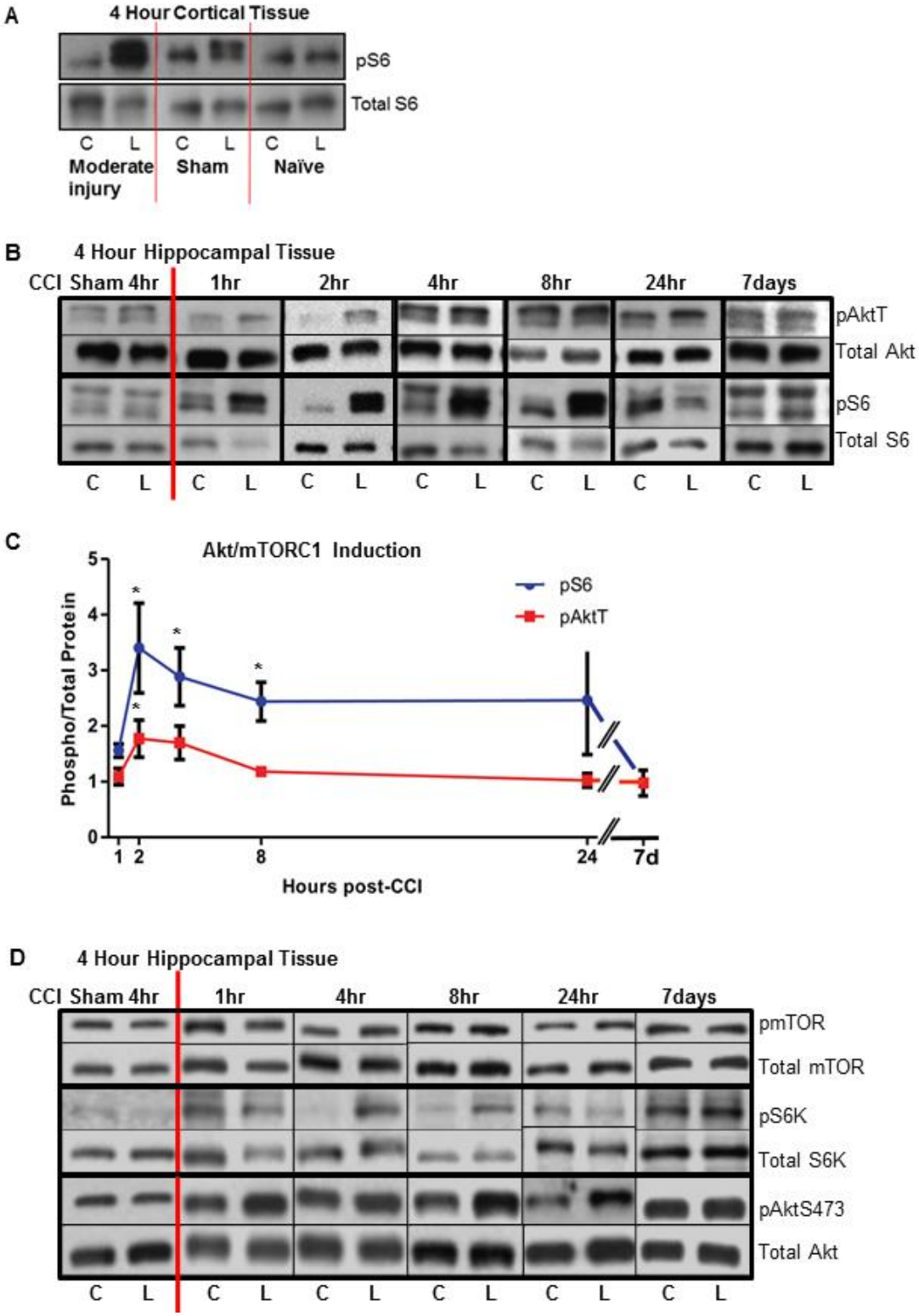
A
4 Hour Cortical Tissue
pS6
Total S6
C L C L C L
Moderate injury
Sham
Naïve
B
4 Hour Hippocampal Tissue
CCI Sham 4hr
1hr
2hr
4hr
8hr
24hr
7days
pAktT
Total Akt
pS6
Total S6
C L C L C L C L C L C L C L
C
Akt/mTORC1 Induction
pS6
pAktT
Phospho/Total Protein
0 1 2 3 4 5
1 2 8 24 7d
Hours post-CCI
D
4 Hour Hippocampal Tissue
CCI Sham 4hr
1hr
4hr
8hr
24hr
7days
pmTOR
Total mTOR
pS6K
Total S6K
pAktS473
Total Akt
C L C L C L C L C L C L

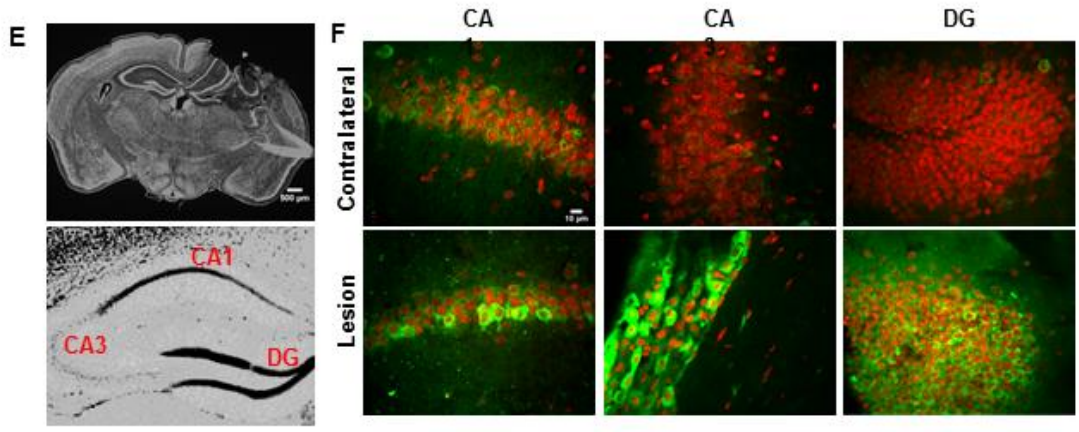

Figure 2. Induction of the Akt/mTORC1 signaling pathway by CCI. (**A**) Representative Western blot data showing Sham surgery-mediated induction of mTORC1 in the L-side cortex. (**B**) Representative Western blot data showing the levels of phosphorylated and total Akt(Thr308) and S6 proteins at each time point in the lesion (L) and contralateral (C) side after CCI or sham surgery. (**C**) Time course of phosphorylation of Akt (pAktT) and S6 (pS6) proteins in the hippocampus after CCI. Values indicate the average ratio of phosphoryated/total proteins in the lesion side relative to the contralateral side of each injured brain (**p*<0.05 by ANOVA). (**D**) Representative Western blot data showing the levels of phosphorylated and total Akt(Ser473), mTOR and S6K proteins at each time point in the lesion (L) and contralateral (C) side after CCI or sham surgery. (**E**) Representative low magnification image of a whole brain section after CCI and sample image of the hippocampus showing the location of regions of interest, such as area CA1, CA3 and dentate gyrus (DG). Both sections were stained with SYTOX nuclear stain. (**F**) High magnification (20x) confocal images of the CA1, CA3 and DG regions in the contralateral and lesion side of the brain after CCI. Sections were stained with fluorophore-conjugated anti-pS6 antibody (green) and Reddot 2 nuclear stain. Scale bars: 500 μm (**E**) and 10 μm (**F**).

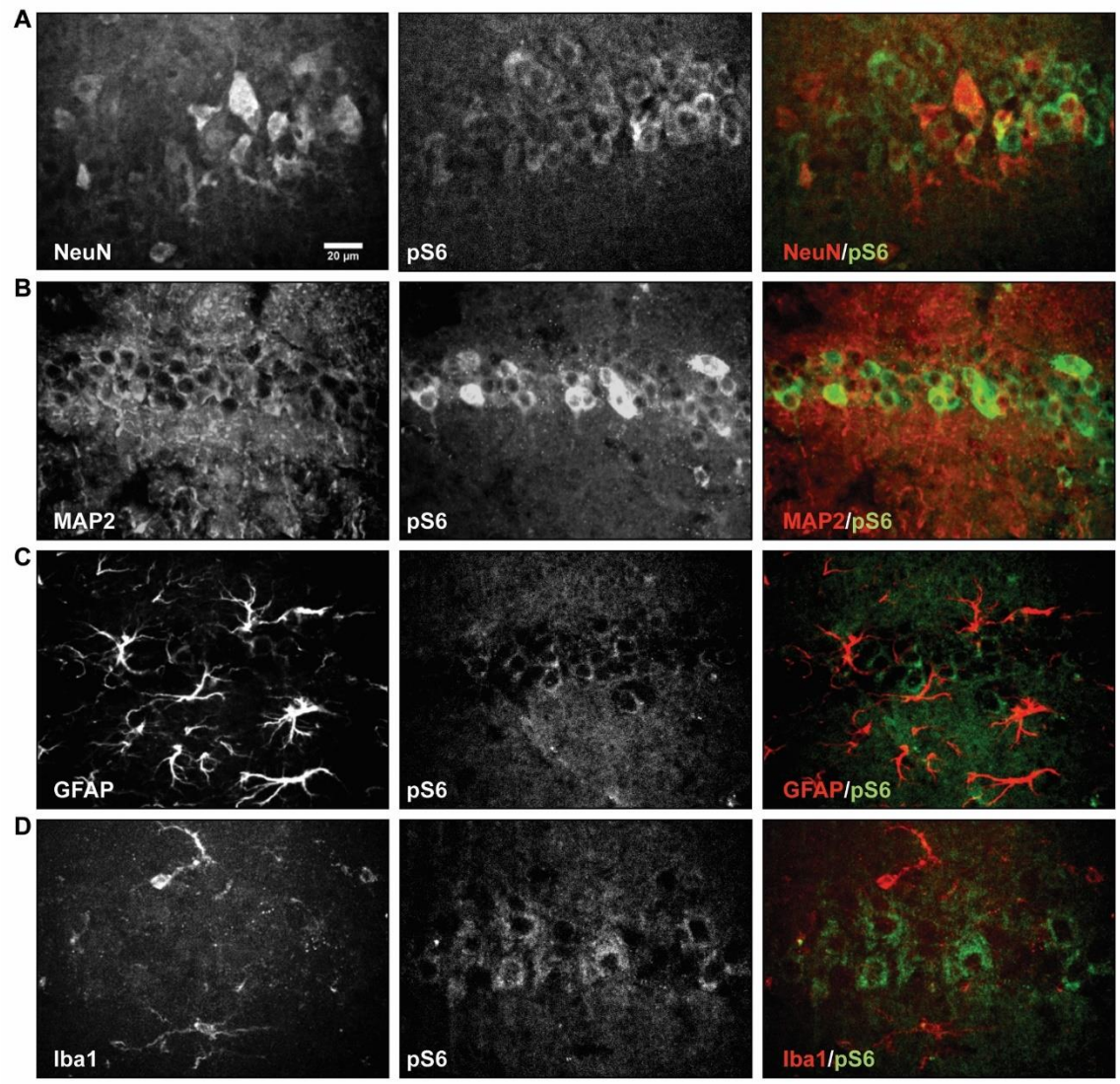

Figure 3. Neuron-specific activation of mTORC1 signaling by CCI. High magnification (20x) confocal images of the CA1 hippocampal area in the lesion side of the brain 4 hours post-CCI. Sections were double labeled with antibodies against pS6 (green) and cell specific markers (red) such as neuronal markers NeuN (**A**) or MAP2 (**B**), astroglia marker GFAP (**C**), and microglia marker Iba1 (**D**). Images are representative of data obtained in *n*=3 mice. Only neuronal markers co-localized with pS6. Scale bar: 20 μm for all panels.

Early mTORC1 activation in the injured hippocampus occurs in neuronal cells

To determine which cell types undergo mTORC1 activation within few hours post-CCI in the L-side hippocampus, we conducted double immunofluorescence using fluorophore-conjugated anti-pS6(Ser235/236) antibody in conjunction with a cell type-specific antibody, such as the neuronal marker NeuN or MAP2, the astroglial marker GFAP, and the microglial marker Iba1. All four markers reliably label the expected cell types in the mouse hippocampus. Sections obtained from mice sacrificed 4 hours post-CCI revealed that only some neuronal cells, identified by either NeuN or MAP2 labeling, expressed high levels of pS6 in the cell body layers of area CA1 (Fig. 3A,B), CA3 and DG (data not shown). GFAP and Iba1 signals did not colocalize with pS6 in any hippocampal region (Fig. 3C,D). These data demonstrate that the early activation of mTORC1 in the injured hippocampus occurs specifically in a subset of neuronal cells within the cell body layers of the hippocampus.

A single rapamycin injection post-CCI suppresses injury-induced mTORC1 activity

To study the significance of mTORC1 activation in CCI-induced tissue damage and recovery, mice were injected with the mTORC1 inhibitor rapamycin one time at 1 hour post-injury. This single injection method was used to determine whether it may be beneficial, modeling a possible strategy for intervention in patients following TBI. Since rapamycin is a potent drug that lingers in the brain for a prolonged period of time (Meikle et al, 2008), we reasoned that an early single injection may be sufficient to suppress the observed transient induction of mTORC1 and to elicit beneficial results, avoiding common side effects associated with prolonged, multi-day treatments with this drug (Barlow et al, 2012; Barlow et al, 2013). Adult mice were subjected to the same moderate CCI described above, and injected once intraperitoneally with 1mg/kg rapamycin or vehicle control 1 hour after injury. Different cohorts of injected mice were

sacrificed at 4 hours post-CCI to assess the effect of the drug on signal transduction, at 24 hours to examine cell damage and astrogliosis, or were analyzed at 3 days for cognitive function (Fig. 4A). At 4 hours post-CCI Western blot analysis of hippocampal tissue revealed that pS6 levels were strongly elevated (by approximately 4 fold) in vehicle-treated mice (Fig. 4B,C), similar to previously analyzed untreated mice (Fig. 2B,C). Rapamycin treatment strongly suppressed this activation, resulting in L-side pS6 levels that were similar to sham controls (Fig. 4B,C). Even though a modest increase in pS6 levels was detected in rapamycin-treated mice when L-side samples were directly compared to C-side values ($p<0.05$ by Student *t*-test), statistical analysis of the whole data set, including sham-treated and vehicle-treated mice, indicated that only the L-side samples of vehicle-treated CCI-exposed mice exhibited significantly elevated levels of pS6 ($p<0.05$ by ANOVA). Interestingly, rapamycin treatment also caused a modest induction of pAktT levels in the L-side versus the C-side hippocampus (Student *t* test, $p<0.05$) (Fig. 4B,D). This likely reflects a positive feedback mechanism that attempts to compensate for the downstream loss of mTORC1 signaling activity (Huang et al, 2009; Das et al, 2012). A very small and not statistically significant induction of pAktT was also seen in vehicle-treated mice (Fig. 4B,D), similar to untreated samples previously analyzed at 4 hour post-CCI (Fig. 2B). However, when the whole pAktT data set was analyzed by ANOVA, no significant effect of any of the treatments was found in either the L-side or the C-side of the hippocampus ($p>0.05$) (Fig. 4D).

To confirm the effectiveness of the rapamycin injection on mTORC1 activity, we also conducted immunofluorescence experiments using a fluorophore-conjugated pS6 antibody. As previously noted for untreated mice (Fig 2 and 3), pS6 levels were strongly induced 4 hours post-CCI in the L-side of vehicle-treated mice in many pyramidal cells of area CA1 (Fig. 4E), as well as in cellular layers of area CA3 and DG (not shown). Rapamycin treatment dramatically suppressed pS6 immunoreactivity in these

hippocampal regions (Fig. 4E and data not shown). Levels of mTORC1 activity were further assessed by counting the number of pS6-positive cells per random field of view in the cell body layers of areas CA1, CA3 and DG in the L-side hippocampus. The number of pS6-positive cells was significantly reduced in rapamycin-treated compared to vehicle-treated mice (Fig. 4F) (Student *t* test, $p<0.05$). No induction of pS6 was detected in the C-side hippocampus of injured rapamycin- or vehicle-treated mice (data not shown). Together, our Western blot and immunofluorescence data demonstrate that a single rapamycin injection delivered 1 hour after CCI effectively suppresses mTORC1 activity in the injured hippocampus.

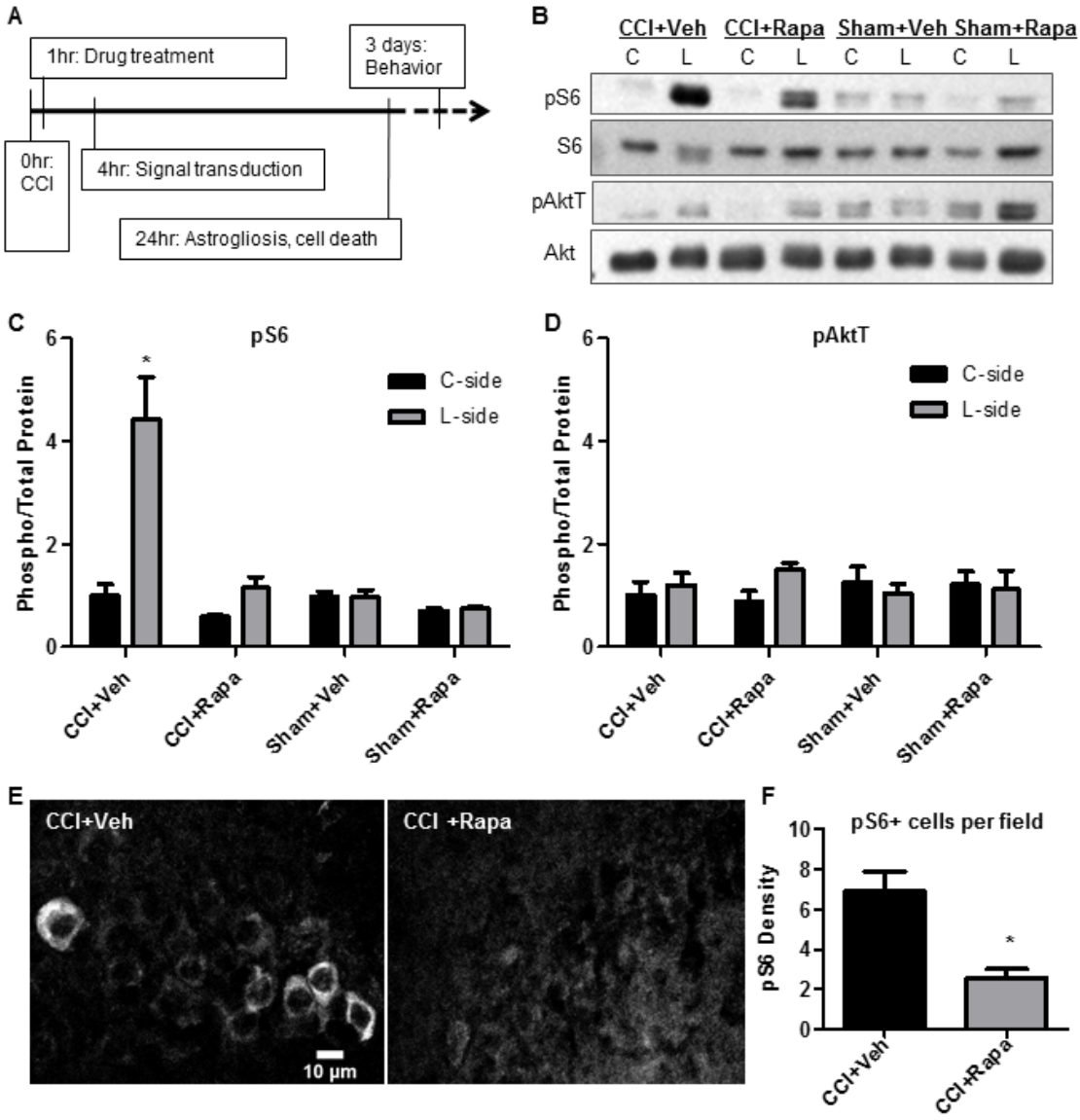

Figure 4. Inhibition of mTORC1 signaling by rapamycin. (**A**) Schematic of the timeline of drug treatments and biological processes analyzed after CCI. (**B**) Western blot analysis of normalized pAktT and pS6 levels in the lesion (L) and contralateral (C) side of the hippocampus in vehicle- (Veh) or rapamycin-treated (Rapa) mice 4 hours post-CCI or sham surgery. Quantification of pS6 (**C**) and pAktT (**D**) data. Values indicate the average ratio of phosphoryated/total proteins in the lesion side (L-side) relative to the contralateral side (C-side) of each injured brain. CCI induced statistically significant pS6 levels only in vehicle-treated, but not in rapamycin-treated mice (*p<0.05 by ANOVA and

post-hoc analysis by Dunnett's test). (**E**) Immunofluorescence analysis of pS6 levels in area CA1 of the lesion-side of the brain 4hr post-CCI in vehicle- or rapamycin-treated mice. (**F**) Quantification of the number of pS6-positive cells per field of view in the pyramidal layer of area CA1. Rapamycin significantly suppresses pS6 induction by CCI (*p<0.05 by Student's t test). Scale bar: 10 μm.

Rapamycin injection post-CCI reduces tissue damage in the injured hippocampus

To evaluate the effects of the single rapamycin treatment on hippocampal tissue damage, we stained brain sections collected 24 hours post-CCI with Fluoro-Jade B (FJB). This time is a recognized early point at which post-CCI deficits can be observed, and is optimal for FJB signal detection in the DG and CA3, but not in the CA1 area (Shein et al, 2008; Zhou et al, 2012). FJB staining is specific for damaged neurons and has been used as a reliable method to quantify post-CCI damage in the L-side of the brain (Schmued and Hopkins, 2000). Indeed, we detected extensive FJB signal in the L-side, and no detectable signal in the C-side hippocampus of vehicle-treated CCI-exposed mice in low magnification images (Fig. 5A). To analyze tissue damage in more detail, we collected higher magnification images of hippocampal regions CA1, CA3 and DG in both vehicle-and rapamycin-treated mice that had been exposed to CCI. The FJB signal was limited to very few cells in the CA1 region of both treatment groups, as expected for the 24 hour time point (Zhou et al, 2012), and this area was therefore not analyzed further (Fig. 5B). In both CA3 and DG, extensive FJB staining was observed in all samples, although the signal appeared reduced in rapamycin-treated compared to vehicle-treated mice (Fig. 5B). Since individual cells could not be easily distinguished, an analysis of the FJB fluorescence signal was performed in the cellular layers of the CA3 and DG. The mean fluorescence signal was significantly reduced in rapamycin-treated

compared to vehicle-treated mice in both hippocampal regions (Fig. 5C,D). The data demonstrate that acute rapamycin treatment post-CCI reduces the extent of tissue damage in the injured hippocampus.

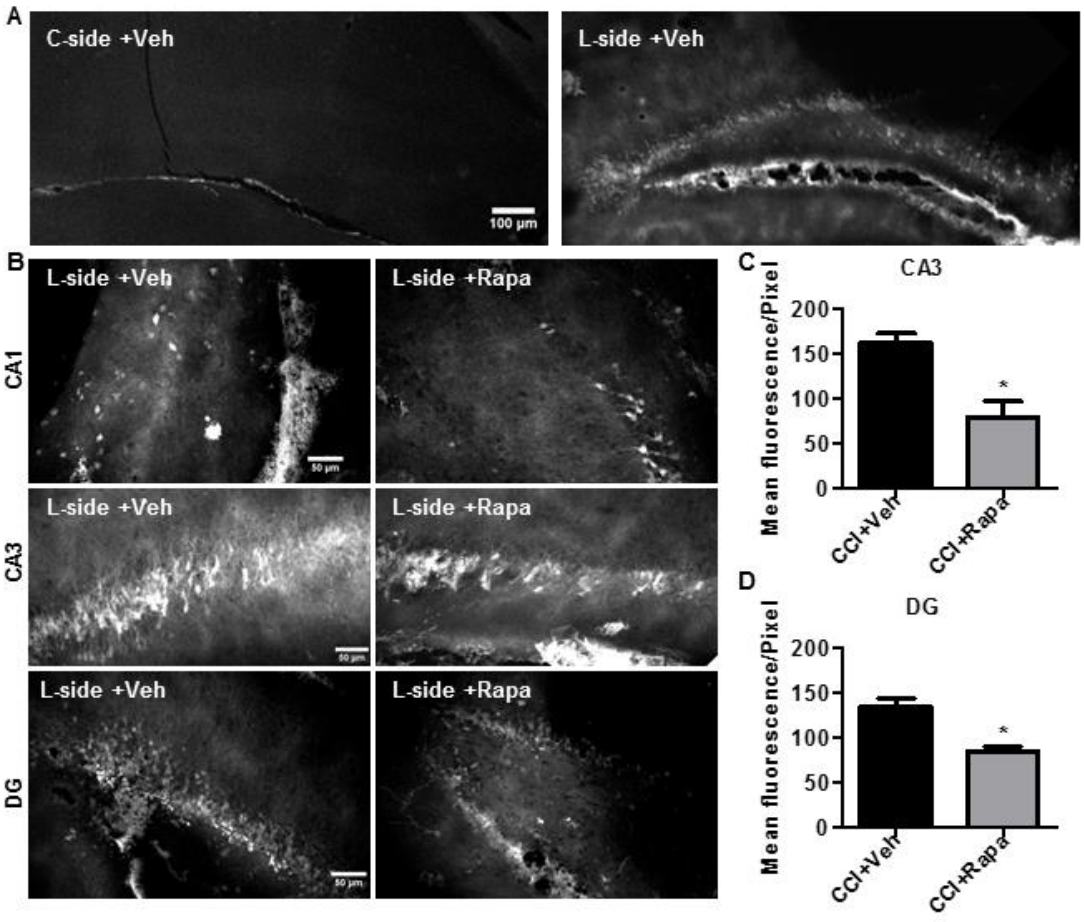

Figure 5. Rapamycin reduces the extent of neuronal damage after CCI. Mice were treated with vehicle (Veh) or rapamycin (Rapa), and analyzed 24 hours after CCI. Sections were stained with Fluoro-Jade B and representative confocal images are shown. (**A**) Low magnification images of the hippocampus in the contralateral (C-side) and lesioned (L-side) hippocampus. (**B**) Higher magnification images of areas CA1, CA3 and DG in the L-side after Veh or Rapa treatment. Quantification of the Fluoro-Jade B signal in the pyramidal layer of area CA3 (**C**) and granule layer of the DG (**D**).

Rapamycin treatment significantly reduced the number of damaged neurons in both areas (*p<0.05 by Student's t test). Scale bars: 100 μm (**A**) and 50 μm (**B**).

Rapamycin injection post-CCI reduces astrogliosis in the injured hippocampus

We examined the effects of CCI and rapamycin treatment on hippocampal astrogliosis by staining sections collected at the 24 hour time point with the astroglial marker GFAP. Low power images of the whole hippocampus revealed that CCI induces extensive astrogliosis in the C-side (Fig. 6B) as well as the L-side hippocampus (not shown), whereas sham surgery did not have any effect (Fig. 6B). Western blot analysis confirmed an increase in GFAP expression in both the C-side and L-side hippocampus of CCI-exposed mice compared to sham-exposed controls (Fig. 6A). CCI-induced astrogliosis was limited to the hippocampus proper areas CA1 and CA3, and did not involve the DG (Fig. 6B). Therefore, these areas were further analyzed in higher magnification images. In area CA1 (Fig. 6D) astrogliosis was present in vehicle-treated CCI-exposed mice in the C-side, and was especially strong in the L-side. Rapamycin reduced astrogliosis in both sides of the hippocampus. The C-side of rapamycin-treated mice appeared indistinguishable from a sham control (Fig. 6C,D), whereas the L-side showed an apparent, but partial improvement compared to vehicle-treated sections. Similar results were obtained when area CA3 was analyzed (Fig. 6E,F). To further quantify the effect of rapamycin treatment on astrogliosis we counted the number of GFAP-positive cells in random fields of area CA1 and CA3 in both the L-side and the C-side of the hippocampus. Statistical analysis indicated a significant reduction in the number of GFAP-positive cells in rapamycin-treated compared to vehicle-treated samples in both areas of the C-side (Student's t-test, p<0.05) (Fig. 6G). However, the number of reactive astrocytes in the L-side was not affected by the rapamycin treatment

(data not shown). These data indicate that a single rapamycin injection 1 hour post-CCI can significantly reduce astrogliosis, particularly in the C-side of the hippocampus.

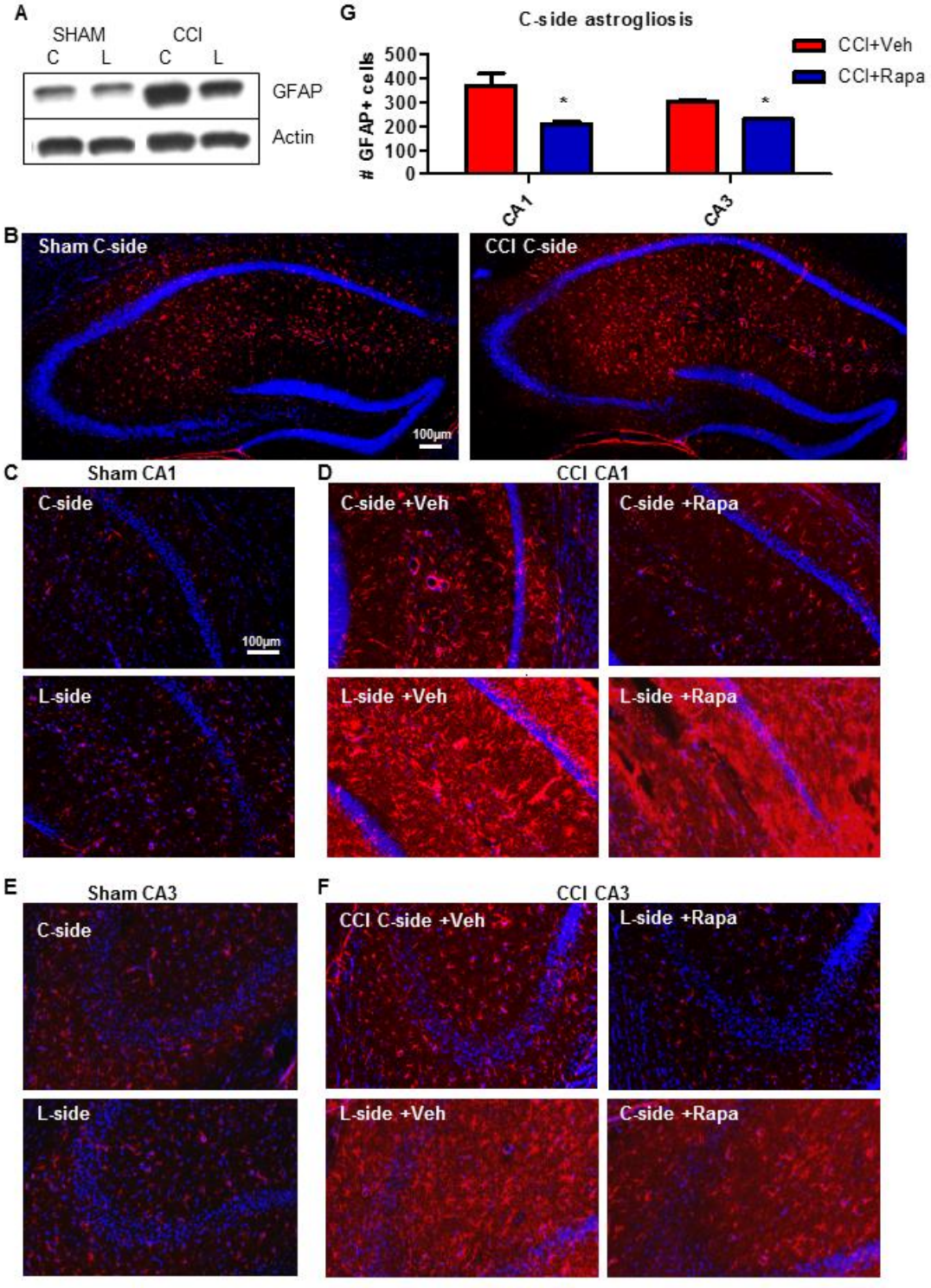

Figure 6. Rapamycin suppresses astrogliosis after CCI. Mice were treated with vehicle (Veh) or rapamycin (Rapa), and analyzed 24 hours after CCI or sham surgery. Sections were stained with GFAP antibodies (red) and counterstained with DAPI or Sytox (blue). (**A**) Western blot analysis of GFAP levels normalized to actin in the contralateral (C-side) or lesion side (L-side) after sham surgery or CCI. GFAP levels are elevated in both sides of the CCI-injured hippocampus. (**B**) Low magnification images of the C-side hippocampus after sham or CCI confirm the increase in the number of GFAP-positive cells after CCI. (**C**) Confocal images of area CA1 in the C-side or L-side after sham surgery. (**D**) Confocal images of area CA1 in the C-side or L-side after CCI and vehicle (Veh) or rapamycin (Rapa) treatment. (**E**) Confocal images of area CA3 in the C-side or L-side after sham surgery. (**F**) Confocal images of area CA3 in the C-side or L-side after CCI and Veh or Rapa treatment. (**G**) Quantification of the number of GFAP-positive cells per area analyzed in the C-side of the brain in CA1 and CA3 regions. Rapamycin treatment significantly reduced astrogliosis in the C-side of both hippocampal areas (*p<0.05 by Student's t test). Scale bars: 100 μm (**A**) and 20 μm (**B-F**).

Given our findings that a single rapamycin injection 1 hour after CCI suppresses mTORC1 activation, early neuronal degeneration, and astrogliosis, our collaborators at Dr. Meaney's laboratory at University of Pennsylvania tested if this treatment also leads to amelioration of cognitive deficits after injury. Morris Water Maze (MWM) deficits were evaluated 3 days after CCI. The overall performance of the animals in acquiring the platform location was calculated over the last four trials of the MWM; performance was significantly worsened by CCI. Rapamycin treatment significantly improved latency time in injured animals relative to vehicle treatment after injury (Nikolaeva et al, 2015).

Discussion

In this study we analyzed the activity of the PI3K/Akt/mTOR signaling pathway in the adult mouse hippocampus following moderate CCI, and found a peak induction of mTORC1 activity at 2-8 hours post-injury in the L-side of the brain, as evidenced by increased pS6 levels. We further showed that this activation is specific to neurons, which lose their tight layer organization in the injured hippocampus, and does not involve astrocytes or microglia. Previous work that examined the induction of pS6 levels 24 hours post-injury indicated that signal activation occurs in glial cells as well as in neurons at this later time point (Park et al, 2012). Thus, it appears that there is a shift in mTORC1 activation from neurons in the early hours after injury to glial cells at later times. This delayed activation may result directly from injury to glial cells, indirectly from neuronal damage, or both. We reasoned that an early intervention with rapamycin 1 hour post-CCI to suppress neuronal mTORC1 activation may reduce not only neuronal damage, but also prevent glial dysfunction at later stages. Indeed, we found that this acute intervention strategy was beneficial in preventing both neuronal and glial abnormalities, and improving functional recovery at least in the short term (3 days after injury). Our results are consistent with a previous study that demonstrated neuroprotection, reduced microglial response and improved behavioral performance when rapamycin was injected 4 hours post-TBI (Erlich et al, 2007). However, no beneficial effect on astrogliosis was seen in that study, nor in a study that administered rapamycin immediately prior to CCI (Park et al, 2012). These studies, taken together with the data presented here, suggest that the most effective time window for an intervention that affects all cell types may be between 1 and 4 hours post-TBI. This treatment paradigm would be applicable to at least some victims of TBI, as it allows a reasonable window of time for patients to be reached by medical personnel.

Previous work on TBI has produced conflicting evidence on the role of the PI3K/Akt/mTOR pathway in recovery from TBI. Unlike this study, some reports suggested that activation, rather than suppression, of the PI3K/Akt/mTOR pathway promotes recovery from TBI. In one study, long-term treatment with simvastatin beginning 24 hours post-CCI, which stimulates Akt phosphorylation, was shown to stimulate neurogenesis and promote spatial learning after TBI (Wu et al, 2008). In another, a single dose of rapamycin given just prior to the injury failed to improve cognitive performance as assessed by the Morris Water Maze using a CCI model, and worsened cognitive performance in a closed-head injury (CHI) model (Park et al, 2012; Zhu et al, 2014). Our findings are consistent with previous studies that demonstrate beneficial effects of mTORC1 signaling inhibition (Erlich et al, 2007; Zhu et al, 2014). Interestingly, in these studies like in ours, rapamycin treatment was initiated in the 1 to 4 hour window after injury. Thus, it is conceivable that the timing or the length of drug treatments targeting the Akt/mTOR pathway play a significant role in determining recovery from TBI.

Rapamycin or rapalogs are widely used to suppress excessive mTORC1 activation in animal models of cortical malformations (Meikle et al, 2007; Zeng et al, 2008; Ljungberg et al, 2009; Kazdoba et al, 2012; Way et al, 2012). In virtually all these models rapamycin treatment not only significantly prolongs survival, prevents or suppresses neuronal abnormalities, and glia pathology, but also strongly suppresses seizures. The overwhelmingly positive effects seen in animal studies led to the development of clinical trials to evaluate the effectiveness of rapalogs in the treatment of epilepsy in these developmental disorders (Krueger et al, 2013). On the other hand, few studies investigated the effects of rapamycin treatment in animal models of TBI. In one study, treatment was initiated 1 hour post-TBI, but continued daily for several weeks, conferring not only protection from neuronal degeneration, but also preventing the

development of posttraumatic epilepsy (Zhu et al, 2014). Together with our studies that demonstrated the beneficial effects of rapamycin on behavioral performance, this work suggests that mTORC1 inhibition may be a viable strategy to ameliorate several aspects of functional recovery after TBI. As for all drugs, however, limitations for the use of rapamycin in the human patient population exist, and warrant caution in the interpretation of these findings. For example, the drug is known to confer non-specific inhibition of other kinase complexes, such as mTORC2 (Sarbassov et al, 2006), and produce considerable side effects in patients especially when treatment is prolonged. These concerns, however, are attenuated if a strategy similar to that used in this animal study, consisting of a single, acute intervention shortly after TBI that is unlikely to cause adverse effects, would be applied to patients.

In this study we showed that rapamycin delivered by systemic injection clearly entered the brain and suppressed the early neuronal phosphorylation of ribosomal protein S6 in the L-side hippocampus, indicating that the treatment successfully reduced mTORC1 activity in the injured brain. Both immunostaining and Western blotting data obtained at the 4 hour time point after injury confirmed this result. By 24 hours post-CCI, neuronal damage was extensive in the L-side, and astrogliosis was apparent in both sides of the injured brain, even though we observed no mTORC1 induction, cell damage or cell body layer disruption in the C-side hippocampus. Rapamycin treatment strongly reduced neuronal and astroglial pathology due to CCI, suggesting that suppression of the early mTORC1 induction in the L-side was sufficient to reduce global astrogliosis. This suggests that early distress signals originating from neurons in the L-side of the brain may cause neuroinflammation in the C-side, and that these secondary effects of the injury may be completely preventable by early rapamycin intervention. However, since we only saw a modest improvement of astrogliosis in the L-side in response to our acute rapamycin treatment, it is possible that repeated or additional forms of intervention

are needed to fully prevent neuronal damage and neuroinflammation in the proximity of the injury. Indeed, a previous study demonstrated that a combination therapy consisting of drugs that inhibit Akt, another kinase component of the PI3K/mTOR signaling pathway, as well as mTORC1 improves function outcome when applied before CCI (Park et al, 2012). However, further studies are needed to determine whether such dual therapy is safe and effective in a clinically-relevant post-TBI paradigm.

In summary, we demonstrate that CCI induces a deleterious activation of mTORC1 activity in hippocampal neurons, which then drives neuronal damage, widespread astrogliosis and cognitive dysfunction. Early intervention with a single dose of rapamycin is greatly beneficial to reduce tissue damage and improve functional recovery. Future studies should investigate the possible application of this intervention strategy to other animal models of TBI and to human patients.

Acknowledgements

Data from this chapter has appeared in Nikolaeva et al., 2015. I want to thank the following people for their contributions to the work presented in this dissertation chapter: the David F. Meaney group at University of Pennsylvania for conducting the CCI procedure and Morris Water Maze experiments, and Beth Crowell for assisting with tissue sectioning.

CHAPTER 3: TARGETING AKT/mTOR IN AN *IN VITRO* MODEL OF SOMATIC AND HEREDITARY BRAIN OVERGROWTH DISORDERS

1. Introduction

The brain overgrowth disorder family includes several cortical malformations, including focal cortical dysplasia (FCD), megalencephaly (MEG), hemimegalencephaly (HMEG), and tuberous sclerosis complex (TSC) (Hevner, 2014). A large percentage of human patients with these disorders have been found to have hyper-activating mutations in the PI3K/Akt/mTOR cell growth pathway (Ljungberg et al, 2006; Jansen et al, 2015). The resulting malformations are highly associated with drug-resistant pediatric epilepsy, and account for over 50% of epilepsy surgery cases in infants and children (Seifer et al, 2012). Thus, there is an urgent need to investigate potential anti-epileptic pharmacological treatments specifically for this family of disorders.

To understand how activation of PI3K/Akt/mTOR signaling affects neuronal development and leads to the hypertrophic neuronal phenotype of brain overgrowth disorders, our laboratory has characterized two novel mouse strains. Kazdoba et al, 2012 developed NEX-*Pten*, a conditional knock out mouse line that exhibits megalencephaly and activation of the PI3K/Akt pathway specifically in postmitotic excitatory neurons of the forebrain (Kazdoba et al., 2012). Mutant mice die shortly after birth, but forebrain neuronal cultures can be readily derived from postnatal day (P) 0 mice. Forebrain *Pten*$^{-/-}$ neurons *in vitro* exhibit dramatic cellular hypertrophy, including increased soma size and dendrite complexity. Crowell et al, 2015 characterized the NEX-*Tsc2* mouse strain as a model for TSC. Under the same promoter as the NEX-*Pten* line, *Tsc2* is deleted via a Cre-Lox mechanism starting at embryonic day (E) 11.5 in forebrain excitatory neurons. Mutant pups display reduced body mass, astrogliosis in the forebrain, and reduced lifespan, with few surviving past 20 days of age (Crowell et al,

2015). mTORC1 suppression, through rapamycin injection in the Kazdoba et al, 2012 study and RAD001 injection in Crowell et al, 2015, improved survival in knockout pups.

We cultured P0 hippocampal neurons from knockout (*Pten*$^{-/-}$, *Tsc2*$^{-/-}$) heterozygous (*Pten*$^{+/-}$, *Tsc2*$^{+/-}$) and wild type (*Pten*$^{+/+}$, *Tsc2*$^{+/+}$) littermates from each mouse strain to characterize their neuronal phenotype *in vitro* and make a comparison between the resulting morphologies. We also hypothesized that brief treatment with novel PI3K/Akt/mTOR inhibitors may be sufficient to reverse mutant phenotypes of *Pten*$^{-/-}$ neurons. We focused our efforts on two compounds currently undergoing clinical trials: Akt inhibitor MK-2206 and mTORC1 inhibitor and rapalog RAD001 (Oki et al, 2015; Rugo et al, 2016).

2. Methods

Mice

The NEX-*Pten* mouse colony was previously characterized by Kazdoba et al, 2012. Briefly, conditional deletion of floxed *Pten* in postmitotic excitatory neurons of the forebrain was driven by the NEX-Cre expression, leading to upregulation of Akt activity. The NEX-*Tsc2* mouse colony was described by Crowell et al, 2015. Briefly, conditional deletion of floxed *Tsc2* in postmitotic excitatory neurons of the forebrain was driven by the NEX-Cre expression, resulting in upregulation of mTORC1 activity.

In order to simplify breeding, breeder mice were all homozygous for the presence of NEX-Cre (*Cre*$^{+/+}$). Therefore, all littermates retain Cre expression and the only difference in genetic background is the presence or absence of LoxP sites at the *Pten* gene (*Pten*$^{+/+}$, *Pten*$^{loxP/+}$ or *Pten*$^{loxP/loxP}$). Because *Cre*$^{+/+}$; *Pten*$^{loxP/loxP}$ (referred to as *Pten*$^{-/-}$ from here on) pups die within days of birth, our breeding strategy was to have heterozygous males (*Cre*$^{+/+}$; *Pten*$^{loxP/+}$, also referred to as *Pten*$^{+/-}$) breed with heterozygous females (*Cre*$^{+/+}$; *Pten*$^{loxP/+}$). This method has the capacity to generate wild-

type and mutant pups in almost every litter, allowing for concurrent study of both genotypes:

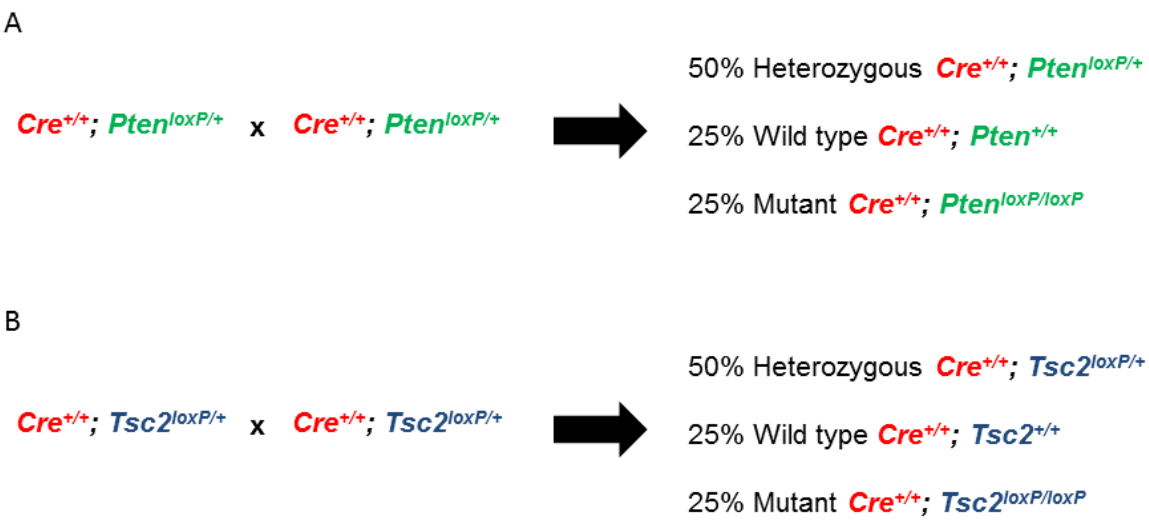

Figure 7. Simple schematic of the breeding strategy for (A) NEX-*Pten* and (B) NEX-*Tsc2* lines in order to generate wild type, heterozygous and mutant cultures for each gene.

Neuronal Cultures

Cortical and hippocampal neuronal cultures were generated from newborn NEX-*Pten* or NEX-*Tsc2* littermates using a papain dissociation kit (Worthington). Cells were strained with a 70 µm filter, and centrifuged for 5 min at 300 x g. The pellet was re-suspended in a solution of Earle's Balanced Salt Solution (EBSS)/deoxyribonuclease I (DNase)/ ovomucoid protease inhibitor. The re-suspension was layered on top of 1 ml ovomucoid protease inhibitor solution, centrifuged for 6 min at 100 x g, and then centrifuged for an additional 6 min at 200 x g to evenly coat the cells with the ovomucoid solution. Cells were re-suspended in a mixture of 98% Neurobasal medium (Gibco), 2% B-27 supplement (Gibco), 0.5 mM glutamine (Gibco) and 0.5 mM PenStrep (Gibco), and

plated onto poly-D-lysine (Sigma) coated glass coverslips at a density of 25-50,000 cells/cm^2 for immunofluorescence studies and 65-100,000 cells/cm^2 for electrophysiology. Cells were maintained at 37°C in 5% CO_2 in a water-jacked incubator for 10 days *in vitro* (DIV) for immunofluorescence studies, 11 DIV for NEX-*Pten* electrophysiological studies and DIV 12 for NEX-*Tsc2* electrophysiological studies. Hippocampal cultures were used for immunofluorescence and electrophysiology experiments and cortical cultures for Western blot analysis.

Drug treatments

10 µM RAD001 and 124 µM MK-2206 stocks in DMSO were stored at -80^{0}C for a maximum of 6 months. Inhibitors were added to cultures at concentrations of 2.5-20 µM RAD001 (Selleck Chemicals), and 0.25-2 µM MK-2206 (Selleck Chemicals) for 4 hours on DIV9 directly to medium. Medium was replaced by fresh Neurobasal+ B27 medium for additional 24 hours for immunofluorescence at 10 DIV and 48 hours for electrophysiology at 11 DIV.

Immunofluorescence and imaging

24 hours post-treatment with inhibitors, cells were washed twice with PBS and fixed for 15min in 4% Paraformaldehyde in PBS at room temperature. Cells were then permeabilized for 10 min in 0.1% Triton-X in PBS, washed, and blocked in 10% Normal Goat Serum. Cells were probed with anti-MAP2 (Covance), anti-Gad67 (Millipore), anti-Pten (Cell Signaling), anti-Tau (AbCam) and 488-fluorophore-conjugated anti-phospho-S6 antibodies (Cell Signaling) and mounted in Vectashield mounting medium with DAPI or Reddot2 as nuclear stains. Images were taken with a Yokogawa CSU-10 confocal spinning disk connected to an Olympus IX50 fluorescence microscope and analyzed using ImageJ.

Western blot

P0 cortexes or DIV 10 cultures were lysed in RIPA lysis buffer (50 mM Tris (pH 7.4), 1% NP40, 0.25% sodium deoxycholate, 150 mM NaCl, 1nM EDTA supplemented with protease and phosphatase inhibitors), and spun at 4^0C, at 3000 rcf for 5-7minutes to remove debris. Protein concentration was measured by a standard Bradford assay. Laemmli sample buffer was added to the lysates, and the samples were boiled for 3 minutes. Proteins (15 μg per sample) were separated by SDS-PAGE using 8.0% or 10.0% gels and transferred onto 0.2 μm nitrocellulose membrane at 4^0C in 20% methanol Tris-Glycine buffer for 2.5 hours at a constant 0.5Amp. Membranes were blocked in 3% milk in TBS-T for 1 hour, and incubated in primary antibodies overnight at 4^0C. Membranes were then incubated for 1 hour in secondary, HRP-conjugated antibodies, and subjected to ECL-Plus Western Blotting Detection System (Pierce/Thermo Fisher, Rockland, IL). Primary antibodies against Pten, pGSK3β(Ser9), pRibosomal Protein S6(Ser235/236), pAkt(Ser473), pAkt(Thr308), Akt, S6 and GSK3β were purchased from Cell Signaling, and anti-actin antibody was purchased from Millipore. All phosphorylated protein levels were normalized to the total amount of each protein. Quantification was performed using the band analysis function of Alpha Imager software (Protein Simple).

Antibody	*Vendor*	*Catalogue#*	*Host*	*Dilution*	*Application*
pAkt(Thr308)	Cell Signaling	2965	Rb	1:1000	WB
pAkt(Ser473)	Cell Signaling	9271	Rb	1:1000	WB
Total Akt	Cell Signaling	4691	Rb	1:2000	WB
pGSK3β(Ser9)	Cell Signaling	9323	Rb	1:1000	WB
Total GSK3β	Cell Signaling	9315	Rb	1:1000	WB
pS6 (Ser235/236)	Cell Signaling	4858	Rb	1:1000	WB
Total S6	Cell Signaling	2317	M	1:1000	WB
488-pS6 (Ser235/236)	Cell Signaling	4803	Rb	1:1000	IF
Pten	Cell Signaling	9559	Rb	1:1000	WB, IF
Actin	Millipore	MAB1501	M	1:5000	WB
MAP2	Covance	SMI-52R	M	1:250	IF
Gad67	Millipore	MAB5406	M	1:100	IF
GFAP	DAKO	Z 0334	Rb	1:500	IF
Tau	AbCam	ab64193	Rb	1:20	IF

Table 3. Primary antibodies used in this study. WB= Western blot, IF=Immunofluorescence. Host: Rb=Rabbit, M=Mouse.

Statistical Analysis

For all analyses, cultures from *n*>2 mice of each genotype were used. Soma size was quantified with the Area measurement tool of ImageJ, and Sholl analysis was carried out manually for MAP2-positive processes crossing ten concentric circles placed at 12.5 µm intervals from each other and centered around the soma. Fluorescence analysis for pS6 and Pten expression was performed by measuring the Integrated

Density of the fluorescent signal in the cell body and subtracting the background (Area x Mean Gray Value of adjacent background). All statistical analyses for 3 groups or more were done by ANOVA and Dunnett's post hoc test if data was normal as determined with Shapiro-Wilk test, and Kruskal-Wallis and Dunn's post hoc test if data was not normal. All statistical analyses for 2 groups were done by Student's t-test if data was normal as determined with Shapiro-Wilk test, and Mann Whitney U test if data was not normal. $p<0.05$ was considered significant.

3. Results

NEX-Cre driven Pten deletion is excitatory neuron-specific

In order to determine the specificity of NEX-Cre expression and *Pten* gene deletion, we bred heterozygous NEX-*Cre*+; $Pten^{+/-}$ mice to generate litters that included wild type, heterozygous and mutant pups. We cultured P0 hippocampal neurons for 10 DIV and performed double immunostaining with antibodies against Pten and either neuronal marker MAP2 or the interneuron marker Gad67. We used only hippocampal neurons for morphological study because they are less heterogeneous than cortical neurons. As expected, our primary cultures consisted primarily of excitatory (MAP2-positive/Gad67-negative) neurons. Therefore, most MAP2-positive cells imaged can be assumed to be excitatory neurons. Both MAP2-positive/Gad67-negative and MAP2-positive/Gad67-positive neurons in $Pten^{+/+}$ cultures stained positive for Pten expression. By comparison, Pten expression was retained exclusively in Gad67-positive interneurons in the $Pten^{-/-}$ culture, and not in MAP2-positive/Gad67-negative excitatory neurons (Fig. 8 A-B). Quantification of corrected total cell fluorescence (CTCF) of the fluorescent Pten signal showed a significant decrease in Pten expression in $Pten^{-/-}$ MAP2-positive neurons ($p<0.0001$, Mann Whitney U test, $n\geq3$ mice per genotype) compared to $Pten^{+/+}$ MAP2-positive neurons (Fig. 8 C). Interestingly, Gad67-positive neurons in the $Pten^{-/-}$ culture showed elevated expression of Pten ($p<0.0001$, Mann

Whitney U test, $n \geq 3$ mice per genotype) as compared to interneurons from the *Pten*$^{+/+}$ culture (Fig 8 D). These data suggest a potential compensatory increase in Pten levels in other cell types surrounding Pten-deficient excitatory neurons. Existing evidence that Pten can be secreted may account for how such a compensatory mechanism could function (Hopkins et al, 2013; Kreis et al, 2014). While this process may help to improve upon pathologies resulting from excess Pten activity, it is likely insufficient to rescue the phenotype as the symptoms of brain overgrowth disorders *in vivo* in the mouse and in humans are quite severe. However, this mechanism may suggest alternative therapies such as Pten protein replacement, which may aid in returning the brain to a normal course of development. Overall, these data confirm that the *Pten* gene is deleted is specifically in excitatory but not in GABAergic interneurons in the forebrain of our NEX-Pten mutant mice.

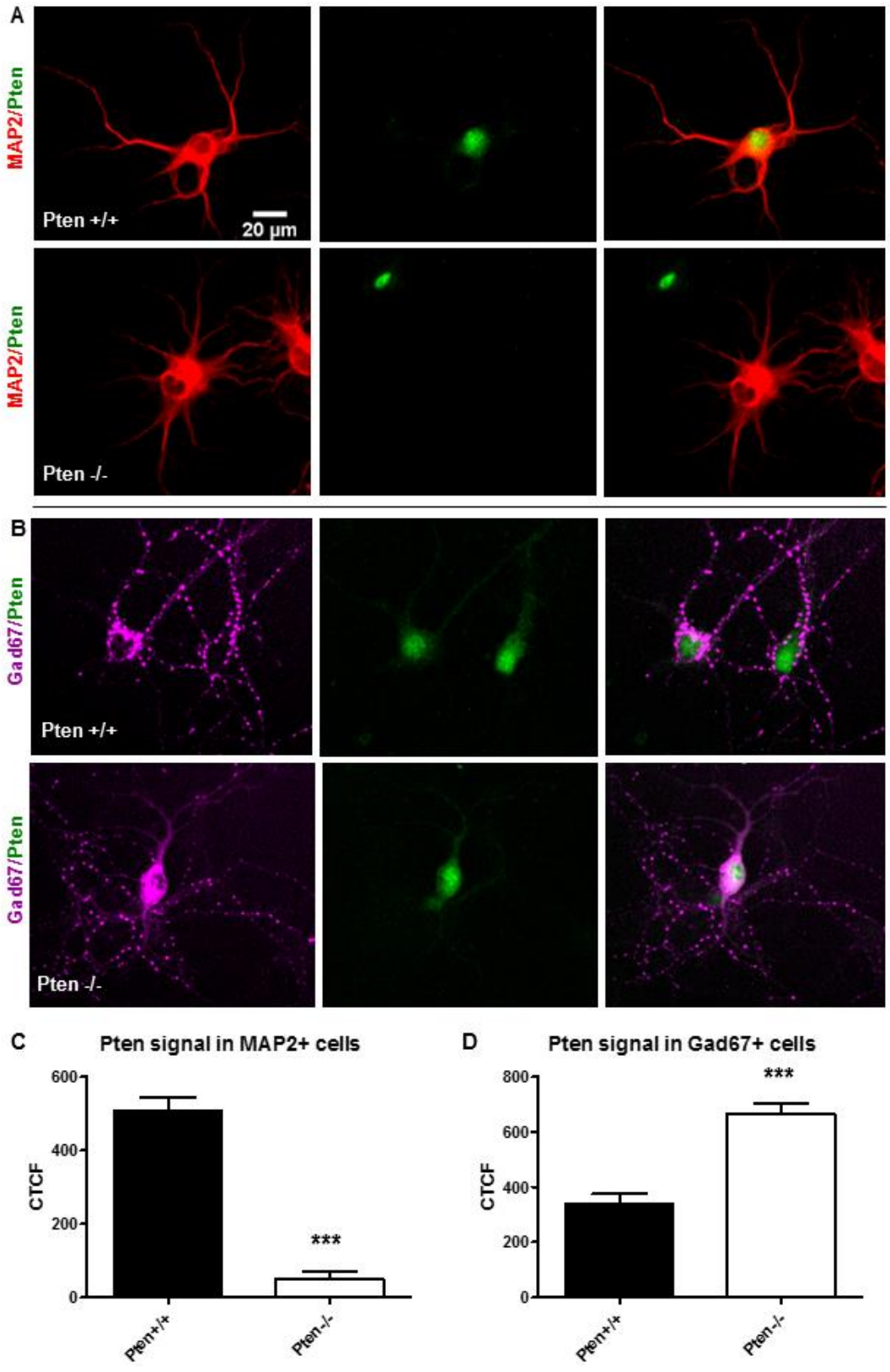
A
MAP2/Pten
Pten +/+
20 µm
MAP2/Pten
Pten -/-
B
Gad67/Pten
Pten +/+
Gad67/Pten
Pten -/-
C
Pten signal in MAP2+ cells
CTCF
600
400
200
0
***
Pten+/+
Pten-/-
D
Pten signal in Gad67+ cells
CTCF
800
600
400
200
0
***
Pten+/+
Pten-/-

Figure 8. Hippocampal neurons from NEX-*Pten* wild type (*Pten*$^{+/+}$) or homozygous mutant (*Pten*$^{-/-}$) mice were cultured for 10 DIV and double labeled with the indicated antibodies. **(A)** Representative images of MAP2-positive (MAP2+) neurons (excitatory). Most neurons obtained from homozygous mutant cultures (excitatory) do not express Pten. **(B)** Representative images of Gad67-positive (Gad67+) neurons (interneurons). Interneurons from mutant cultures cultures retain Pten expression. **(C)** CTCF of Pten signal in MAP2-positive DIV 10 hippocampal neurons from wild type or homozygous mutant neurons ($p<0.0001$, Mann Whitney U test, $n\geq3$ mice per genotype). **(D)** CTCF of Pten signal in Gad67-positive DIV 10 hippocampal neurons from wild type or homozygous mutant neurons ($p<0.0001$, Mann Whitney U test, $n\geq3$ mice per genotype). Bar graphs show the mean values ± SEM

Pten-deficient excitatory neurons show altered Akt/mTORC1 signaling, enlarged soma and greater dendritic arborization

We performed a Western blot for pathway activity in DIV 10 cortical NEX-*Pten* cultures and in the P0 cortex of wild type, heterozygous and mutant mice to assess whether *Pten* deletion has an effect on PI3K/Akt/mTOR signaling. Cortical cultures were selected for Western blotting over hippocampal cultures because they allow us to collect more cells for protein extraction. Samples were probed for phospho(p)-specific antibodies against pAkt(Thr308), pAkt(Ser473), pS6 (Ser235/236) and pGSK3β(Ser9) and normalized individually to their respective total levels of protein in cultures from $n=1$ mouse per genotype and in P0 brains from $n=3$ mice per genotype. We did not have sufficient cortical cultures to do statistical analysis on PI3K/Akt/mTOR signaling by Western blot, but are able to provide representative Western blot results of my preliminary data in Fig. 9 B from 1 culture each of *Pten*$^{+/+}$, *Pten*$^{+/-}$ and *Pten*$^{-/-}$ cortical

neurons. As expected, *Pten*$^{-/-}$ cortexes showed significantly increased Akt and mTORC1 signaling, as evidenced by excess phosphorylation of Akt at the Thr308 and Ser473 sites, and of pS6 at the Ser235/236 residues (p=0.05, p<0.05, and p<0.05 respectively, Kruskal-Wallis test, n=3 mice per genotype) as compared to *Pten*$^{+/+}$ and *Pten*$^{+/-}$ pups (Fig. 9 A, D-F). Excess PI3K/Akt/mTOR activity in Pten-deficient NEX-*Pten* mice was also demonstrated by Kazdoba et al, 2012. No change was observed in Akt-mediated phosphorylation of GSK3β at Ser9, and therefore was not analyzed further (Fig. 9 G). Representative Western blots of DIV 10 cultured wild type, heterozygous and knockout neurons suggest the signaling defect and Pten deficiency persist in mature cultured neurons from the respective pup genotypes Fig. 9 B).

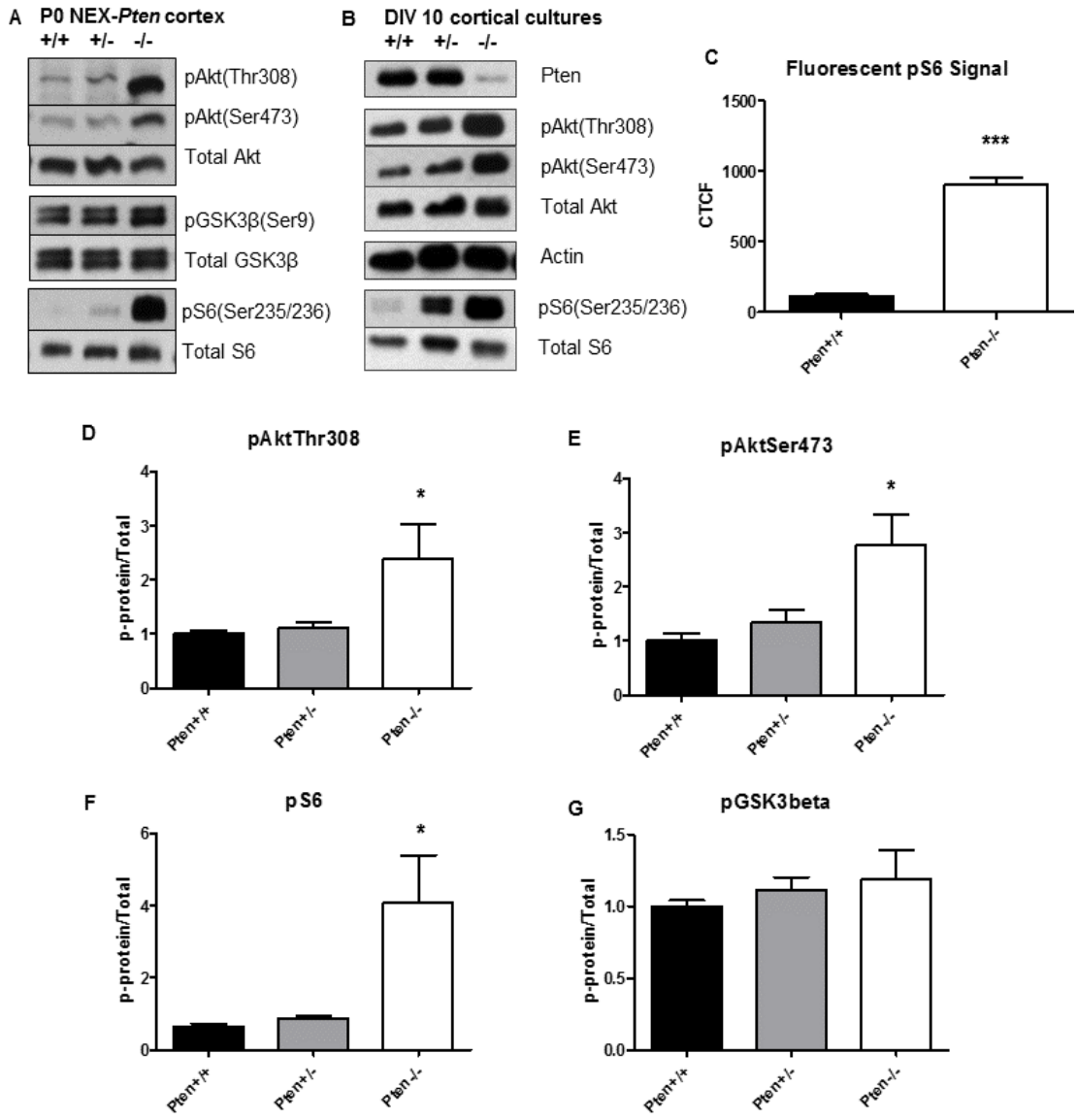

Figure 9. Western blot analysis of the PI3K/Akt/mTOR pathway in NEX-*Pten* cortex and cortical cultures. **(A)** Representative Western blots of phosphorylated and total Akt, S6 and GSK3β in P0 mouse cortex of *Pten*$^{+/+}$, *Pten*$^{+/-}$ and *Pten*$^{-/-}$ pups. **(B)** Representative Western blots of Pten expression and phosphorylated and total Akt and S6 in DIV 10 cortical neurons. **(C)** CTCF of 488-pS6 (Ser235/236) signal in MAP2-positive cells of *Pten*$^{+/+}$ and *Pten*$^{-/-}$ DIV 10 hippocampal cultures (p<0.0001 by Mann Whitney U test, n=2-3 mice per genotype). **(D-G)** Quantification of Western blot data for PI3K/Akt/mTOR

signal in P0 *Pten*$^{+/+}$, *Pten*$^{+/-}$ and *Pten*$^{-/-}$ cortex. (* p<0.05 by Kruskal-Wallis test, n=3 mice per genotype.) Bar graphs show the mean values ± SEM

We also probed hippocampal DIV 10 cultures with fluorophore-conjugated anti-pS6(Ser235/236) antibody, using MAP2 neuronal marker labeling as a counterstain. Since pS6 is a reliable readout of mTORC1 activity, we used CTCF to quantify the fluorescent signal of pS6 in cultured *Pten*$^{+/+}$ and *Pten*$^{-/-}$ neurons (n=2-3 mice per genotype). *Pten*$^{-/-}$ neurons showed significantly elevated levels of pS6 per pixel, controlling for cell size (p<0.0001, Mann Whitney U test, n=2-3 mice per genotype), indicating that *Pten*$^{-/-}$ hippocampal neurons have sustained elevated mTORC1 activity as compared to *Pten*$^{+/+}$ controls.

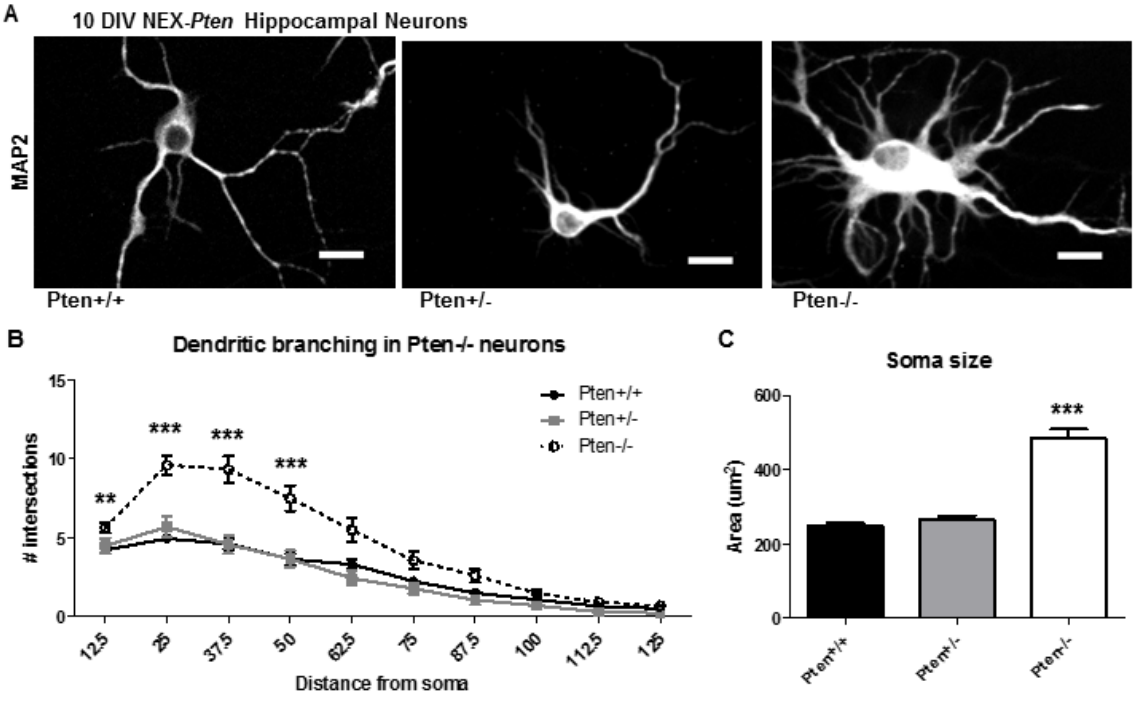

Figure 10. **(A)** Representative images of *Pten*$^{+/+}$, *Pten*$^{+/-}$, and *Pten*$^{-/-}$ DIV 10 hippocampal neurons labeled with MAP2. **(B)** Sholl analysis of *Pten*$^{+/+}$, *Pten*$^{+/-}$ and *Pten*$^{-/-}$

MAP2+ processes of DIV 10 hippocampal neurons. **(C)** Quantification of soma area in DIV 10 hippocampal MAP2+ neurons. *Pten*$^{-/-}$ neurons have larger soma and more branched dendrites, but a normal number of axons. (* $p<0.05$, ** $p<0.01$, *** $p<0.001$ by Kruskal-Wallis test, $n\geq3$ mice per genotype). Bar graphs show the mean values ± SEM. Scale bar: 20µm.

Previous studies have reported enlarged neuron cell bodies both in human brain tissue from FCD and HMEG patients, and mouse models with increased PI3K/Akt/mTOR signaling (Ljungberg et al, 2006; D'Arcangelo et al, 2009; Yasin et al, 2013). In order to determine whether our mouse model exhibits neuronal hypertrophy *in vitro*, we quantified the dendritic branching and soma area of DIV 10 cultured P0 hippocampal *Pten*$^{+/+}$, *Pten*$^{+/-}$, and *Pten*$^{-/-}$ neurons. We probed cultures with an anti-MAP2 antibody and measured cell body area and dendritic branching by Sholl analysis from 10x confocal images. *Pten*$^{+/+}$ and heterozygous *Pten*$^{+/-}$ neurons have indistinguishable soma size and dendritic morphology, but *Pten*$^{-/-}$ neurons have, on average, almost 2-fold larger soma ($p<0.0001$, Kruskal-Wallis test, $n\geq3$ mice per genotype) and significantly increased dendritic branching between 12.5 and 50 µm from the soma ($p<0.001$ and $p<0.01$ respectively, Kruskal-Wallis test, $n\geq3$ mice per genotype) (Fig 10 B-C). Unpublished data from previous lab member Dr. Tatiana Kazdoba-Leach suggests no axonal abnormalities in *Pten*$^{-/-}$ hippocampal neurons between 2 and 15 DIV (data not shown). Since heterozygous neurons showed a wild type morphological and signaling phenotype, they were not studied further except for use as controls where sufficient wild type animals were not available.

Effect of RAD001and MK-2206 treatment on the soma size phenotype of NEX-Pten-/- neurons

We hypothesized that suppressing the PI3K/Akt/mTOR pathway might normalize the size of hypertrophic *Pten*$^{-/-}$ excitatory neurons. We selected the Akt inhibitor MK-2206 and the mTORC1 inhibitor RAD001 because of their promising performance in safety and efficacy human trials (Oki et al, 2015; Rugo et al, 2016). We chose a treatment scheme whereby we introduced one of four doses of the drug into the culture medium on DIV 9, several days after the hypertrophic phenotype of NEX-Pten -/- neurons was observable (unpublished data from Dr. Tatiana Kazdoba performed in our lab indicates that hypertrophic phenotype of knockout neurons is observable as early as 4 DIV). We used a brief, 4 hour treatment, as previous work has shown that sustained inhibition of Akt or mTORC1 can reduce soma size and dendritic branching even in wild type neurons (Jaworski et al, 2005). After 4 hours of incubation with the drug, neurons received fresh medium and were allowed to recover for 24 hours. On DIV 10, we fixed and probed DMSO-treated control wild type and knockout neurons, and drug-treated knockout neurons for MAP2. MAP2-positive cells were imaged, and soma size was quantified using the Area tool of ImageJ. Both mTORC1 and Akt suppression were individually sufficient to reduce soma size of *Pten*$^{-/-}$ excitatory neurons (Fig. 11 B). We found that 5.0 µM RAD001 and 2.0 µM MK-2206 were the most effective doses for reducing soma size ($p<0.05$ from wild type for RAD001, and $p>0.05$ from wild type for MK-2206, Kruskal-Wallis test, n≥3 mice per genotype). Of the two drugs, only MK-2206 was able to restore normal soma size area in knockout neurons, bringing values within statistically non-significant levels of wild type neurons. While MK-2206 treated neurons showed a dose-dependent reduction in soma size, no such gradient was observed in response to RAD001 treatments. Furthermore, 10.0 µM and 20.0 µM RAD001 treated

cells showed signs of cytotoxicity (data not shown). We therefore decided to continue with 2.0 µM MK-2206 and 5.0 µM RAD001 treatments and evaluate their effects on excess dendritic branching observed in *Pten*$^{-/-}$ neurons.

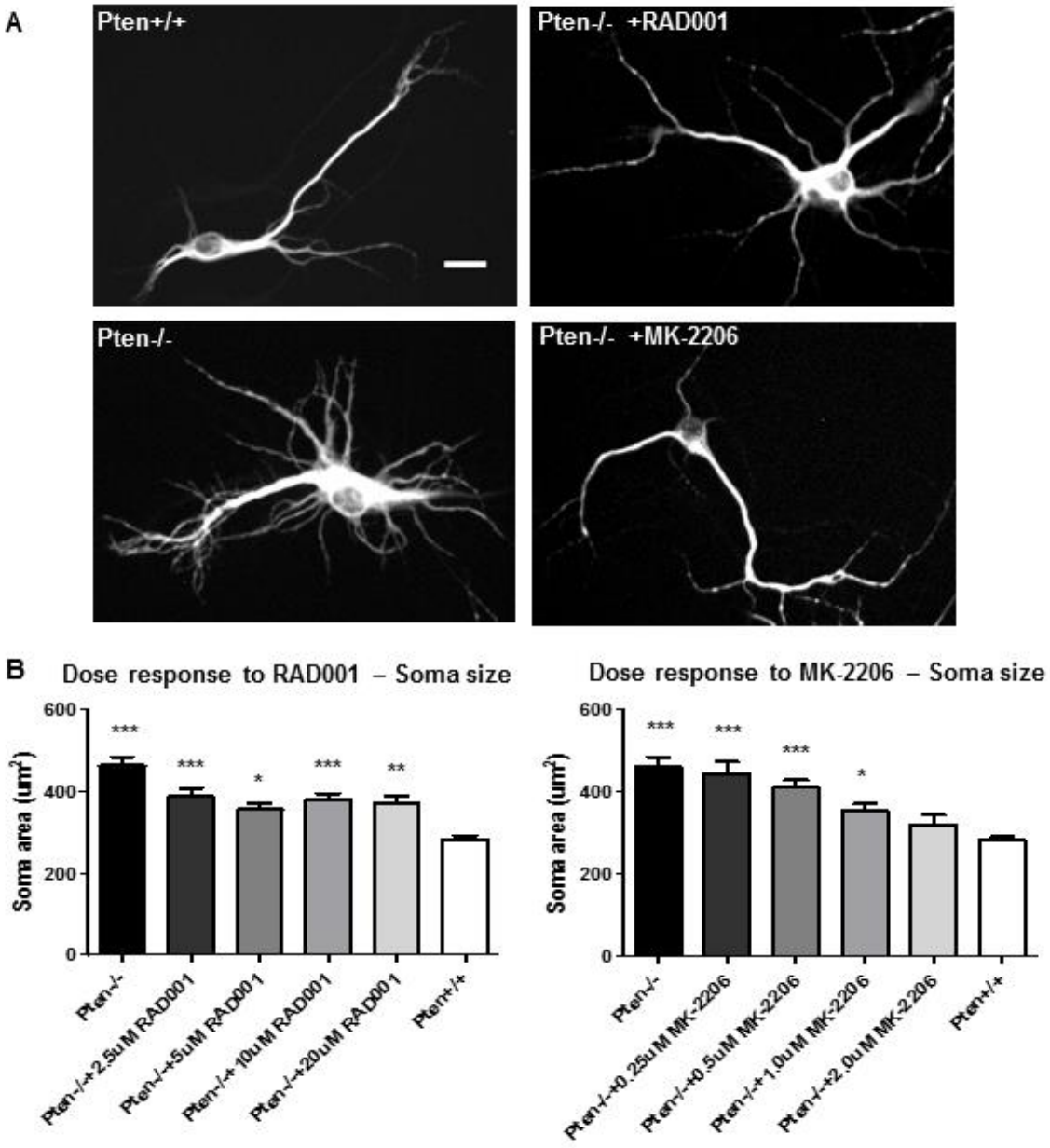

Figure 11. Hippocampal neurons from NEX-*Pten* wild type (*Pten*$^{+/+}$) or homozygous mutant (*Pten*$^{-/-}$) mice were cultured for 9 DIV, treated for 4 hr with vehicle DMSO, 5.0 µM RAD001 or 2.0 µM MK-2206, fixed and stained for MAP2 24 hours later. **(A)**

Representative images of wild type, untreated knockout and RAD001 or MK-2206 treated knockout MAP2-positive neurons. **(B)** Quantification of soma size in hippocampal neurons without drug or treated with increasing doses of RAD001 or MK-2206 (* $p<0.05$, ** $p<0.01$, *** $p<0.001$ by Kruskal-Wallis test; denotes significant difference from $Pten^{+/+}$, $n\geq2$ mice per treatment). Bar graphs show the mean values ± SEM

Both RAD001 and MK-2206 reverse dendritic branching phenotype, but MK-2206 is more effective

We used our 4 hour treatment and 24 hour recovery scheme to evaluate the effects of MK-2206 and RAD001 on dendritic branching in NEX-*Pten* knockout neurons. Sholl analysis was performed in blind on anti-MAP2 immunostained DIV 10 hippocampal neuronal cultures for processes up to 125 µm from the soma. Arborization of RAD001-treated neurons trended higher than wild type neurons between 25 and 75 µm from the soma, and was statistically significantly different from wild type neurons at 50 µm from the soma ($p<0.05$, Kruskal-Wallis test, $n=3$ mice per gentoype). Knockout neurons that received 2.0 µM MK-2206 treatment had statistically significantly fewer dendrites 12.5 µm from the soma ($p<0.0001$, Kruskal-Wallis test, $n=3$ mice per gentoype), and trending toward fewer dendrites than wild types from 12.5 µm to 62.5 µm from the soma. Overall, MK-2206 was more successful at reversing the dendritic branching phenotype of knockout neurons (Fig. 12 A-B).

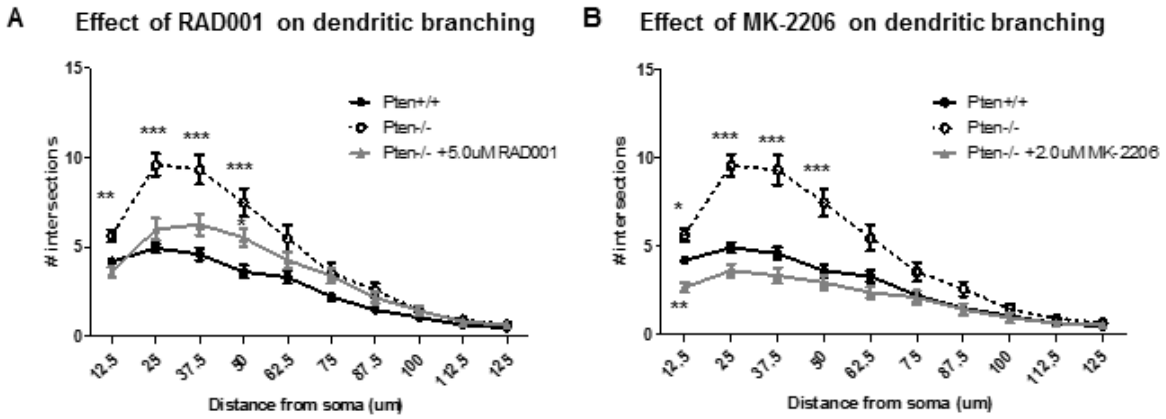

Figure 12. Sholl analysis of MAP2-positive dendrites of neurons without drug or treated with 5.0 µM RAD001 **(A)** or 2.0 µM MK-2206 **(B)**. (* p<0.05, ** p<0.01, *** p<0.001 by Kruskal-Wallis test; denotes significant difference from $Pten^{+/+}$, n≥3 mice per treatment). Error bars show ± SEM

Brief RAD001 and MK-2206 treatments suppress PI3K/Akt/mTOR signal but do not affect soma size and dendritic branching of regular neurons

Previous studies have shown that prolonging treatment with mTORC1 or Akt inhibitors to 3-6 days can reduce soma size and dendritic branching in wild type neurons as well as neurons with elevated PI3K/Akt/mTOR signaling activity (Jaworski et al, 2005). We quantified effects of a 4 hour incubation in the presence of RAD001 or MK-2206 on PI3K/Akt/mTOR activity in wild type and heterozygous neurons by Western blot to confirm that the pathway is significantly suppressed in our treatment scheme. Our results showed that both RAD001 and MK-2206 prevented phosphorylation of S6, suggesting that both drugs are capable of inhibiting mTORC1 activity (Fig. 13 A,D). RAD001 suppressed Akt activity downstream of PI3K to about 70% of its regular levels, while MK-2206 brought Akt phosphorylation at Thr308 down to less than 20% of the

untreated samples (Fig. 13 B). Therefore, we concluded that any differences in effects between the two drugs are due to their differential modulation of Akt activity upstream of mTORC1. Finally, it is important to note that based on levels of Akt(Ser473) phosphorylation, neither treatment scheme affects mTORC2 signaling (Fig. 13 C).

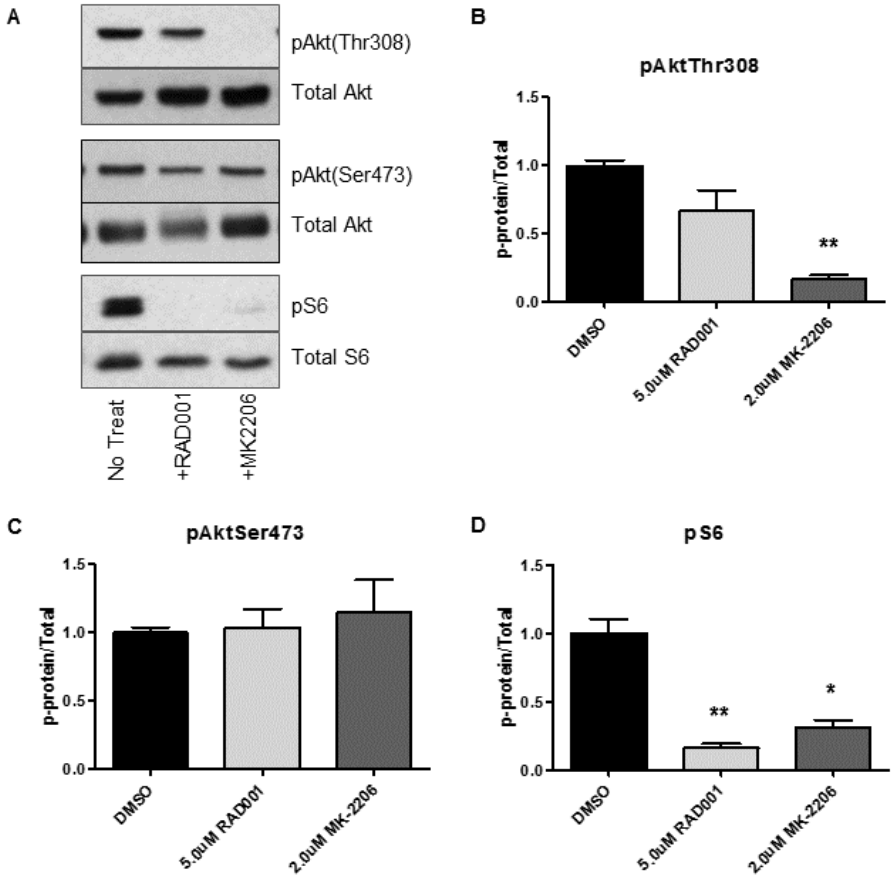

Figure 13. Western blot analysis of levels of Akt and S6 phosphorylation in treated or untreated *Pten*$^{+/+}$ cultures. RAD001 preferentially suppresses pS6, whereas MK-2206 suppresses both pAkt and pS6 levels. **(A)** Representative images of Western blot for pAkt(Thr308), pAkt(Ser473) and pS6 (Ser235/236) in DIV 10 wild type cortical cultures treated with DMSO control, 5.0 µM RAD001 or 2.0 µM MK-2206 for 4 hours. **(B-D)** Quantification of p-protein over total for pAkt(Thr308), pAkt(Ser473) and

pS6(Ser235/236); (*p<0.05, **p<0.01 by Kruskal-Wallis test, n>4 mice per treatment.) . Bar graphs show the mean values ± SEM

We wanted to ensure that our treatment, while sufficient to reverse the hypertrophic phenotype of *Pten*$^{-/-}$ neurons, was mild enough not to cause morphological changes in wild type neurons with baseline PI3K/Akt/mTOR signaling activity. We therefore tested whether heterozygous neurons retain their morphology after drug treatments. We used heterozygotes because they were readily available in every culture and are indistinguishable in signaling and morphology from wild type neurons. We found that heterozygous neurons do not lose soma area or dendritic branching as a result of MK-2206 or RAD001-mediated Akt or mTORC1 suppression (Fig. 14 A-B), suggesting that there may be viable treatments schemes for *in vivo* use that will naturally target neurons with endogenous excess PI3K/Akt/mTOR signaling, while leaving healthy neurons unaffected.

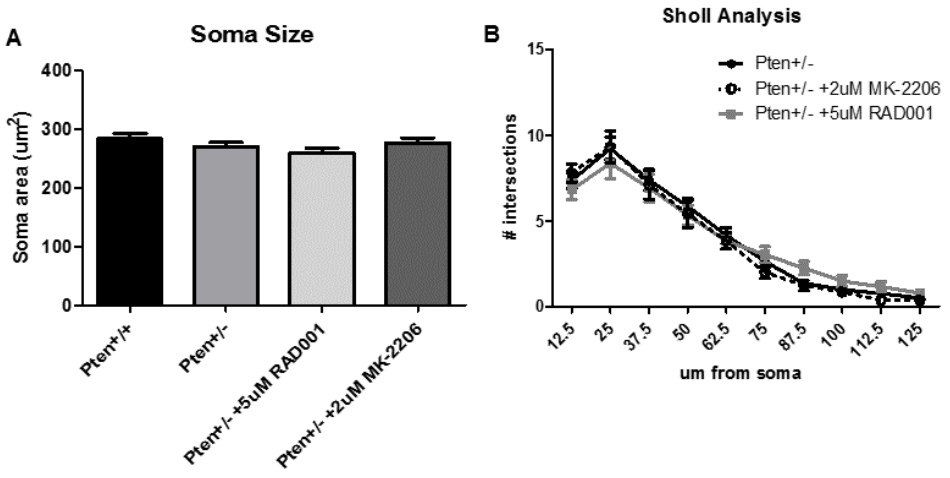

Figure 14. (A) Soma size quantification of morphologically normal *Pten*$^{+/-}$ neurons treated for 4 hours with DMSO or 5. 0μM RAD001 or 2.0 μM MK-2206 (p>0.05, by

Kruskal-Wallis test, *n*=3 mice per treatment). **(B)** Sholl analysis of dendrites from morphologically normal *Pten*$^{+/-}$ neurons treated for 4 hours with DMSO, 5.0 µM RAD001 or 2.0 µM MK-2206 ($p>0.05$, by Kruskal-Wallis test, *n*=3 mice per treatment). Bar graphs show the mean values ± SEM

Since brain overgrowth disorders are consistently accompanied by epilepsy (Inoki et al, 2002; D'Arcangelo, 2009; Jansen et al, 2015; Moavero et al, 2015; Roy et al, 2015), we hypothesized that *Pten*$^{-/-}$ neurons will exhibit signaling abnormalities and increased excitability *in vitro*. We cultured wild type and knockout hippocampal neurons for 11 DIV before sending them to Dr. Bonnie Firestein's laboratory for the recording miniature excitatory post-synaptic currents (mEPSCs) by Przemyslaw Swiatkowski. Briefly, results showed no differences in amplitude of mEPSCs between *Pten*$^{+/+}$ and *Pten*$^{-/-}$ cells. However, cultured *Pten*$^{-/-}$ neurons experienced higher frequency of mEPSCs than wild type *Pten*, which suggests increased spontaneous vesicle release at the presynaptic terminal. This finding supports the possibility that enlargement of cells in the brain leads to heightened excitability and the potential for epileptogenesis.

NEX-Cre driven Tsc2 deletion is excitatory neuron-specific

Since *Pten* and *Tsc2* gene deletion activate different components of the PI3K/Akt/mTOR signaling cascade, we wanted to analyze differences *in vitro* between NEX-*Pten* and NEX-*Tsc2* mutant neurons. Just like with the *Pten*$^{-/-}$ neurons described above, we confirmed that only excitatory neurons, and not interneurons or astrocytes, experience mTORC1 activation as revealed by increased pS6 fluorescent signal. This is as an indirect way of assessing NEX-Cre expression and gene knockout specificity ($p<0.001$, $p>0.05$, and $p>0.05$, respectively, Mann Whitney U test, *n*=3 mice per genotype) (Fig. 15 A-B). Furthermore, the approximate increase in pS6 fluorescence

from wild type to *Tsc2*$^{-/-}$ neurons is 9.5-fold, which is extremely similar to the 8.3-fold increase in pS6 signal that we observed in *Pten*$^{-/-}$ knockout neurons when we compared them to their wild type counterparts.

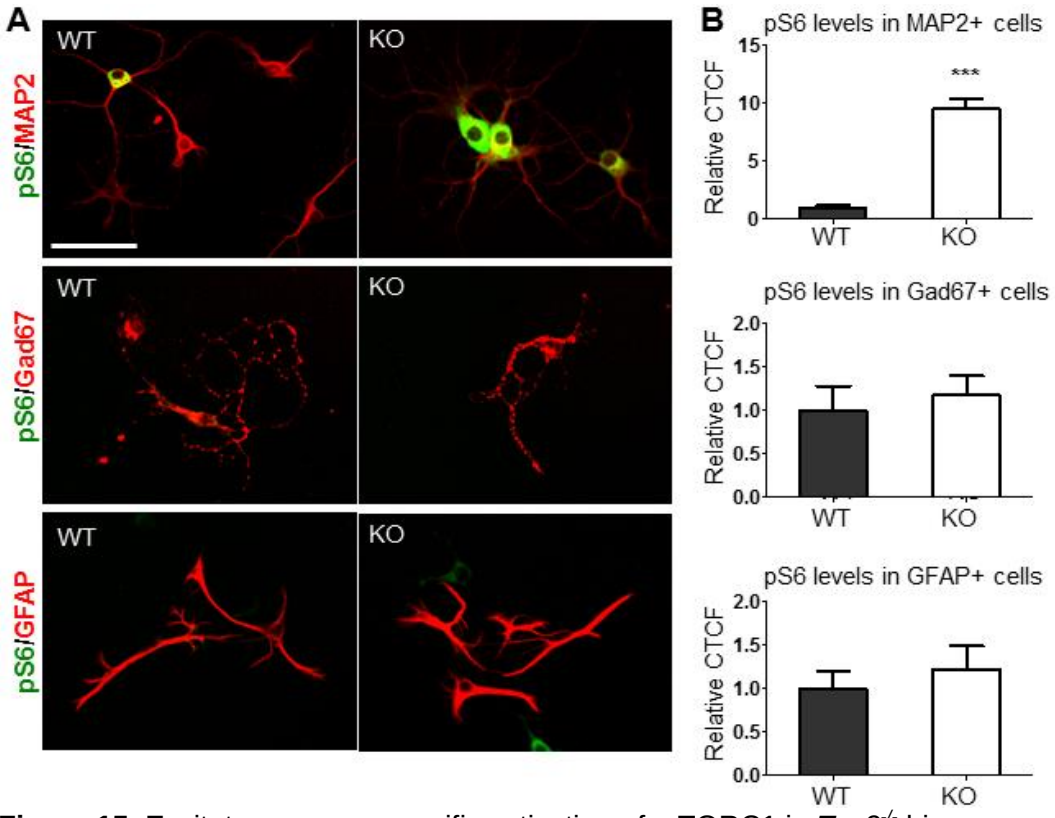

Figure 15. Excitatory neuron-specific activation of mTORC1 in *Tsc2*$^{-/-}$ hippocampal cultures. **(A)** Strong pS6 signal was seen preferentially in knockout cultures, and co-localized with the MAP2 signal in neurons, but not with the Gad67 signal in inhibitory neurons or the GFAP signal in astrocytes. **(B)** Quantification of the CTCF for pS6 levels in different cell types demonstrates that only MAP2+ neurons exhibit a statistically significant increase in pS6 levels in *Tsc2*$^{-/-}$ cultures compared to WT. (p<0.001, p>0.05, p>0.05 for MAP2+, Gad67+ and GFAP+ cells, respectively, by Mann Whitney U test, n=3 mice per genotype) Bar graphs show the mean values relative to *Tsc2*$^{+/+}$ ± SEM; Scale bar: 20µm.

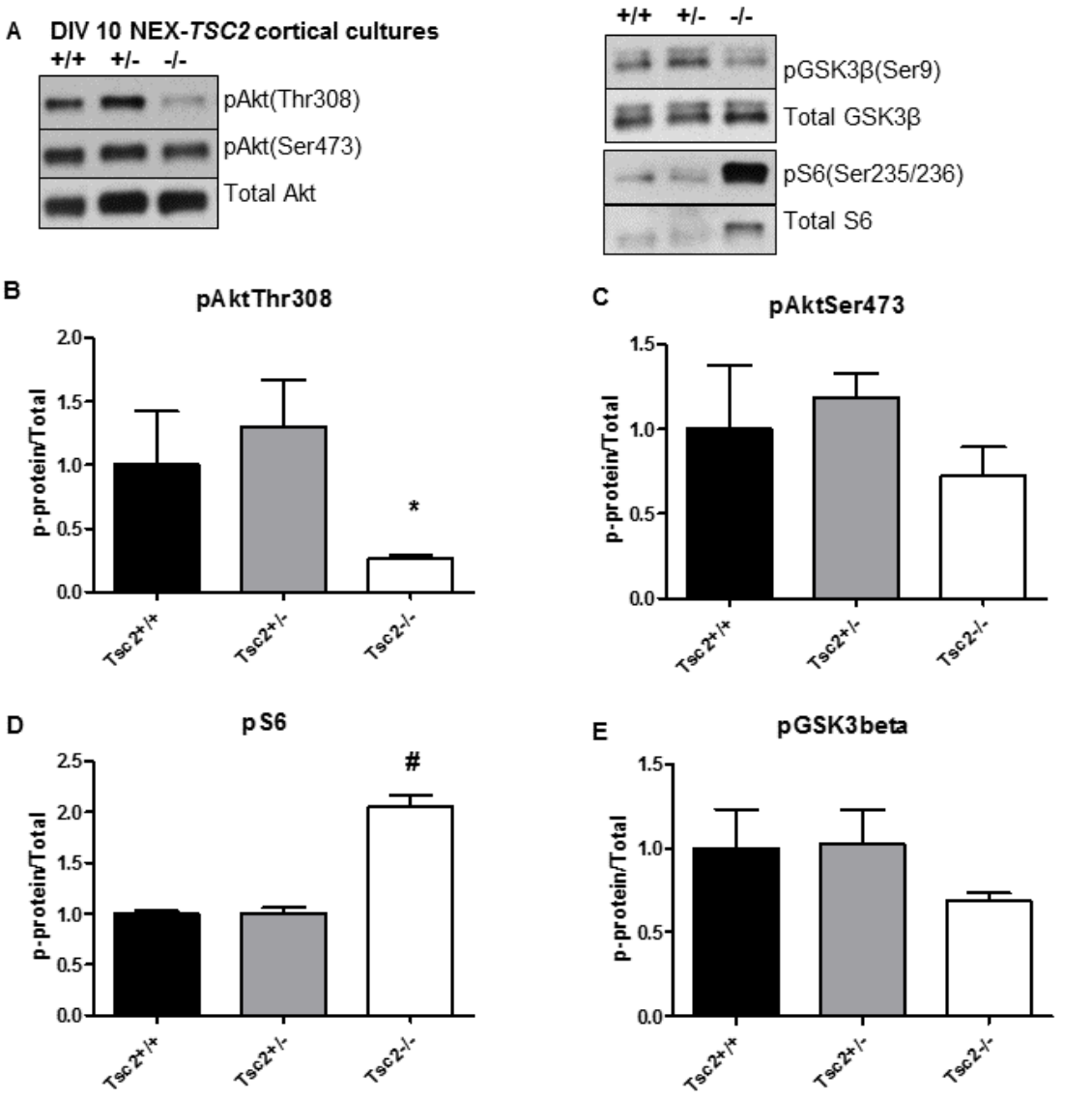

Figure 16. Western blot analysis of the PI3K/Akt/mTOR pathway in NEX-*Tsc2* cortical cultures. **(A)** Representative Western blots of phosphorylated and total Akt, S6 and GSK3β in DIV 10 cortical cultures from $Tsc2^{+/+}$, $Tsc2^{+/-}$ and $Tsc2^{-/-}$ mice. **(B-E)** Quantification of Western blot data for PI3K/Akt/mTOR signal in DIV 10 cortical neuron cultures from $Tsc2^{+/+}$, $Tsc2^{+/-}$ and $Tsc2^{-/-}$ mice. (* p<0.05, # p<0.1 by Kruskal-Wallis test, n=3 mice per genotype.) Bar graphs show the mean values ± SEM

$Tsc2^{-/-}$ neurons exhibit enlarged soma and increased dendritic arborization; both $Tsc^{+/-}$ and $Tsc2^{-/-}$ neurons have increased number of axons per cell

We assessed soma size, axon count and dendritic branching of DIV 10 $Tsc2^{+/+}$, $Tsc2^{+/-}$, and $Tsc2^{-/-}$ hippocampal neurons by staining with antibodies against axonal marker Tau and dendritic marker MAP2. Similar to NEX-*Pten* knockout neurons, NEX-*Tsc2* knockout neurons exhibit enlarged soma and increased dendritic branching when compared to wild type neurons from the same litter. It is interesting to note that the soma size phenotype in $Tsc2^{-/-}$ neurons is not as extreme as it is in $Pten^{-/-}$ neurons. The average fold increase in soma area from wild type to Pten-deficient neurons is 2x, while it is only 1.5x for Tsc2-deficient neurons. Furthermore, both $Tsc2^{+/-}$ and $Tsc2^{-/-}$ neurons exhibit an increased axon number phenotype (Fig. 17 A, D). This abnormal morphology was not observed in either the heterozygous or homozygous knockout Pten neurons (unpublished data, Dr. Tatiana Kazdoba-Leach). These data raise several questions about the control of growth, polarity and branching in neurons by PI3K/Akt/mTOR. Our comparison of $Tsc2^{-/-}$ and $Pten^{-/-}$ neurons *in vitro* suggest that Akt and mTORC1 have overlapping, yet not identical, roles in dendritic branching and soma size, and distinct effects on neuronal polarity and axonal development. These differences in function may account for some of the variety and severity of symptoms in brain overgrowth disorder patients. Furthermore, our findings suggest that not all PI3K/Akt/mTOR activity disorders can be treated with one “silver bullet” compound; it may be necessary to develop targeted inhibitors for each affected kinase in order to confer maximum benefits to every patient.

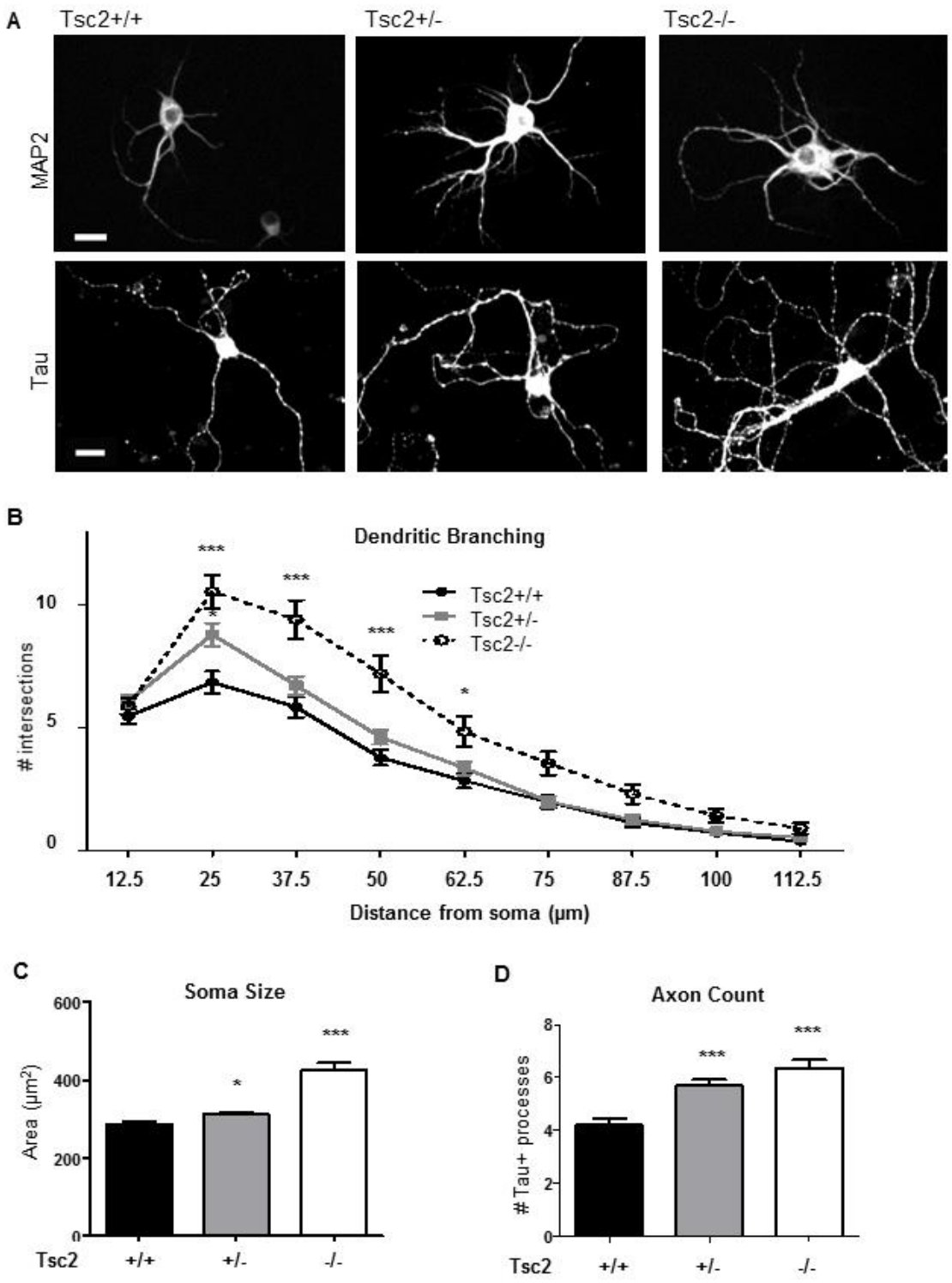

Figure 17. **(A)** Representative images of dendritic (MAP2) and axonal (Tau) markers of *Tsc2*$^{+/+}$, *Tsc2*$^{+/-}$ and *Tsc2*$^{-/-}$ P0 DIV 10 hippocampal neurons. **(B)** Sholl analysis of MAP2+ processes of *Tsc2*$^{+/+}$, *Tsc2*$^{+/-}$ and *Tsc2*$^{-/-}$ DIV 10 hippocampal neurons (* p<0.05 by

Kruskal-Wallis test, $n \geq 3$ mice per genotype). **(C)** Quantification of soma area in DIV 10 hippocampal MAP2+ neurons (*** $p<0.001$ by Kruskal-Wallis test, $n \geq 3$ mice per genotype). **(D)** Axon count of Tau+ processes longer than the diameter of the soma. *Tsc2*$^{-/-}$ neurons have larger soma, more branched dendrites and higher number of axons (* $p<0.05$, *** $p<0.001$ by ANOVA, $n \geq 3$ mice per genotype). Bar graphs show the mean values ± SEM. Scale bar: 20µm.

---

4. Discussion

Brain overgrowth disorders are a devastating group of diseases that can present with crippling epilepsy, intellectual disability, and lesions or benign tumors in the brain. When the epileptic seizures cannot be controlled pharmacologically, the only available treatment is surgical resection of the seizure foci. The PI3K/Akt/mTOR pathway has long been associated with the pathology of these disorders. Many patients of brain overgrowth disorders carry somatic mutations in *PTEN*, *PI3K*, *AKT* or *MTOR*, or hereditary mutations in *TSC1* or *TSC2* (Jansen et al, 2015). It is therefore important to study how loss or gain of function at different levels of the pathway impacts neurons, and whether defects can be pharmacologically reversed in order to avoid brain surgery or improve upon brain surgery outcomes.

In this study, we characterized Pten-deficient and Tsc2-deficient primary cultured hippocampal neurons, and showed that certain hypertrophic phenotypes are pharmacologically reversible in the *Pten*$^{-/-}$ model without influencing wild type neuronal morphology. Finally, we also compared hypertrophic phenotypes of *Pten*$^{-/-}$ neurons to those observed in *Tsc2*$^{-/-}$ neurons of the same age and found both similarities and differences in their morphological abnormalities.

Pten$^{-/-}$ neurons have enlarged soma and increased dendritic branching but show no change in the number of their axons. Both the soma and dendrite phenotype can be reversed by a transient treatment with mTORC1 inhibitor RAD001 or Akt inhibitor MK-2206. Our study showed that neither of these treatments affects neurons with wild type-level PI3K/Akt/mTOR signaling. The RAD001 treatment had a much weaker impact on Akt activity than MK-2206, which may account for the differences in their efficacies to suppress hypertrophy. While MK-2206 returned soma size to fully within wild type levels, RAD001 significantly reduced soma size but *Pten*$^{-/-}$ neurons remained statistically distinct from *Pten*$^{+/+}$ neurons. Furthermore, MK-2206 caused a consistently greater decrease of dendritic branching in mutant cells than RAD001 did. MK-2206 had a less pronounced effect on pS6 levels and, by extension, mTORC1 activity. However, it was extremely effective in suppressing pAkt(Thr308) levels. Therefore, it is reasonable to speculate that mTORC1 is not completely responsible for the hypertrophic phenotype of *Pten*$^{-/-}$ neurons, especially with regard to the soma enlargement. Our data suggest that Akt modulates mTORC1-dependent and independent processes that control soma size and dendritic branching in mature neurons.

To support this, we examined *Tsc2*$^{-/-}$ neurons using the same NEX-Cre recombinase, breeding strategy and culturing conditions. Since Tsc2 acts as a negative regulator immediately upstream of the mTORC1 signaling cascade, any effects on morphology from this mutation can be reasonably attributed to excess mTORC1 activity. Indeed, *Tsc2*$^{-/-}$ neurons exhibited both an enlarged soma and increased dendritic tree, but the former was less extreme than the change we observed in Pten-deficient neurons. Unexpectedly, we also found a neuronal polarity phenotype in both heterozygous and homozygous knockout *Tsc2*$^{-/-}$ neurons. Both sets of neurons had a higher number of axons than wild type counterparts by DIV 10, which was not observed in *Pten*$^{+/-}$ or *Pten*$^{-/-}$ neurons (unpublished data). PI3K/Akt/mTOR pathway signaling differences were also

evident between the two mutant strains. While *Pten*$^{-/-}$ neurons experience excess Akt, mTORC1 and mTORC2 signaling (measured by pAkt(T308), pS6 and pAkt(S473), respectively), *Tsc2*$^{-/-}$ neurons have reduced Akt, increased mTORC1 and unaltered mTORC2 activity. Therefore, it is likely that other targets of Akt and mTORC2 can regulate soma size and neuronal polarity independent of mTORC1.

These findings raise two key questions that require further study. First, could pharmacological treatments against the PI3K/Akt/mTOR signaling cascade successfully reverse the hypertrophic neuronal phenotype *in vivo* and ameliorate epilepsy in brain overgrowth disorder patients? And second, what mechanisms might lie behind Akt and mTORC2's effects on soma size and dendritic branching and mTORC1's effects on axon number? This study suggests that even if pharmacological alternatives to surgery for brain overgrowth disorders are developed, patients with a mutation upstream of *TSC1/2* may respond differently to PI3K/Akt/mTOR inhibitor therapy than patients with mutations downstream of *TSC1/2.* Therefore, patients with these disorders may benefit heavily from the growing trends in personalized medicine research, as patients might need to receive tailored treatments in order to gain optimal symptom relief with minimal side effects.

CHAPTER 4: CONCLUSION AND FUTURE DIRECTIONS

1. Modulation of PI3K/Akt/mTOR signal following traumatic brain injury

With the incidence of traumatic brain injury on the rise, researchers have focused many efforts on studying the complex responses of the damaged and healing brain. Modulation of these processes may lead to minimization of long term negative effects experienced by victims of TBI. TBI sequelae can manifest days or months after the initial injury, but the groundwork for post-traumatic conditions such as epilepsy or behavioral defects is laid much sooner than that (Don et al, 2012; Zhou et al, 2012; Guo et al, 2013; Park et al, 2013). Therefore, by the time symptoms appear, the therapeutic window has mostly closed and treatment options are limited. Research has shown that the PI3K/Akt/mTOR pathway is involved in both the repair response necessary to restore as much of the damaged tissue and connections as possible, and as a medium for secondary damage by stimulating inflammation and exacerbating neuronal death (Erlich et al, 2007; Wu et al, 2013; Zhu et al, 2014) (Table 3). It is therefore essential for researchers to determine what is the appropriate level and timing of PI3K/Akt/mTOR induction for optimal benefits and minimal side effects in the brain.

In the study presented in Chapter 2, we analyzed the time course of PI3K/Akt/mTORC1 activation and selected mTORC1 activity as our drug target. We hypothesized that the highest peak of mTORC1 induction is where activity is in excess and stimulates detrimental pathways. We targeted that peak induction with a single rapamycin injection following brain injury and successfully suppressed it down to basal levels of mTORC1 signaling, as measured by its downstream target pS6. This single-injection treatment strategy was sufficient to reduce neuronal damage in the hippocampus by 24 hours after injury as measured by FJB staining, and to reduce astrocyte-mediated inflammation on the C-side of the brain. The notion that the inflammatory response occurs in the uninjured side of the brain following TBI is a fairly

recent one, and very few research groups have studied it to date (Clausen et al, 2009; Wiley et al, 2015). Most TBI studies focus on a sham versus a CCI- or FP-injured cortex and hippocampus without looking at the adjacent uninjured side (Chen et al, 2007; Park et al, 2012). However, the reach and effects of secondary damage following TBI are now shown to extend across to the furthest parts of the patient's brain (Clausen et al, 2009; White et al, 2013).

When we compared our treatment strategy to other studies using rapamycin in conjunction with various models of TBI, we discovered that our treatment results in many of the benefits scattered across other studies (Table 3). When we plotted treatments in literature on a time course, we realized that there is likely an optimal time to administer rapamycin suppression. Furthermore, beginning at 24 hours post-TBI, it becomes unclear whether the benefits of suppressing the pathway outweigh the benefits of inducing it. Rapamycin treatment after injury over the course of 4 weeks decreased incidence of TBI-induced epilepsy. However, prolonged treatment with simvastatin, which induces the pathway at the Akt level, rescued cell division post-TBI (Wu et al, 2008; Guo et al, 2013). Finally, based on our discussion on the differential effects of Akt and mTORC1 on neuronal growth and polarity in Chapter 3, it may be necessary to analyze the activity and optimal suppression timing of each of the 3 major kinases of the PI3K/Akt/mTORC1 pathway, as they may have distinct roles during healing and secondary damage in the brain.

Future studies should combine the timed suppression and induction schedules of PI3K/Akt/mTORC1 for an optimal protocol to be followed in TBI patients after injury. Effects may be dependent upon the type of brain injury suffered and its severity. Finally, such treatments may be able to partially or fully offset the additive deficits caused by repetitive TBI, thereby improving patient outcomes.

				Observed benefits				
Author, Year	**Type of TBI**	**mTORC1 ↑ or ↓**	**Time course**	**↓ Inflammation**	**↑ Cell division**	**↓ Neuronal death/ damage**	**Behavioral improvement**	**↓ Seizures**
Wu et al, 2008	CCI in rats	↑ (indirectly by simvastatin)	Day 1 after TBI, then daily for 14 days		√		√	
Guo et al, 2013	CCI in mice	↓ (rapamycin)	1hr post-TBI, then daily for 4 weeks			√		√
Park et al, 2012	CCI in mice	↓ (rapamycin + Akt inhibitor VIII)	Immediately before CCI	X		√	√	
Erlich et al, 2007	CHI in mice	↓ (rapamycin)	4hr post-TBI	√ (microgliosis only; no effect on astrogliosis)		√	√	
Zhu et al, 2014	CHI in mice	↓ (rapamycin)	Immediately before CHI				XX	
Rozas et al, 2014	CHI in mice	↑ (Tsc2+/-)	N/A - genetic	X		X	XX	
Mao et al, 2013	stroke in mice	↑ (bpV)	14 days, starting 24hrs post-occlusion			√	√	
Nikolaeva et al, 2015	CCI in mice	↓ (rapamycin)	1hr post-TBI	√		√	√	

Table 4. Comparison of strategy and findings of studies using mTORC1 modulation following TBI. √=improvement; **X**=no change; **XX**= deterioration; gray box=not tested.

---

2. Akt inhibition in a Pten-deficient model of brain overgrowth

Brain overgrowth disorders such as focal cortical dysplasia, hemimegalencephaly and tuberous sclerosis complex commonly present with intractable (drug-resistant) epilepsy. Patients with such seizures have only one treatment option: surgical resection of any discernable seizure foci. These surgical procedures are only effective approximately 60% of the time. Furthermore, many surgical candidates are children and infants, and can be as young as only a few months of age (Kloss et al, 2002; Ljungberg et al, 2006; D'Arcangelo, 2009; Hu et al, 2015; Jansen et al, 2015). While regular anti-epileptic drugs have no effect on intractable epilepsy, experimental treatments in targeting synaptogenesis, network rearrangement, and cell growth in rodents have shown promising reversal of epileptiform activity and cell dysmorphism in models of brain overgrowth (Kazdoba et al, 2012; Andersen et al, 2014; Roy et al, 2015). Intractable epilepsy and dysmorphic neurons with increased PI3K/Akt/mTORC1 signaling are present in most cases of brain overgrowth. Enlargement of the cerebral cortex is caused by increased cell division, enlarged cell size or a combination of the two. Other features of the disease are only present in a subset of cases, such as neuronal migration defects and balloon cells (Hung et al, 2005; Ljungberg et al, 2006; Guerrini and Barba, 2010; Bozzi et al, 2012; Mirzaa and Poduri, 2014; Rossini et al, 2014; Chen et al, 2015). While neuronal migration defects are present in some animal models as well, they do not need to be corrected by drug treatments in order to reduce or eliminate seizures in rodents (Kazdoba et al, 2012; Baek et al, 2015; Roy et al, 2015).

We therefore hypothesized that targeting the enlargement defect in the cells of FCD, HMEG and TSC patients may hold the key to reducing seizure activity.

In the study described in Chapter 3, we showed that Pten-deficient neurons *in vitro* show enlarged soma size and increased dendritic branching. This phenotype also appeared to be associated with increased excitability, as demonstrated in electrophysiological experiments conducted at our collaborator Dr. Bonnie Firestein's lab (data not shown). We were able to reverse the overgrowth phenotype with Akt inhibitor MK-2206, without affecting wild type neurons. mTORC1 suppressor RAD001 was able to partially reverse both the dendritic and soma size phenotype, suggesting that Akt may send additional signals through mTORC1-independent pathways to stimulate cell growth in neurons. If future experiments *in vitro* indicate that MK-2206 can also return electrical properties of dysmorphic neurons back to normal levels, studies will have to focus on testing the drug for phenotype reversal in live mouse and other rodent models. If drugs such as RAD001 and MK-2206 can actively reverse neuronal hypertrophy *in vivo*, and ameliorate electrical properties of the neurons, they may provide pharmacological alternatives to surgical resection of seizure foci in the brain. It is important to note that we have not investigated effects of either drug on balloon cells, such as those present in FCDIIb (D'Arcangelo, 2009). These cells are electrically inactive, and are somewhat unlikely candidates for seizure induction; nevertheless, their impaired-autophagy phenotype may eventually lead to other neurological disorders if left untreated. Since balloon cells are considered to be primarily the result of faulty differentiation, a stem-cell model or very early embryonic Pten deletion may be a more appropriate model for such cells (Ljungberg et al, 2006; D'Arcangelo, 2009; Yasin et al, 2013).

Genetic studies in patients with brain overgrowth disorders, such as FCD and HMEG, have identified loss-of-function mutations in the negative regulator *PTEN* gene, and gain-of-function mutations in *AKT*, *MTOR*, and *PI3K* (Le Belle et al, 2014; Mirzaa

and Poduri, 2014; Chen et al, 2015; Jansen et al, 2015; Lim et al, 2015; Lin et al, 2015; Winden et al, 2015). Furthermore, hereditary brain overgrowth disorder TSC is caused primarily by loss-of-function mutations in mTORC1 negative regulators *TSC1* or *TSC2* genes (Feliciano et al, 2013; Tavazoie et al, 2015). Studies *in vivo* in rodents have suggested that treatments such as rapamycin or PI3K inhibitor BKM120 can reverse the growth phenotype and reduce seizure activity (Kazdoba et al, 2012; Baek et al, 2015; Roy et al, 2015). In our study, we used mTORC1 inhibitor RAD001 and Akt inhibitor MK-2206 to reverse the overgrowth phenotype of *Pten*$^{-/-}$ neurons *in vitro*. There are two benefits to this approach. Performing the assay *in vitro* allowed us to do detailed morphological analysis of neurons and do statistical comparisons of exact soma size and branching phenotypes to directly compare the two inhibitors. Furthermore, our study is of high translational value as both RAD001 and MK-2206 are currently showing promising results in terms of drug safety in clinical trials, and can both be administered orally instead of via injection. Finally, both are highly soluble as compared to rapamycin and other PI3K/Akt/mTORC1 inhibitors (Schuler et al, 1997; Hirai et al, 2010, Pal et al, 2010).

3. Comparison of Pten- and Tsc2-deficient neurons

TSC is known as the hereditary member of the brain overgrowth disorder group. Affecting on average 1 person in every 6-10 000, the disease's underlying cause is an inactivating mutation either in the *TSC1* or *TSC2* gene (Napolioni et al, 2009; Tsai et al, 2012; Feliciano et al, 2013). Recent studies into the genetics of the disorder suggest that about 30% of patients have an inherited germline mutation, another ~50% carry some form of mosaicism for a mutation, 2-3% of patients have a *de novo* sporadic mutation, and the remaining 10-15% show no detectable alteration in either gene (Feliciano et al, 2013; Tuburczy et al, 2015). Studies focusing on these two genes have shown that deletion of *Tsc1* in mouse neuronal progenitor cells lead to formation of the TSC

equivalent of dysmorphic neurons, referred to as giant cells. Giant cells generated *in vivo* in a mouse model in this way have a more complex dendritic tree than wild types, at a similar fold increase of branching as what we observed *in vitro* in Chapter 3 for *Tsc2*$^{-/-}$ neurons (Goto et al, 2011). Other reported abnormalities in Tsc1- or Tsc2-deficient cells include enlarged soma, spine density defects, altered gene expression, and increased electrical excitability (Tavazoie et al 2005; Nie et al, 2015).

Our study reveals a new phenotype in Tsc2-haploinsufficient hippocampal neurons, which has not been previously reported in this cell type. Brain overgrowth disorders can be caused by both the heterozygous and homozygous gene inactivation of the PI3K/Akt/mTOR pathway. TSC cases are associated with heterozygous mutations, with predicted loss of heterozygosity in at least some of the cells of cortical tubers and lesions, which form in the brain. Other proposed genetic mechanisms of TSC include autosomal dominant mutations, and dosage effect (Tavazoie et al 2005; Nie et al, 2010; Goto et al, 2011; Feliciano et al, 2013). However, in mouse neurons, a developmental phenotype in *Tsc1*$^{+/-}$ or *Tsc2*$^{+/-}$ cells is rarely observed, and only in specific cell types to date. Two examples are enlarged soma and dendritic branching in *Tsc1*$^{+/-}$ Purkinje cells and impaired axonal growth cone collapse in *Tsc2*+/- retinal cells (Nie et al, 2010; Tsai et al, 2012). Here, we report that excitatory neurons in the *Tsc2*$^{+/-}$ condition have a slightly enlarged soma and dendritic branching phenotype, accompanied by clear increase in number of axons. Furthermore, just like homozygous *Tsc1*$^{-/-}$ hippocampal neurons, *Tsc2*$^{-/-}$ neurons also form more axons than wild type counterparts (Nie et al, 2010). Increase in axonal number appears to be a *Tsc1/Tsc2*-deletion specific phenotype, since genetic upregulation of the pathway starting at the PI3K or Akt level does not have the same effect unless an injury is used to stimulate axonal regeneration (Park et al, 2008; unpublished data).

We generated cultures from *Tsc2*-deficient mice in order to compare their phenotype to that of *Pten*$^{-/-}$ neurons. We observed that while Pten-deficient neurons have a more severe soma size enlargement, *Tsc2*-negative neurons have an axonal phenotype not previously observed in the NEX-*Pten* strain in our lab. We hypothesize that differential signaling (lowered Akt and unchanged mTORC2 signaling) in mTORC1-independent targets is responsible for governing neuronal polarity. One potential target to explain this difference was GSK3β; however, the signaling differences between wild type and knockout cultures were not statistically significant. Even if statistical significance had been achieved, the more GSK3β is phosphorylated and inhibited by Akt, the more axons each neuron should grow (Jiang et al, 2004). Since Akt and GSK3β are both less active in the *Tsc2*$^{-/-}$ neurons, GSK3β signaling is unlikely to be the underlying mechanism. From the signaling proteins we probed for, only two differed in trends from wild type to mutant between the NEX-*Pten* and NEX-*Tsc2* cultures: pAkt(Ser473) (mTORC2 target) and pAkt(Thr308). mTORC1-dependent pS6 phosphorylation levels were similarly induced in Pten and Tsc2 knockouts, as measured both by Western blot and immunofluorescence. It is therefore more likely that neuronal polarity and the decision to generate extra axons is mediated by an mTORC1-independent target of mTORC2 or Akt. Nie et al suggest Ephrin signaling as a potential mediator of axonal growth cone collapse (Nie et al, 2010). Other studies into the *Tsc1*$^{-/-}$ multi-axonal phenotype implicate the SAD family of kinases (Choi et al, 2008). Finally, a study from 2006 suggests ubiquitination and depletion of Akt from the dendrites stimulates axon formation; perhaps depleting active Akt in the neuron as compensation for overactive mTOR has the same effect (Yan et al, 2006). More studies need to be performed in order to elucidate the mechanism through which Tsc1/Tsc2 controls axonal outgrowth.

In conclusion, our study indicates targeting different members of the PI3K/Akt/mTORC1 pathway may need to be tailored to each patient's underlying genetic makeup. While mutations in *PTEN*, *PI3K*, *AKT*, and *MTOR* do not appear to account for the majority of brain overgrowth disorders in humans, an overactive PI3K/Akt/mTORC1 pathway is almost always observed in cytomegalic neurons of resected brain tissue. Therefore, even if the underlying mutation is not in one of the major players of the signaling cascade, it results in uncontrolled activation of the pathway and Akt or mTORC1 inhibitors could still be used to counteract the events of overgrowth in such patients. In the case of TSC, up to 85% of patients are found to have mutations in *TSC1* or *TSC2*, and therefore mTORC1 inhibitors specifically may prove most beneficial to them. The studies presented here hint at the delicate balance of the PI3K/Akt/mTOR signaling cascade, which must be maintained during development and healing in the brain. The wrong timing or level of induction of the pathway is sufficient to cause destructive medical conditions such as epilepsy, intellectual disability and behavioral difficulties. We must continue to examine the pathway and generate more data about the boundaries between benefit and detriment before clinical trials can be undertaken in younger patients or victims of brain injury.

BIBLIOGRAPHY

Albertson AJ, Yang J, Hablitz JJ. (2011) Decreased hyperpolarization-activated currents in layer 5 pyramidal neurons enhances excitability in focal cortical dysplasia. *J Neurophysiol.* 106:2189-2200.

Andersen L, Hampton D, Taylor-Weiner A, Morel L, Yang Y, Maguire J, Dulla CG. (2014) Gabapentin attenuates hyperexcitability in the freeze-lesion model of developmental cortical malformation. *Neurobiol Dis.* 71:305-316.

Auguin D, Barthe P, Auge-Senegas MT, Stern MH, Noguchi M, Roumestand C. (2004) Solution structure and backbone dynamics of the pleckstrin homology domain of the human protein kinase B (PKB/Akt). Interaction with inositol phosphates. *J Biomol NMR.* 28: 137-155.

Baar EL, Carbajal KA, Ong IM, Lamming DW. (2015) Sex- and tissue-specific changes in mTOR signaling with age in C57BL/6J mice. *Aging Cell.* DOI: 10.1111/acel.12425.

Backman SA, Stambolic V, Suzuki A, Haight J, Elia A, Pretorius J, Tsao MS, Shannon P, Bolon B, Ivy GO, Mak TW. (2001) Deletion of *Pten* in mouse brain causes seizures, ataxia and defects in soma size resembling Lhermitte-Duclos disease. *Nat Gen.* 29: 396-403.

Baek ST, Copeland B, Yun EJ, Kwon SK, Guemez-Gamboa A, Schaffer AE, Kim S, Kang HC, Song S, Mathern GW, Gleeson JG. (2015) An AKT3-FOXG1-reelin network underlies defective migration in human focal malformations of cortical development. *Nat Med.* DOI: 10.1038/nm.3982.

Barlow AD, Xie J, Moore CE, Campbell SC, Shaw JA, Nicholson ML, Herbert TP. (2012) Rapamycin toxicity in MIN6 cells and rat and human islets is mediated by the inhibition of mTOR complex 2 (mTORC2). *Diabetologia*. 55(5):1355-136

Bassi C, Ho J, Srikumar T, Dowling RJO, Gorrini C, Miller SJ, Mak TW, Neel BG, Raught B, Stambolic V. (2013) Nuclear PTEN controls DNA repair and sensitivity to genotoxic stress. *Science*. 341: 395-399.

Bhattacharya A, Mamcarz M, Mullins C, Choudhury A, Boyle RG, Smith DG, Walker DW, Klann E. (2015) Targeting translation control with p70 S6 kinase 1 inhibitors to recerse phenotypes in Fragile X Syndrome mice. *Neuropsychopharmacology.* DOI: 10.1038/npp.2015.369.

Bozzi Y, Casarosa S, Caleo M. (2012) Epilepsy as a neurodevelopmental disorder. *Front Psych.* DOI:10.3389/fpsyt.2012.00019.

Briaud I, Dickson LM, Lingohr MK, McCuaig JF, Lawrence JC, Rhodes CJ. (2005) Insulin receptor substrate-2 proteasomal degradation mediated by a mammalian target of rapamycin (mTOR)-induced negative feedback down-regulates protein kinase B-mediated signaling pathway in β-cells. *J Biol Chem.* 280(3): 2282-2293.

Browne KD, Chen XH, Meaney DF, Smith DH. (2011) Mild traumatic brain injury and diffuse axonal injury in swine. *Journal of Neurotrauma*, 28(9):1747-1755.

Buel GR, Blenis J. (2016) Seeing mTORC1 specificity. *Science*. 351(6268):25-26.

Cafferkey R, Young PR, McLaughlin MM, Bergsma DJ, Koltin Y, Sathe GM, Faucette L, Eng WK, Johnson RK, Livi GP. (1993) Dominant missense mutation in a novel yeast protein related to mammalian phosphatidylinositol 3-kinase and VPS34 abrogate rapamycin cytotoxicity. *Mol Cell Biol.* 13(10): 6012-6023.

Calikoglu C, Aytekin H, Akgul O, Akgul MH, Gezen AF, Akyuz F, Cakir M. (2015) Effects of pregabalin in preventing secondary damage in traumatic brain injury: an experimental study. *Med Sci Monit.* 21: 813-820.

Cardamone M, Flanagan D, Mowat D, Kennedy SE, Chopra M, Lawson JA. (2014) Mammalian target of rapamycin inhibitors for intractable epilepsy and subepndymal giant cell astrocytomas in tuberous sclerosis complex. *J Pediatr.* 164(5):1195-1200.

Carroll B, Maetzel D, Maddocks ODK, Otten G, Ratcliff M, Smith GR, Dunlop EA, Passos JF, Davies OR, Jaenisch R, Tee AR, Sarkar S, Korolchuk VI. (2016) Control of TSC2-Rheb signaling axis by arginine regulates mTORC1 activity. *eLife*. 10.7554/eLife.11058.

Carson RP, Kelm ND, West KL, Does MD, Fu C, Weaver G, McBrier E, Parker B, Grier MD, Ess KC. (2015) Hypomyelination following deletion of *Tsc2* in oligodendrocyte precursors. *Ann Clin Transl Neurol.* 2(12): 1041-1054.

Chen CC, Hung TH, Lee CY, Wang LF, Wu CH, Ka CH, Chen SF. (2014) Berberine protects against neuronal damage via suppression of glia-mediated inflammation in traumatic brain injury. *PLoS ONE*. 9(12):e115694, DOI: 10.1371/journal.pone.0115694.

Chen S, Atkins CM, Liu CL, Alonso OF, Dietrich WD, Hu BR. (2007) Alterations in mammalian target of rapamycin signaling pathways after traumatic brain injury. *Cerebral Blood Flow & Metabolism*, 27:939-949.

Chen Y, Huang WC, Sejourne J, Clipperton-Allen AE, Page DT. (2015) *Pten* mutations alter brain growth trajectory and allocation of cell types through elevated β-catenin signaling. *Neurobiol Disease.* 35(28): 10252-10267.

Choi DW, Maulucci-Gedde M, Kriegstein AR. (1987) Glutamate neurotoxicity in cortical cell culture. *Journal of Neuroscience*, 7(2):357-368.

Choi YJ, Di Nardo A, Kramvis I, Meikle L, Kwiatkowski DJ, Sahin M, He X, (2008) Tuberous sclerosis complex proteins control axon formation. *Genes Dev.* 22(18): 2485-2495.

Choo AM, Miller WJ, Chen YC,Nibley P, Patel TP, Goletiani C, Morrison B 3rd, Kutzing MK, Firestein BL, Sul JY, Haydon PG, Meaney DF. (2013) Antagonism of purinergic signalling improves recovery from traumatic brain injury. *Brain*. 136(Pt 1):65-80.

Clausen F, Hanell A, Bjork M, Hillered L, Mir AK, Gram H, Marklund N. (2009) Neutralization of interleukin-1β modifies the inflammatory response and improves histological and cognitive outcome following traumatic brain injury in mice. *Eur J Neurosci.* 30: 385-396.

Coffey RT, Shi Y, Long MJ, Marr MT 2nd, Hedstrom L. (2016) Ubiquilin mediated small molecule inhibition of mammalian target of rapamycin complex 1 (mTORC1) signaling. *J Biol Chem*. jbc.M115.691584 [Epub ahead of print]

Cortes-Vieyra R, Silva-Garcia O, Oviedo-Boyso J, Huante-Mendoza A, Bravo-Patino A, Valdez-Alarcon JJ, Finlay BB, Baizabal-Aguirre VM. (2015) The Glycogen Synthase Kinase 3α and β isoforms differentially regulates Interleukin-12p40 expression in endothelial cells stimulated with peptidoglycan from Staphylococcus aureus. *PLoS ONE*. 10(7): e0132867. DOI: 10.1371/journal.pone.0132867

Costa HA, Leitner MG, Sos ML, Mavrantoni A, Rychkova A, Johnson JR, Newton BW, Yee MC, De La Vega FM, Ford JM, Krogan NJ, Shokat KM, Oliver D, Halaszovich CR, Bustamante CD. (2015) Discovery and functional characterization of a neomorphic PTEN mutation. *P Natl Acad Sci.* 112(45): 13976-13981.

Crowell B, Lee GH, Nikolaeva I, Dal Pozzo V, D'Arcangelo G. (2015) Complex neurological phenotype in mutant mice lacking Tsc2 in excitatory neurons in the developing forebrain. *eNeuro.* 10.1523/ENEURO.0046-15.2015

D'Arcangelo G. (2009) From human tissue to animal models: insights into the pathogenesis of cortical dysplasia. *Epilepsia.* Suppl 9:28-33

Das BB, Shoemaker L, Subramamian S, Johnsrude C, Recto M, Austin EH. (2007) Acute sirolimus pulmonary toxicity in an infant heart transplant recipient: case report and literature review. *J Heart Lung Transplant*. 26(3):296-298.

Das F, Ghosh-Choudhury N, Dey N, Mandal CC, Mahimainathan L, Kasinath BS, Abboud HE, Choudhury GG. (2012) Unrestrained mammalian target of rapamycin complexes 1 and 2 increase expression of phosphatase and tensin homolog deleted on chromosome 10 to regulate phosphorylation of Akt kinase. *J Biol Chem*. 287(6):3808-3822.

Deane JA, Fruman DA. (2004) Phosphoinositide 3-kinase: diverse roles in immune cell activation. *Annu Rev Immunol.* 22: 563-598.

Dixon CE, Lyeth BG, Povlishock JT, Findling RL, Hamm RJ, Marmarou A, Young HF, Hayes RL. (2010) A fluid percussion model of experimental brain injury in the rat. *Journal of Neurosurgery*, 112(2):110-119.

Don AS, Tsang CK, Kazdoba TM, D'Arcangelo G, Young W, Zheng XF. (2012) Targeting mTOR as a novel therapeutic strategy for traumatic CNS injuries. *Drug Discovery Today*, 17(15-16):861-8.

Downward J. (2004) PI 3-kinase, Akt and cell survival. *Semin Cell Dev Biol.* 15:177-182.

Drinjakovic J, Jung H, Campbell DS, Strochlic L, Dwivedy A, Holt CE. (2010) E3 Ligase Nedd4 promotes axon branching by downregulating PTEN. *Neuron.* 65(3): 341-357.

Edinger AL, Linardic CM, Chiang GG, Thompson CB, Abraham RT. (2003) Differential effects of rapamycin on mammalian target of rapamycin signaling functions in mammalian cells. *Cancer Res.* 63: 8451-8460.

Ehninger D, Han S, Shilyansky C, Zhou Y, Li W, Kwiatkowski DJ, Ramesh V, Silva AJ. (2008) Reversal of learning deficits in a Tsc2+/- mouse model of tuberous sclerosis. *Nat Med.* 14(8): 843-848.

Elder GA, Sosa MAG, De Gasperi R, Stone JR, Dickstein DL, Haghighi F, Hof PR, Ahlers ST. (2015) Vascular and inflammatory factors in the pathophysiology of blast-induced brain injury. *Front Neurol.* Volume 6, Article 48.

Erdman J, Oria M, Pillsbury L. Nutrition and Traumatic Brain Injury: Improving Acute and Subacture Health Outcomes in Military personnel. *Committee on Nutrition, Trauma, and the Brain.* Washington: National Academy of Sciences, 2011

Erlich S, Alexandrovich A, Shohami E, Pinkas-Kramarski R. (2007) Rapamycin is a neuroprotective treatment for traumatic brain injury. *Neurobiology of Disease*, 26:86-93.

Ewald F, Norz D, Grottke A, Bach J, Herzberger C, Hofmann BT, Nashan B, Jucker M. (2015) Vertical targeting of AKT and mTOR as well as dual targeting of AKT and MEK signaling is synergistic in hepatocellular carcinoma. *J Cancer.* 6(12): 1195-1205.

Faden AI, Demediuk S, Panter SS, Vink R. (1989) The role of excitatory amino acids and NMDA receptors in traumatic brain injury*. Science*, 244:798-800.

Feliciano DM, Lin TV, Hartman NW, Bartley CM, Kubera C, Hsieh L, Lafourcade C, O'Keefe RA, Bordey A. (2013) A circuitry and biochemical basis for tuberous sclerosis symptoms: from epilepsy to neurocognitive deficits. *Int J Dev Neurosci.* 31(7): DOI:10.1016/j.ijdevneu.2013.02.008.

Fingar DC, Salama S, Tsou C, Harlow E, Blenis J. (2002) Mammalian cell size is controlled by mTOR and its downstream targets S6K1 and 4EBP1/eIF4E. *Gene Dev*. 16:1472-1487.

Fraser MM, Bayazitov IT, Zakharenko SS, Baker SJ. (2008) Pten deficiency in brain causes defects in synaptic structure, transmission and plasticity, and myelination abnormalities. *Neuroscience.* 151(2): 476-488.

Gao X, Deng-Bryant Y, Cho W, Carrico KM, Hall ED, Chen J. (2008) Selective death of newborn neurons in hippocampal dentate gyrus following moderate experimental traumatic brain injury. *J Neurosci Res*. 86: 2258-2270.

Gao X, Deng P, Xu ZC, Chen J. (2011) Moderate traumatic brain injury causes acture dendrite and synaptic degeneration in the hippocampal dentate gyrus. *PLoS ONE.* 6(9): e24566 DOI: 10.1371/journal/pone.0024566,

Garami A, Zwartkruis FJT, Nobukuni T, Joaquin M, Roccio M, Stocker H, Kozma SC, Hafen E, Bos JL, Thomas G. (2003) Insulin activation of Rheb, a mediator of mTOR/S6K/4E-BP signaling, is inhibited by TSC1 and 2. *Mol Cell.* 11: 1457-1466.

Gong R, Park CS, Abbassi NR, Tang SJ. (2006) Roles of glutamate receptors and the mammalian target of rapamycin (mTOR) signaling pathway in activity-dependent dendritic protein synthesis in hippocampal neurons. *J Biol Chem*. 281(27):18802-18815.

Goto J, Talos DM, Klein P, Qin W, Chekaluk YL, Anderl S, Malinowska IA, Di Nardo A, Bronson RT, Chan JA, Vinters HV, Kernie SG, Jensen FE, Sahin M, Kwiatkowski DJ. (2011) Regulable neural progenitor-specific *Tsc1* loss yields giant cells with organellar dysfunction in a model of tuberous sclerosis complex. *Proc Natl Acad Sci*. 108(45): E1070-E1079.

Groszer M, Erickson R, Scripture-Adams DD, Lesche R, Trumpp A, Zack JA, Kornblum HL, Liu X, Wu H. (2001) Negative regulation of neural stem/progenitor cell proliferation by the *Pten* tumor suppressor gene *in vivo*. *Science.* 294: 2186-2189.

Guerrini R, Barba C. (20120) Malformations of cortical development and aberrant cortical networks: epileptogenesis and functional organization. *J Clin Neurophysiol.* 27(6): 372-379.

Guo D, Zeng L, Brody DL, Wong M. (2013) Rapamycin attenuates the development of posttraumatic epilepsy in a mouse model of traumatic brain injury. *PLoS ONE.* 8(5): e64078 DOI: 10.1371/journal.pone.0064078.

Hevner RF. (2015) Brain overgrowth in disorders of RTK-PI3K-AKT signaling: a mosaic of malformations. *Semin Perinatol.* 39: 36-43.

Hietakangas V, Cohen SM. (2007) Re-evaluating AKT regulation: role of TOR complex 2 in tissue growth. *Gene Dev.* 21: 632-637.

Hirai H, Sootome H, Nakatsuru Y, Miyama K, Taguchi S, Tsujioka K, Ueno Y, Hatch H, Majumder PK, Pan BS, Kotani H. (2010) MK-2206, an allosteric Akt inhibitor, enhances antitumor efficacy by standard chemotherapeutic agents or molecular targeted drugs *in vitro* and *in vivo. Mol Cancer Ther.* 9(7):1956-1967.

Hiraoka D, Okomura E, Kishimoto T. (2011) Turn motif phosphorylation negatively regulates activation loop phosphorylation in Akt. *Oncogene*. 30(44):4487-4497.

Hopkins BD, Fine B, Steinbach N, Dendy M, Rapp Z, Shaw J, Pappas K, Yu JS, Hodakoski C, Mense S, Klein J, Pegno S, Sulis MS, Goldstein H, Amendolara B, Lei L, Maurer M, Bruce J, Canoli P, Hibshoosh H, Parsons R. (2013) A secreted PTEN phosphatase that enters cells to alter signaling and survival. *Science*. 341: 399-402.

Hosokawa N, Hara T, Kaizuka T, Kishi C, Takamura A, Miura Y, Iemura S, Natsume T, Takehana K, Yamada N, Guan JL, Oshiro N, Mizushima N. (2009) Nutrient-dependent mTORC1 association with the ULK1-Atg13-FIP200 complex required for autophagy. *Mol Biol Cell.* 20: 1981-1991.

Hu WH, Zhang C, Zhang K, Shao XQ, Zhang JG. (2015) Hemispheric surgery for refractory epilepsy: a systematic review and meta-analysis with emphasis on seizure predictors and outcomes. *J Neurosurg.* Doi:10.3171 [epub ahead of print]

Huang J, Manning BD. (2009) A complex interplay between Akt, TSC2, and the two mTOR complexes. *Biochem Soc Trans*. 37(1):217-222.

Hung PC, Wang HS. (2003) Hemimegalencephaly: cranial sonogrpahic findigns in neonates. *J Clin Ultrasound.* 33(5): 243-247.

Inoki K, Li Y, Zhu T, Wu J, Guan KL. (2002) TSC2 is phosphorylated and inhibited by Akt and suppresses mTOR signaling. *Nat Cell Biol.* 4: 648-657.

Inoki K, Li Y, Xu T, Guan KL. (2003) Rheb GTPase is a direct target of TSC2 GAP activity and regulates mTOR signaling. *Gene Dev.* 17: 1829-1834.

Inoki K, Ouyang H, Zhu T, Lindvall C, Wang Y, Zhang X, Yang Q, Bennett C, Harada Y, Stankunas K, Wang C, He X, MacDougald OA, You M, Williams BO, Guan KL. *Cell.* 126: 955-968.

Inverardi F, Chikhladze M, Donzelli A, Moroni RF, Regondi MC, Pennacchio P, Zucca I, Corradini I, Braida D, Sala M, Franceschetti S, Frassoni C. (2013) Cytoarchitectural, behavioral and neurophysiological dysfunctions in the BCNU-treated rat model of cortical dysplasia. *Eur J Neurosci.* 37(1):150-162.

Iyer G, Hanrahan AJ, Milowsky MI, Al-Ahmadie H, Scott SN, Janakiraman M, Pirun M, Sander C, Socci ND, Ostrovnaya I, Viale A, Heguy A, Peng L, Chan TA, Bochner B, Bajorin DF, Berger MF, Taylor BS, Solit DB. (2012) Genome sequencing identifies a basis for everolimus sensitivity. *Science*. 338(6104): 221.

Jansen LA, Mirzaa GM, Ishak GE, O'Roak BJ, Hiatt JB, Roden WH, Gunter SA, Christian SL, Collins S, Adams C, Riviere JB, St-Onge J, Ojemann JG, Shendure J, Hevner RF, Dobyns WB. (2015) PI3K/AKT pathway mutations cause a spectrum of brain malformations from megalencephaly to focal cortical dysplasia. *Brain.* 138(6):1613-1628.

Jaworski J, Spangler S, Seeburg DP, Hoogenraad SS, Sheng M. (2005) Control of dendritic arborization by the phosphoinositide-3-kinase-Akt-mammalian target of rapamycin pathway. *J Neurosci.* 25(49): 11300-11312.

Jiang H, Guo W, Liang X, Rao Y. (2005) Both the establishment and the maintenance of neuronal polarity require active mechanisms: critical roles of GSK-3beta and its upstream regulators. *Cell.* 120(1): 123-135.

Jimenez PM, Olmedo MR, Marin GD, Lozano RJM, de la Cruz LJ, Rodrigo LJM. (2006) Pulmonary toxicity associated with sirolimus therapy in liver transplantation. *Gastroenterol Hepatol.* 29(10):616-618.

Johnston O, Rose CL, Webster AC, Gill JS. (2008) Sirolimus is associated with new-onset diabetes in kidney transplant recipients. *J Am Soc Nephrol.* 19(7):1411-1418.

Kahan BD. (1992) Cyclosporin A, FK506, rapamycin: the use of a quantitative analytic tool to discriminate immunosuppressive drug interactions. *J Am Soc Nephrol.* 2: S222-S227.

Karisson E, Magic I, Bostner J, Dyrager C, Lysholm F, Hallbeck AL, Stal O, Lundstrom P. (2015) Revealing different roles of the mTOR-targets S6K1 and S6K2 in breast cancer by expression profiling and structual analysis. *PLoS ONE* 10(12): e0145013. DOI:10.1371/journal.pone.0145013.

Kazdoba TM, Sunnen CN, Crowell B, Lee GH, Anderson AE, D'Arcangelo G. (2012) Development and characterization of NEX- Pten, a novel forebrain excitatory neuron-specific knockout mouse. *Dev Neurosci*. 34(2-3):198-209.

Kennedy SG, Wagner AJ, Conzen SD, Jordan J, Bellacosa A, Tsichlis PN, Hay N. (1997) The PI 3-kinase/Akt signaling pathway delivers an anti-apoptotic signal. *Gene Dev.* 11: 701-713.

Kim K, Qiang L, Hayden MS, Sparling DP, Purcell NH, Pajvani UB. (2015) mTORC1-independent Raptor prevents hepatic steatosis by stabilizing PHLPP2. *Nat Comms.* DOI10.1038/ncomms10255.

Kloss S, Pieper T, Pannek H, Holthausen H, Tuxhorn I. (2002) Epilepsy surgery in children with focal cortical dysplasia (FCD): results of long-term seizure outcome. *Neuropediatrics.* 33(1):21-26.

Kreis P, Leondaritis G, Lieberam I, Eickholt BJ. (2014) Subcellular targeting and dynamic regulation of PTEN: implications for neuronal cells and neurological disorders. *Frontiers Mol Neurosci.* 7: DOI: 10.3389/fnmol.2014.00023.

Krueger DA., Wilfong AA., Holland-Bouley K, Anderson AE, Agricola K, Tudor C, Mays M, Lopez CM, Kim MO, Franz DN. (2013) Everolimus treatment of refractory epilepsy in tuberous sclerosis complex. *Ann Neurol*. 74(5):679-687.

Kwon CH, Zhu X, Zhang J, Knoop LL, Tharp R, Smeyne RJ, Eberhart CG, Burger PC, Baker SJ. (2001) Pten regulates neuronal soma size: a mouse model of lhermitte-Duclos disease. *Nat Gen.* 29: 404-411.

Kwon CH, Luikart BW, Powell CM, Zhou J, Matheny SA, Zhang W, Li Y, Baker SJ, Parada LF. (2006) Pten regulates neuronal arborization and social interaction in mice. *Neuron.* 50: 377-388.

Lachyankar MB, Sultana N, Schonhoff CM, Mitra P, Poluha W, Lambert S, Quesenberry PJ, Litofsky NS, Recht LD, Nabi R, Miller SJ, Ohta S, Neel BG, Ross AH. (2000) A role for nuclear PTEN in neuronal differentiation. *J Neurosci.* 20(4): 1404-1413.

Laplante M, Sabatini DM. (2009) mTOR signaling at a glance. *Journal of Cell Science*, 122:3589-3594.

Lau A, Arundine M, Sun HS, Jones M, Tymianski M. (2006) Inhibition of caspase-mediated apoptosis by peroxynitrite in traumatic brain injury. *J Neurosci.* 26(45): 11540-11553.

Le Belle JE, Sperry J, Ngo A, Ghochani Y, Laks DR, Lopez-Aranda M, Silva AJ, Kornblum HI. (2014) Maternal inflammation contributes to brain overgrowth and autism-associated behaviors through altered redox signaling in stem and progenitor cells. *Stem Cell Rep.* 3: 725-734.

Lee JJ, Loh K, Yap YS. (2015) PI3K/Akt/mTOR inhibitors in breast cancer. *Cancer Biol Med.* 12(4): 342-354.

Lee JO, Yang H, Georgescu MM, Di Cristofano A, Maehama T, Shi Y, Dixon JE, Pandolfil P, Pavletich NP. (1999) Crystal structure of PTEN tumor suppressor: implications for its phosphoinositide phosphatase activity and membrane association. *Cell*. 99: 323-334.

Leslie NR, Brunton VG. (2013) Where is PTEN? *Science*. 355-356.

Lim JS, Lee JH. (2015) Brain somatic mutations in *MTOR* leading to focal cortical dysplasia. *Nat Med.* 21(4): 395-400.

Liaw D, Marsh DJ, Li J, Dahia PLM, Wang SI, Zheng Z, Bose S, Call KM, Tsou HC, Peacoke M, Eng C, Parsons R. (1997) Germline mutations of the *PTEN* gene in Cowden disease, an inherited breast and thyroid cancer syndrome. *Nat Genet.* 16:64-67.

Lin YX, Lin K, Liu XX, Kang DZ, Ye ZX, Wang XF, Zheng SF, Yu LH, Lin ZY. (2015) PI3K-AKT pathway polymerase chain reaction (PCR) array analysis of epilepsy induced by type II focal cortical dysplasia. *Gen Mol Res.* 14(3): 9994-10000.

Liu J, Reeves C, Michalak Z, Coppola A, Diehl B, Sisodiya SM, Thom M. (2014) Evidence for mTOR pathway activation in a spectrum of epilepsy-associated pathologies. *Acta Neuropathol Commun.* 2:71-84.

Liu Y, Wang L, Long Z, Wu Y, Wan Q, Jiang J, Wang Z. (2013) Inhibiting PTEN protects hippocampal neurons against stretch injury by decreasing membrane translocation of AMPA receptor GluR2 subunit. *PLoS ONE.* 8(6): e65431.

Ljungberg MC, Bhattacharjee MB, Lu Y, Armstrong DL, Yoshor D, Swann JW, Sheldon M, D'Arcangelo G. (2006) Activation of mammalian target of rapamycin in cytomegalic neurons of human cortical dysplasia. *Ann Neurol.* 60(4):420-429.

Ljungberg MC, Sunnen CN, Lugo JN, Anderson AE, D'Arcangelo G. (2009) Rapamycin suppresses seizures and neuronal hypertrophy in a mouse model of cortical dysplasia. *Dis Model Mech*. 2(7-8):389-398.

Lloyd E, Somera-Molina K, Van Eldik LJ, Watterson DM, Wainwright MS. (2008) Suppression of acute proinflammatory cytokine and chemokine upregulation by post-injury administration of a novel small molecule improves long-term neurologic outcome in a mouse model of traumatic brain injury. *J Neuroinflamm.* 5:28-42.

LoPiccolo J, Kim SJ, Shi Y, Wu B, Wu H, Chait BT, Singer RH, Sali A, Brenowitz M, Bresnick AR, Backer JM. (2015) Assembly and molecular architecture of the phosphoinositide 3-kinase p85α homodimer. *J Biol Chem.* 290(51): 30390-30405.

Ma L, Chen Z, Erdjument-Bromage H, Tempst P, Pandolfi PP. (2005) Phosphorylation and functional inactivation of TSC2 by Erk: implications for tuberous sclerosis and cancer pathogenesis. *Cell.* 121:179-193.

Mao L, Jia J, Zhou X, Xiao Y, Wang Y, Mao X, Zhen X, Guan Y, Alkayed NJ, Cheng J. (2013) Delayed administration of a Pten inhibitor bpV improves functional recovery after experimental stroke. *Neuroscience.* 231: 272-281.

McMahon J, Huang X, Yang J, Komatsu M, Yue Z, Qian J, Zhu X, Huang Y. (2012) Impaired autophagy in neurons following disinhibition of mTOR and its contribution to epileptogenesis. *J Neurosci.* 32(45):15704-15714.

Mego M, Svetlovska D, Miskovska V, Obertova J, Palacka P, Rajec J, Sycova-Mila Z, Chovanec M, Rejlekova K, Zuzak P, Ondrus D, Spanik S, Reckova M, Mardiak J. (2015) Phase II study of everolimus in refractory testicular germ cell tumors. *Urol Oncol.* Doi: 10.1016/j.urolonc.2015.10.010.

Meikle L, Pollizzi K, Egnor A, Kramvis I, Lane H, Sahin M, Kwiatkowski DJ. (2008) Response of a neuronal model of tuberous sclerosis to mammalian target of rapamycin (mTOR) inhibitors: effects on mTORC1 and Akt signaling lead to improved survival and function. *J Neurosci*. 28(21):5422-5432.

Meikle L, Talos DM, Onda H, Pollizzi K, Rotenberg A, Sahin M, Jensen FE, Kwiatkowski DJ. (2007) A mouse model of tuberous sclerosis: neuronal loss of Tsc1 causes dysplastic and ectopic neurons, reduced myelination, seizure activity, and limited survival. *J Neurosci*. 27(21):5546-5558.

Merritt VC, Arnett P (2014) Premorbid predictors of postconcussion symptoms in collegiate athletes. *J Clin Exp Neuropsychol*. 36(10):1098-1111.

Mirzaa GM, Poduri A. (2014) Megalencepahly and hemimegalencephaly: Breakthroughs in molecular etiology. *Am J Med Gen.* 166C: 156-172.

Moavero R, Folgiero V, Carai A, Miele E, Ferretti E, Po A, Camassei FD, Lepri FR, Vigevano F, Curatolo P, Valeriani M, Colafati GS, Locatelli F, Tornesello A, Mastronuzzi A. (2015) Metastatic group 3 medulloblastoma in a patient with tuberous sclerosis complex: case description and molecular characterization of the tumor. *Pediatr Blood Cancer*. DOI: 10.1002/pbc25851.

Muddassar M, Pasha FA, Neaz MM, Saleem Y, Cho SJ. (2009) Elucidation of binding mode and three dimensional quantitative structure-activity relationship studies of a novel series of protein kinase B/Akt inhibitors. *J Mol Model.* 15: 183-192.

Nakanishi Y, Walter K, Spoerke JM, O'Brien C, Huw LY, Hampton GM, Lackner MR. (2016) Activating mutations in *PIK3CB* confer resistance to PI3K inhibition and define a novel oncogenic role for p110β. *Cancer Res.* DOI: 10.1158/0008-5472 [ePub ahead of print].

Naguib A, Bencze G, Cho H, Zheng W, Tocilj A, Elkayam E, Faehnle CR, Jaber N, Pratt CP, Chen M, Zong WX, Marks MS, Joshua-Tor L, Pappin DJ, Trotman LC. (2015) PTEN functions by recruitment to cytoplasmic vesicles. *Mol Cell.* 58: 255-268.

Napolioni V, Moavero R, Curatolo P. (2009) Recent advances in neurobiology of tuberous sclerosis complex. *Brain Dev.* 31(2): 104-113.

Nelen MR, van Staveren WCG, Peeters EAJ, Hassel MB, Gorlin RJ, Hamm H, Lindobe CF, Fryns JP, Sijmons RH, Woods DG, Mariman ECM, Padberg GW, Kremer H. (1997) Germline mutations in the *PTEN/MMAC1* gene in patients with Cowden disease. *Hum Mol Genet.* 6(8): 1383-1387.

Nie D, Di Nardo A, Han JM, Baharanyi H, Kramvis I, Huynh TT, Dabora S, Codeluppi S, Pandolfi PP, Pasquale EB, Sahin M. (2010) Tsc2-Rheb signaling regulates EphA-mediated axon guidance. *Nat Neurosci.* 13(2): 163-172.

Nie D, Chen Z, Ebrahimi-Fakhari D, Di Nardo A, Julish K, Robson VK, Cheng YC, Woolf CJ, Heiman M, Sahin M. (2015) The stress-induced Atf3-gelsolin cascade underlies dendritic spine deficits in neuronal models of tuberous sclerosis complex. *J Neurosci.* 35(30): 10762-10772.

Nikolaeva I, Crowell B, Valenziano J, Meaney DF, D'Arcangelo G. (2015) Beneficial effects of early mTORC1 inhibition after traumatic brain injury. *J Neurotrauma.* 33(2): 183-193.

Ohtake Y, Park D, Abdul-Muneer PM, Li H, Xu B, Sharma K, Smith GM, Selzer ME, Li S. (2014) The effect of systemic PTEN antagonist peptides on axon growth and functional recovery after spinal cord injury. *Biomaterials.* 35(16): 4610-4626.

Ohtake Y, Hayat U, Li S. (2015) PTEN inhibition and axon regeneration and neural repair. *Neural Regen Res.* 10(9): 1363-1368.

Oki Y, Fanale M, Romaguerra J, Fayad L, Fowler N, Copeland A, Samaniego F, Kwak LW, Neelapu S, Wang M, Feng L, Younes A. (2015) Phase II study of an AKT inhibitor MK2206 in patients with relapsed or refractory lymphoma. *Brit J Haematol*. 171: 463-470.

Okie S. (2005) Traumatic brain injury in the war zone. *N Engl J Med*. 352(20):2043-2047.

Pal SK, Reckamp K, Yu H, Figlin RA. (2010) Akt inhibitors in clinical development for the treatment of cancer. *Expert Opin Investig Drugs.* 19(11): 1355-1366.

Palmini A, Najm I, Avanzini G, Babb T, Guerrini R, Foldavy-Schaefer N, Jackson G, Luders HO, Prayson R, Spreafico R, Vinters HV. (2004) Terminology and classification of the cortical dysplasias. *Neurology*. 62:S2-S8.

Panzer MB, Matthews KA, Yu AW, Morrison III B, Meaney DF, Bass CR. (2012) A multiscale approach to blast neurotrauma modeling: part I – development of novel test devices for *in vivo* and *in vitro* blast injury models*. Frontiers in Neurology*, 3(Article 46):1-11.

Park J, Zhang J, Qiu J, Zhu X, Degterev A, Lo EH, Whalen MJ. (2012) Combination therapy targeting Akt and mammalian target of rapamycin improves functional outcome after controlled cortical impact in mice. *Journal of Cerebral Blood Flow & Metabolism,* 32:330-340.

Park KK, Liu K, Hu Y, Smith PD, Wang C, Cai B, Xu B, Connolly L, Kramvis I, Sahin M, He Z. (2008) Promoting axon regeneration in the adult CNS by modulation of the PTEN/mTOR pathway. *Science.* 32295903): 963-966.

Park Y, Luo T, Zhang F, Liu C, Bramlett HM, Dietrich WD, Hu B. (2013) Downregulation of Src-kinase and glutamate-receptor phosphorylation after traumatic brain injury. *J Cerebr Blood F Met.* 33: 1642-1649.

Poduri A, Evrony GD, Cai X, Elhosary PC, Beroukhim R, Lehtinen MK, Hills LB, Heinzen EL, Hill A, Hill RS, Barry BJ, Bourgeois BF, Riviello JJ, Barkovich AJ, Black PM, Ligon KL, Walsh CA. (2012) Somatic activation of AKT3 causes hemispheric developmental malformations. *Neuron.* 74(1):41-48.

Prestwich GD. (2004) Phosphoinositide signaling: from affinity probes to pharmaceutical targets. *Chem Biol.* 11: 619-637.

Rose ME, Huerbin MB, Melick J, Marion DW, Palmer AM, Sciding JK, Kochanek PM, Graham SH. (2002) Regulation of interstitial excitatory amino acid concentrations after cortical contusion injury. *Brain Research*, 943:15-22.

Rossini L, Medici V, Tassi L, Cardinale F, Tringali G, Bramerio M, Villani F, Spreafico R, Garbelli R. (2014) Layer-specific gene expression in epileptogenic type II focal cortical dysplasia: normal-looking neurons reveal presence of a hidden laminar organization. *Acta Neuropath Comm.* 2:45-60.

Roy A, Skibo J, Kalume F, Ni J, Rankin S, Lu Y, Dobyns WB, Mills GB, Zhao JJ, Baker SJ, Millen KJ. (2015) Mouse models of human PIK3CA-related brain overgrowth have acutely treatable epilepsy. *eLife.* Doi: 10.7554 [epub ahead of print]

Rozas NS, Redell JB, Hill JL, McKenna J 3rd, Moore AN, Gambello MJ, Dash PK. (2015) Genetic activation of mTORC1 signaling worsens neurocognitive outcome after traumatic brain injury. *J Neurotrauma.* 32(2): 149-158.

Ru W, Peng Y, Zhong L, Tang SJ. (2012) A role of the mammalian target of rapamycin (mTOR) in glutamate-induced down-regulation of tuberous sclerosis complex proteins 2 (TSC2). *J Mol Neurosci.* 47: 340-345.

Rugo HS, Hortobagyi GN, Yao J, Pavel M, Ravaud A, Franz D, Ringeisen F, Gallo J, Rouyrre N, Anak O, Motzer R. (2016) Meta-analysis of stomatitis in clinical studies of everolimus: incidence and relationship with efficacy. *Ann Oncol*. PMID:26759276 [epub ahead of print]

Sansal I, Sellers WR. (2004) The biology and clinical relevance of the *PTEN* tumor suppressor pathway. *J Clin Oncol.* 22(14): 2954-2963.

Sarbassov DD, Ali SM, Kim DH, Guertin DA, Latek RR, Erdjument-Bromage H, Tempst P, Sabatini DM. (2004) Rictor, a novel binding partner of mTOR, defines a rapamycin-insensitive and Raptor-independent pathway that regulates the cytoskeleton. *Curr Biol.* 14: 1296-1302.

Sarbassov DD, Guertin DA, Ali SM, Sabatini DM. (2005) Phosphorylation and regulation of Akt/PKB by the Rictor-mTOR complex. *Science.* 307: 1098-1101.

Sarbassov DD, Ali SM, Sengupta S, Sheen JH, Hsu PP, Bagley AF, Markhard AL, Sabatini DM. (2006) Prolonged rapamycin treatment inhibits mTORC2 assembly and Akt/PKB. *Mol Cell*. 22(2):159-168.

Schuler W, Sedrani R, Cottens S, Haberlin B, Schulz M, Schuuman HJ, Zenke G, Zerwes HG, Schreier MH. (1997) *Transplantation.* 64(1): 36-42.

Seifer G, Blenkmann A, Princich JP, Consalvo D, Papayannis C, Muravchik C, Kochen S. (2012) Noninvasive approach to focal cortical dysplasias: clinical, EEG, and neurimaging features. *Epilepsy Res Treat.* DOI: 10.1155/2012/736784.

Schmued LC, Hopkins KJ. (2000) Fluoro-Jade B: a high affinity fluorescent marker for the localization of neuronal degeneration. *Brain Res*. 874(2):123-130.

Shein NA, Grigoriadis N, Alexandrovich AG, Simeonidou C, Spandou E, Tsenter J, Yatsiv I, Horowitz M, Shohami E. (2008) Differential neuroprotective properties of endogenous and exogenous erythropoietin in a mouse model of traumatic brain injury. *J Neurotrauma*. 25(2):112-123.

Shimobayashi M, Hall MN. (2016) Multiple amino acid sensing inputs to mTORC1. *Cell Res.* 26: 7-20.

Shin S, Wolgamott L, Yu Y, Blenis J, Yoon SO. (2011) Glycogen synthase kinase (GSK)-3 promotes p70 ribosomal protein S6 kinase (p70S6K) activity and cell proliferation. *Proc Natl Acad Sci.* 108(47): E1204-E1213.

Shum M, Bellmann K, St-Pierre P, Marette A. (2016) Pharmacological inhibition of S6K1 increases glucose metabolism and Akt signalling in vitro and in diet-induced obese mice. *Diabetologia.* DOI: 10.1007/s00125-015-3839-6.

Smith DH, Soares HD, Pierce JS, Perlman KG, Saatman KE, Meaney DF, Dixon CE, McIntosh TK. (1995) A model of parasagittal controlled cortical impact in the mouse: cognitive and histopathologic effects. *J Neurotrauma*. 12(2):169-178.

Sperow M, Berry RB, Bayazitov IT, Zhu G, Baker SJ, Zakharenko SS. (2012) Phosphatase and tensin homolog (PTEN) regulates synaptic plasticity independently of its effect on neuronal morphology and migration. *J Physiol.* 590(4): 777-792.

Spinelli L, Black FM, Berg JN, Eickholt BJ, Leslie NR. (2014) Functionally distinct groups of inherited PTEN mutations in autism and tumor syndromes. *J Med Genet.* 52(2): 128-134.

Sunnen CN, Brewster AL, Lugo JN, Vanegas F, Turcios E, Mukhi S, Parghi D, D'Arcangelo G, Anderson AE. (2011) Inhibition of the mammalian target of rapamycin blocks epilepsy progression in NS-PTEN conditional knockout mice. *Epilepsia.* 52(11): 2065-2075.

Tavazoie SF, Alvarez VA, Ridenour DA, Kwiatkowski DJ, Sabatini BI. (2005) Regulation of neuronal morphology and function by the tumor suppressors Tsc1 and Tsc2. *Nat Neurosci.* 8(12): 1727-1734.

Tee AR, Manning BD, Roux PP, Cantley LC, Blenis J. (2003) Tuberous sclerosis complex gene products, tuberin and hamartin, control mTOR signaling by acting as a GTPase-activating protein complex toward Rheb. *Curr Biol.* 13: 1259-1268.

Thompson HJ, Lifshitz J, Maklund N, Grady MS, Graham DI, Hovda DA, McIntosh TK. (2005) Lateral fluid percussion brain injury: a 15-year review and evaluation. *Journal of Neurotrauma*, 22(1):42-75.

Thompson SN, Gibson TR, Thompson BM, Deng Y, Hall ED. (2006) Relationship of calpain-mediated proteolysis to the expression of axonal and synaptic plasticity markers following traumatic brain injury in mice. *Exp Neurol.* 201: 253-265.

Tsai PT, Hull C, Chu YX, Greene-Colozzi E, Sadowski AR, Leech JM, Steinberg J, Crawley JN, Regehr WG, Sahin M. (2012) Autistic-like behavior and cerebellar dysfunction in Purkinje cell *Tsc1* mutant mice. *Nature.* 488: 647-651.

Tyburczy ME, Dies KA, Glass J, Camposano S, Chekaluk Y, Thorner AR, Lin L, Krueger D, Franz DN, ThieleEA, Sahin M, Kwiatkowski DJ. (2015) Mosaic and intronic mutations in *TSC1/TSC2* explain the majority of TSC patients with no mutation identified by conventional testing. *PLoS Genet.* 11(11): e1005637. DOI:10.1371/journal.pgen.1005637.

van Diepen MT, Eickholt BJ. (2008) Function of PTEN during the formation and maintenance of neuronal circuits in the brain. *Dev Neurosci.* 30: 59-64.

Wang L, Chen L, Yu M, Xu LH, Cheng B, Lin YS, Gu Q, He XH, Xu J. (2016) Discovering new mTOR inhibitors for cancer treatment through virtual screening methods and *in vitro* assays. *Nature Sci Reports.* 6:18987 DOI: 10.1038/srep18987.

Way SW, Rozas NS, Wu HC, McKenna J, Reith RM, Hashmi SS, Dash PK, Gambello MJ. (2012) The differential effects of prenatal and/or postnatal rapamycin on neurodevelopmental defects and cognition in a neuroglial mouse model of tuberous sclerosis complex. *Hum Mol Genet*. 21(14):3226-3236.

Webster SJ, Van Eldik LJ, Watterson DM, Bachstetter AD. (2015) Closed head injury in age-related Alzheimer mouse model leads to an altered neuroinflammatory response and persistent cognitive impairment. *J Neurosci*. 35(16):6554-6569.

White TE, Ford GD, Surles-Ziegler MC, Gates AS, Laplaca MC, Ford BD. (2013) Gene expression patterns following unilateral traumatic brain injury reveals a local pro-inflammatory and remote anti-inflammatory response. *BMC Genomics.* 14: 282.

Wiley CA, Bonneh-Barkay D, Dixon CE, Lesniak A, Wang G, Bissel SJ, Kochanek PM. (2015) Role of mammalian chitinase 3-like protein 1 in traumatic brain injury. *Neuropathology.* 35: 95-106.

Williams MR, DeSpenza Jr T, Li M, Gulledge AT, Luikart BW. (2015) Hyperactivity of newborn Pten knockout neurons results from increased excitatory synaptic drive. *J Neurosci.* 35(3):943-959.

Winden KD, Yuskaitis CJ, Poduri A. (2015) Megalencephaly and macroencephaly. *Semin Neurol.* 35:277-287.

Wong M, Crino PB. (2012) mTOR and epileptogenesis in developmental brain malformations. Jasper's Basic mechanisms of the Epilepsies. 4th ed, Bethesda, MD, 2012

Woodcock T, Morganti-Kossmann MC. (2013) The role of markers of inflammation in traumatic brain injury. *Front Neurol.* Volume 4, Article 18.

Wu H, Lu D, Jiang H, Xiong Y, Qu C, Li B, Mahmood A, Zhou D, Chopp M. (2007) Simvastatin-mediated upregulation of VEGF and BDNF, activation of the PI3K/Akt pathway, and increase of neurogenesis are associated with therapeutic improvement after traumatic brain injury. *Journal of Neurotrauma*, 25:130-139.

Xu L, Ryu J, Nguyen JV, Arena J, Rha E, Vranis P, Hitt D, Marsh-Armstrong N, Koliatsos VE. (2015) Evidence for accelerated tauopathy in the retina of transgenic P301S tau mice exposed to repetitive mild traumatic brain injury. *Exp Neurol.* 273: 168-176.

Yan D, Guo L, Wang Y. (2006) Requirement of dendritic Akt degradation by the ubiquitin-proteasome system for neuronal polarity. *J Cell Biol.* 174(3): 415-424.

Yang H, Rudge DG, Koos JD, Vaidialingam B, Yang HJ, Pavletich NP. (2013) mTOR kinase structure, mechanism and regulation. *Nature.* 497(7448): 217-223.

Yap TA, Yan L, Patnaik A, Fearen I, Olmos D, Papadopoulos K, Baird RD, Delgado L, Taylor A, Lupinacci L, Riisnaes R, Pope LL,Heaton SP, Thomas G, Garrett MD, Sullivan DM, de Bono JS, Tolcher AW. (2011) First-in-man clinical trial of the oral pan-AKT inhibitor MK-2206 in patients with advanced solid tumors. *J Clin Oncol.* 29(35):4688-4695.

Yasin SA, Ali AM, Tata M, Picker SR, Anderson GW, Latimer-Bowman E, Nicholson SL, Harkness W, Cross JH, Paine SML, Jacques TS. (2013) mTOR-dependent abnormalities in autophagy characterize human malformations of cortical development: evidence from focal cortical dysplasia and tuberous sclerosis. *Acta Neuropathol.* 126:207-218.

Zeng LH, Xu L, Gutmann DH, Wong M. (2008) Rapamycin prevents epilepsy in a mouse model of Tuberous Sclerosis Complex. *Ann Neurol*. 23(4):444-453.

Zeng LH, Rensing NR, Wong M. (2009) Developing antiepileptic drugs for acquired epilepsy: targeting the mammalian target of rapamycin (mTOR) pathway. *Mol Cell Pharmacol.* 1(3): 124-129.

Zhao S, Fu J, Liu X, Wang T, Zhang J, Zhao Y. (2012) Activation of Akt/GSK-3beta/beta-catenin signaling pathway is involved in survival of neurons after traumatic brain injury in rats. *Neurol Res.* 34(4): 400-407.

Zhou H, Chen L, Gao X, Luo B, Chen J. (2012) Moderate traumatic brain injury triggers rapid necrotic death of immature neurons in the hippocampus. *J Neuropathol Exp Neurol*. 71(4):348-359.

Zhou J, Blundell J, Ogawa S, Kwon CH, Zhang W, Sinton C, Powell CM, Parada LF. (2009) Pharmacological inhibition of mTORC1 suppresses anatomical, cellular, and behavioral abnormalities in neural-specific *Pten* knock-out mice. *J Neurosci.* 29(6): 1773-1783.

Zhu X, Park J, Golinski J, Qiu J, Khuman J, Lee CC, Lo EH, Degterev A, Whalen MJ. Role of Akt and mammalian target of rapamycin in functional outcome after concussive brain injury in mice. *J Cereb Blood Flow Metab*. 2014;34(9):1531-1539.